

DEVELOPMENT OF A BIOSENSOR BASED ON LINEAR DICHROISM SPECTROSCOPY

SANDEEP KAUR SANDHU

A thesis submitted to the University of Birmingham for the degree of
Doctor of Philosophy

School of Biosciences

College of Life and Environmental Science

University of Birmingham

Edgbaston, Birmingham

B15 2TT

September 2014

UNIVERSITY OF
BIRMINGHAM

University of Birmingham Research Archive

e-theses repository

This unpublished thesis/dissertation is copyright of the author and/or third parties. The intellectual property rights of the author or third parties in respect of this work are as defined by The Copyright Designs and Patents Act 1988 or as modified by any successor legislation.

Any use made of information contained in this thesis/dissertation must be in accordance with that legislation and must be properly acknowledged. Further distribution or reproduction in any format is prohibited without the permission of the copyright holder.

Abstract

Existing methodologies for biomolecular detection are limited in several key areas. Heterogeneous assays struggle with various wash steps which can prolong assay time, while other assays require costly reagents, lack mobility and can be highly complex in nature. This project demonstrates how a bio-nano particle in the form of M13 bacteriophage (M13) can be used for the basis of a novel homogeneous immunoassay which incorporates the use of linear dichroism spectroscopy (LD).

M13 has a high aspect ratio which allows it to align easily in shear flow, this in turn generates a large LD signal. This property of M13 has been manipulated for use in a new *in-vitro* diagnostic technique.

Existing M13 production yields are much lower than those required for this assay. A new method was developed which increased the yield 10 fold. Chemical modifications were made by covalently attaching chromophores, this enabled the M13 LD signal to be visualised in the visible region and develops the potential for multiplexing.

By chemically modifying M13 with chromophores and antibodies it was possible to create an assay capable of detecting 10^5 cells/mL of *Escherichia coli* O157. This is 100 times more sensitive than the M13 based assay developed by Pacheco-Gomez *et al.* (2012). The assay was reassembled to detect small molecules and was found to have a sensitivity of 0.01 mM.

The assays presented form a sensitive, specific, fast diagnostic tool capable of detecting pathogens and small molecules. It offers significant improvements over existing methods, and could act as a platform in developing a multimodal detection system.

I would like to dedicate this thesis to my Mum and Dad.

Thank you for believing in me and always encouraging me to aim higher.

Acknowledgments

Firstly I would like to thank my two supervisors Professor Tim Dafforn and Professor Charles Penn for all of their help and support throughout my PhD. I would also like to thank everyone in the Dafforn lab both past and present including Matt Hicks, Craig Harris, Julia Kramer and Mohammed Jamshad. I would also like to give a special thank you to Raul Pacheco-Gomez who has not only been a wonderful colleague to work with but has also been a lovely friend. In addition I would like to acknowledge everyone on the 7th floor in Biosciences (Rosemary, Eva, Richard, Martin, Jack, Nick, Penny, Maria and Ian) who have been incredibly supportive and have made my time here extremely fun. I would also like to thank my parents and family for their encouragement, support and interest during my PhD.

I also would like to appreciate Professor Petra Oyston, Dr Roman Lukaszewski, Dr Sarah Goodchild and Dr Stephen Nicklin from Defence Science and Technology Laboratory (dstl) for their help and guidance.

Finally I would like to thank EPSRC and dstl for their financial support.

Table of Contents

1	CHAPTER 1 - INTRODUCTION	1
1.1.	Bio-detection.....	1
1.1.1.	Major methods	2
1.1.1.1.	Microbial culture for detection of pathogens.....	2
1.1.1.2.	Antibody based methods (homogeneous and heterogeneous)	3
1.1.1.2.1.	Agglutination assays	4
1.1.1.2.2.	Enzyme-linked immunosorbent assay	5
1.1.1.2.2.1.	Sandwich assay	6
1.1.1.2.2.2.	Indirect assays.....	7
1.1.1.2.3.	Lateral flow methods	9
1.1.1.2.4.	Homogenous methods.....	12
1.1.1.2.4.1.	Enzyme multiplied immunoassay technique	13
1.1.1.2.4.2.	Fluorescence polarisation immunoassay	14
1.1.2.	Summary	17
1.2.	Linear dichroism.....	20
1.2.1.	Theory and instrumentation and history	20
1.2.1.1.	Absorbance	20
1.2.1.2.	Theory of linear dichroism	22
1.2.1.3.	Molecular alignment methods.....	25
1.2.2.	Applications in Biology	27
1.2.2.1.	LD and structural studies of DNA.....	27
1.2.2.2.	Protein fibres.....	29
1.2.2.3.	Bacteriophage	30
1.3.	Synthetic biology.....	36
1.3.1.	Synthetic biology and detection	36

1.4. LD in immune detection.....	37
1.4.1. Theory	37
1.4.2. Previous work on an M13/LD based assay	39
1.5. Aims.....	42
2 CHAPTER 2 - MATERIALS AND METHODS	43
2.1. Materials	43
2.2. Methods.....	43
2.2.1. Production of M13 bacteriophage.....	43
2.2.1.1. Method based on Sambrook and Russell (2001)	43
2.2.1.2. Method from New England Biolabs (2011).....	44
2.2.1.3. New method for M13 bacteriophage production	45
2.2.1.4. Optimising precipitation time for M13 bacteriophage production	45
2.2.1.5. Measurement of M13 bacteriophage concentration	46
2.2.1.6. Collection of LD data	47
2.2.1.7. Calibration of LD instrument.....	48
2.2.2. Labelling of M13 bacteriophage with extrinsic chromophores	50
2.2.2.1. Labelling M13 bacteriophage with fluorescamine	50
2.2.2.2. Labelling M13 bacteriophage with rhodamine B isothiocyanate	50
2.2.2.3. Labelling M13 bacteriophage with fluorescein isothiocyanate isomer 1	50
2.2.2.4. Labelling M13 bacteriophage with 4-chloro-7-nitrobenzofurazan.....	51
2.2.2.5. Labelling M13 bacteriophage with black hole quencher-10	51
2.2.2.6. Labelling M13 bacteriophage with eosin-5-maleimide	51
2.2.2.7. Measurement of labelling efficiency	52
2.2.2.8. LD measurements of chromophore labelled M13.....	53
2.2.2.9. Fluorescence measurements	54
2.2.3. Conjugation of wt M13 with purified goat-anti-mouse.....	54
2.2.3.1. Thiolation of wt M13 bacteriophage (method 1)	55

2.2.3.2. Maleimide derivatisation of affinity purified goat anti-mouse antibody	55
2.2.3.3. Bioconjugation	56
2.2.4. Electron microscopy.....	57
2.2.4.1. Sample preparation	57
2.2.4.2. Preparation of carbon-coated grids for electron microscopy	57
2.2.4.2.1. Glow discharge of the carbon-coated copper grids.....	57
2.2.4.2.2. Staining and visualisation.....	58
2.2.5. Conjugation of wt M13 with goat anti- <i>E. coli</i> O157 and BHQ-10	58
2.2.5.1. Thiolation of wt M13 bacteriophage (method 2)	59
2.2.5.2. Maleimide derivatisation of goat anti- <i>E. coli</i> O157	59
2.2.5.3. Bioconjugation and labelling with BHQ-10	60
2.2.6. Detection of <i>E. coli</i> O157 using M13 bacteriophage and LD	61
2.2.6.1. <i>E. coli</i> O157 preparation	61
2.2.6.2. <i>E. coli</i> XL10 preparation	61
2.2.6.3. Sample preparation	62
2.2.6.4. LD measurements	62
2.2.7. Conjugation of wt M13 with anti-FITC antibody.....	63
2.2.7.1. Thiolation of wt M13 bacteriophage (method 2)	63
2.2.7.2. Maleimide derivatisation of anti-FITC antibody	64
2.2.7.3. Bioconjugation	64
2.2.8. Detection of fluorescein using the M13 bacteriophage aggregation assay	65
2.2.8.1. Fluorescein preparation.....	65
2.2.8.2. Rhodamine 6G preparation	66
2.2.8.3. Sample preparation	66
2.2.8.4. LD measurements	67
3 CHAPTER 3 - OPTIMISATION OF M13 PRODUCTION	68
3.1. Production of M13 bacteriophage.....	68

3.1.1. Production of M13 bacteriophage using the method based on Sambrook and Russell (2001)	71
3.1.2. Production of M13 bacteriophage using the New England Biolabs method (2011)	73
3.1.3. New method of M13 bacteriophage production	73
3.1.4. Optimisation of precipitation time in M13 production	78
3.1.5. Conclusion	82
4 CHAPTER 4 - FLUORESCENT LABELLING OF M13 FOR USE IN ASSAYS	85
4.1. Labelling M13 bacteriophage with fluorescamine	90
4.2. Labelling M13 bacteriophage with rhodamine B isothiocyanate	93
4.3. Labelling M13 bacteriophage with 4-chloro-7-nitrobenzofurazan	96
4.4. Labelling M13 bacteriophage with black hole quencher-10	99
4.5. Summary	103
4.6. Conclusion	110
5 CHAPTER 5 - DEVELOPMENT OF A HIGH SENSITIVITY ASSAY USING M13 BACTERIOPHAGE AND LINEAR DICHROISM	113
5.1. Conjugation methods	116
5.2. Labelling M13 bacteriophage with eosin-5-maleimide	120
5.3. M13 bacteriophage conjugated with GAM	124
5.4. Production of double labelled M13 reagent	128
5.5. Detection of <i>E. coli</i> O157 using double labelled M13 and LD	131
5.6. Conclusion	136
6 CHAPTER 6 - DETECTION OF SMALL MOLECULES USING M13 BACTERIOPHAGE AND LINEAR DICHROISM	138
6.1. Why small molecule detection?	139
6.2. Detection methods for toxins, illicit drugs and explosives	141
6.3. Small molecule detection	144
6.4. M13 bacteriophage aggregation assay	150

6.4.1. Production of M13 labelled with FITC and M13 labelled with anti- FITC	150
6.4.2. Detection of fluorescein using LD and anti-FITC and FITC labelled M13	154
6.5. Conclusion.....	160
7 CHAPTER 7 - CONCLUSIONS AND FURTHER WORK	162

List of Figures

Figure 1.1 - Agglutination assay process.....	4
Figure 1.2 - Sandwich ELISA process	7
Figure 1.3 - Indirect ELISA process	8
Figure 1.4 - Lateral flow process	10
Figure 1.5 - Human serum albumin signal using a semi-quantitative lateral flow system	12
Figure 1.6 - EMIT process.....	13
Figure 1.7 - FPIA mechanism.....	15
Figure 1.8 - FPIA process	15
Figure 1.9 - Simple Jabłoński diagram.....	20
Figure 1.10 - LD schematic diagram (parallel)	23
Figure 1.11 - LD schematic diagram (perpendicular)	23
Figure 1.12 - The effect of molecular alignment on LD	24
Figure 1.13 - LD instrument	26
Figure 1.14 - Quartz Couette and sample chamber.....	26
Figure 1.15 - Capillary and rod used to produce shear flow in LD.....	27
Figure 1.16 - Flow LD spectra of PCR amplimers	29
Figure 1.17 - Difference in absorbance of perpendicular and parallel light by bacteriophage ..	31
Figure 1.18 - Structure of M13 bacteriophage	32
Figure 1.19 - Schematic diagram of M13 bacteriophage.....	33
Figure 1.20 - M13 bacteriophage lifecycle.....	35
Figure 1.21 - Principle behind an existing M13/LD based assay.....	40
Figure 1.22 - <i>E. coli</i> O157 detection using an existing M13/LD based assay	41
Figure 2.1 - Components of the LD instrument	47
Figure 2.2 - LD spectra of various dilutions of M13 bacteriophage.....	49
Figure 2.3 - LD signal at 280 nm for various dilutions of M13 bacteriophage.....	49
Figure 3.1 - Comparison of two existing M13 production methods.....	71
Figure 3.2 - New M13 production method	74
Figure 3.3 - Comparison of M13 production yields and specific activities	76
Figure 3.4 - LD spectrum of M13 bacteriophage generated from the new method	78
Figure 3.5 - The effect of precipitation time on M13 production yield and specific activity	80
Figure 4.1 - M13 production, labelling and LD measurement process.....	86

Figure 4.2 - Schematic illustrating the principle behind an M13/LD assay capable of multiplexing	87
Figure 4.3 - Images illustrating the location of the p8 coat proteins within M13	89
Figure 4.4 - Labelling M13 with fluorescamine.....	90
Figure 4.5 - UV/Vis absorbance spectra, LD spectra and fluorescence spectra of fluorescamine and M13 labelled with fluorescamine.....	92
Figure 4.6 - Labelling M13 with rhodamine	94
Figure 4.7 - UV/Vis absorbance spectra, LD spectra and fluorescence spectra of rhodamine and M13 labelled with rhodamine	95
Figure 4.8 - Labelling M13 with NBD chloride	97
Figure 4.9 - UV/Vis absorbance spectra, LD spectra and fluorescence spectra of NBD chloride and M13 labelled with NBD chloride.....	98
Figure 4.10 - Labelling M13 with BHQ-10	100
Figure 4.11 - UV/Vis absorbance spectra and LD spectra of BHQ-10 and M13 labelled with BHQ-10.....	101
Figure 4.12 - Schematic diagram illustrating M13 labelled with NBD chloride and M13 labelled with BHQ-10	110
Figure 5.1 - A schematic diagram of the M13 reagent used by Pacheco-Gomez <i>et al.</i> (2012)	114
Figure 5.2 - A schematic diagram illustrating the principle behind the pathogen detection assay used by Pacheco-Gomez <i>et al.</i> (2012).	114
Figure 5.3 - A schematic diagram of the M13 reagent proposed for a detection assay.....	115
Figure 5.4 - A schematic diagram illustrating the development of the M13/LD based assay ..	116
Figure 5.5 - Chemistry used to conjugate M13 to an antibody.	119
Figure 5.6 - Labelling M13 with eosin-5-maleimide	121
Figure 5.7 - UV/Vis absorbance spectra, LD spectra and fluorescence spectra of eosin-5-maleimide and M13 labelled with eosin-5-maleimide.....	122
Figure 5.8 - Image showing the change in colour during the labelling process.....	123
Figure 5.9 - The UV/Vis and LD spectra of the process of bioconjugating M13 with GAM	126
Figure 5.10 - Transmission electron microscopy images of M13 conjugated with GAM	127
Figure 5.11 - Covalently linking thiol labelled M13 with maleimide labelled BHQ-10	129
Figure 5.12 - UV/Vis spectrum and LD spectrum of double labelled M13	130
Figure 5.13 - Detection of <i>E. coli</i> O157 using double labelled M13 and LD.....	134
Figure 6.1 - Diagram illustrating the idea of creating a multimodal detection system	139

Figure 6.2 - Schematic diagram of how a radioimmunoassay works	142
Figure 6.3 - Schematic diagram illustrating how fluoroimmunoassays work.....	143
Figure 6.4 - Schematic diagram illustrating how microspheres, M13 and LD may be used to detect small molecules	146
Figure 6.5 - LD spectra produced from the microsphere aggregation assay.....	148
Figure 6.6 - Schematic diagram illustrating how LD and M13 bacteriophage are able to detect small molecules	149
Figure 6.7 - Labelling M13 with FITC.....	150
Figure 6.8 - Absorbance spectra of M13 conjugated with anti-FITC when it is subjected to size exclusion chromatography	151
Figure 6.9 - UV/Vis spectra of M13 conjugated with anti-FITC and M13 conjugated with FITC	152
Figure 6.10 - LD spectra of M13 conjugated with anti-FITC and M13 conjugated with FITC ...	152
Figure 6.11 - LD spectra illustrating how M13 conjugated with FITC and M13 conjugated with anti-FITC can disrupt the LD signal	155
Figure 6.12 - LD spectra illustrating how the presence of fluorescein can re-establish the LD signal.....	156
Figure 6.13 - Sensitivity of the small molecule detection assay	157
Figure 6.14 - Schematic diagram illustrating the principle of this small molecule detection assay	159
Figure 6.15 - LD spectra illustrating the specificity of this small molecule detection assay.....	160

List of Tables

Table 1.1 - Brief comparative table providing examples of bio-detection methods.....	18
Table 2.1 - UV/Vis-Spectrophotometer (Jasco V550 UV/Vis spectrophotometer) parameters .	46
Table 2.2 - Jasco (Japan) J-715 spectropolarimeter parameters used to gather LD spectra.....	48
Table 2.3 - UV/Vis-Spectrophotometer (Jasco V550 UV/Vis spectrophotometer) parameters .	53
Table 2.4 - Jasco (Japan) J-715 spectropolarimeter parameters used to record LD spectra.....	54
Table 2.5 - Fluorescence parameters.....	54
Table 2.6 - Assay constituents for the detection of <i>E. coli</i> O157	62
Table 2.7 - Jasco (Japan) J-715 spectropolarimeter parameters used to gather LD spectra.....	63
Table 2.8 - Assay constituents for the detection of fluorescein	67
Table 2.9 - Jasco (Japan) J-715 spectropolarimeter parameters used to gather LD spectra.....	67
Table 3.1 - M13 yield based on UV absorbance	72
Table 3.2 - M13 yield based on LD absorbance	72
Table 3.3 - Comparison of M13 production methods.....	75
Table 3.4 - Comparison of M13 yields and specific activities	79
Table 4.1 - The dyes proposed to label M13 bacteriophage.	89
Table 4.2 - Percentage labelling and dye LD to M13 LD ratios	103
Table 4.3 - Factors affecting the LD signal of chromophore labelled M13.....	107
Table 6.1 - Table displaying the percentage labelling of M13 conjugated with FITC and the FITC to M13 LD ratio.....	153
Table 6.2 - Comparing the structures of rhodamine 6G and FITC.	158

List of Equations

Equation 1.1 - Beer-Lambert Law	21
Equation 2.1 - Rearranged Beer-Lambert law	47
Equation 2.2 - Labelling efficiency of M13.....	53
Equation 3.1 - Specific activity definition	72

Abbreviations

AEM	N-(2-Aminoethyl) maleimide
BHQ-10	Black hole quencher-10
CCD	Charge-coupled device
CFU	Colony forming unit
DMSO	Dimethyl sulfoxide
DNA	Deoxyribonucleic acid
EDTA	Ethylene diamine tetra acetic acid
ELISA	Enzyme-linked immunosorbent assay
EM	Electron Microscope
EMIT	Enzyme multiplied immunoassay technique
FITC	Fluorescein isothiocyanate isomer 1
FPIA	Fluorescence polarisation immunoassay
FtsZ	Filamenting temperature-sensitive mutant Z
GAE	Goat anti- <i>E. coli</i> O157 antibody
GAM	Goat anti-mouse antibody
GC-MS	Gas chromatography-mass spectrometry
GTP	Guanosine-5'-triphosphate
HRP	Horseradish peroxidase
IgG	Immunoglobulin G
IMS	Ion mobility spectrometry
LB	Luria broth
LD	Linear dichroism

M13	M13 bacteriophage
MWCO	Molecular weight cut off
NaCl	Sodium chloride
NBD chloride	4-Chloro-7-nitrobenzofurazan
NEM	<i>N</i> -Ethylmaleimide
OD	Optical density
PCR	Polymerase chain reaction
PEG	Polyethylene glycol
RIA	Radioimmunoassay
Rhodamine	Rhodamine B isothiocyanate
SATA	N-Succinimidyl-S-acetyl thioacetate
SEC	Size exclusion chromatography
SMCC	Succinimidyl-4-(N-maleimidomethyl)cyclohexane-1-carboxylate
STEC	Shiga-toxin-producing <i>Escherichia coli</i>
TEM	Transmission electron microscopy
TSS	Toxic shock syndrome
TSST-1	Toxic shock syndrome toxin-1
UA	Uranyl acetate
UV	Ultra Violet
Vis	Visible
Wt	Wild-type

CHAPTER 1 - INTRODUCTION

It is the aim of this project to investigate whether linear dichroism spectroscopy (LD) can be used in combination with a bio-nanoparticle based on M13 bacteriophage (M13) to produce a novel bio-detection system. This introduction aims to provide an overview of the two key elements of this project, bio-molecular detection and linear dichroic spectroscopy.

1.1. Bio-detection

Bio-detection can be defined as the application of methods that allow the presence of a specific biological agent to be identified and quantified. As such bio-detection has an important place in many commercial sectors including healthcare, environmental monitoring, defence and agriculture. In this project a bio-detection system will be developed that has wide ranging applications but initially is focused on detecting targets that are important in human disease and health. In these applications effective bio-detection is extremely important as it can be used to determine the source, diagnosis, and treatment of infections. To underline the importance of bio-detection, a number of reports including the Pennington report (Pennington, 2009), and articles written by Rice (Rice, 2011) and Kuehn (Kuehn, 2013) have highlighted a lack of effective bio-detection methods, emphasising the need for new and improved methods.

One of the major aims of this project is to explore whether LD can be used to provide such a new bio-detection platform that is able to detect a wide range of biomolecules. There are already a number of methods that can be used to detect material of a biological origin. The majority of these rely on detecting proteins, toxins and DNA from an organism or antibodies produced by the host in response to the organism. In this section a number of the methods

used in microbial bio-detection will be summarised. This is not an exhaustive survey but provides a broad view of what is currently used in commercial laboratories. The methods discussed range from traditional microbial cultures to antibody based methods, including both homogeneous and heterogeneous assays.

1.1.1. Major methods

1.1.1.1. Microbial culture for detection of pathogens

Microbial culturing is a common diagnostic technique used within pathology laboratories. Microbial cultures rely on the development of either a visually observable colony with a characteristic morphology on a plate or a turbid liquid culture. Cultures can be obtained from a range of sources including urine, sputum, stool, skin and soft tissue, as well as blood (Abubakar *et al.*, 2007).

Blood cultures are used as the principle method for detecting bacteremia and fungemia (Reimer *et al.*, 1997) with blood samples being incubated in anaerobic and aerobic bottles which contain media to support the growth of bacteria or fungi. A large volume of blood is required from the patient for a blood culture (approximately 20 mL for an adult)(Reimer *et al.*, 1997). The blood culture bottles are then placed into incubators for 5-7 days with most pathogens usually growing within 2 days. The bottles are monitored for microbial growth by measuring the carbon dioxide production and resulting pH change in the bottle. If the sample is flagged as being positive by the system then an inoculum is taken for Gram staining and another inoculum is taken for growth on media plates for susceptibility testing (the media plates used depend on the result of Gram staining) (Reimer *et al.*, 1997).

A urine culture is carried out by simply inoculating plates containing specific growth media with the urine sample and incubating. Colony forming units are counted and calculated per mL (Lipsky *et al.*, 1987).

Skin and soft tissue cultures can be used for wounds, abscesses and burns, and require swabs to be taken from the infected area. The swabs are stored in a collection tube and the specimens are inoculated onto growth media plates and allowed to incubate (Stevens *et al.*, 2005). Sputum and stool cultures are done in a similar way.

Although these methods have been established for more than 50 years there are limitations with using culturing as a diagnostic technique, arguably the major one being its time consuming nature. This is inherent in the methods as it is a requirement that the bacteria have to multiply to a level that they become visible to the naked eye as a colony or turbid solution. For example, methicillin resistant *Staphylococcus aureus* (MRSA) can take more than 24 hours to form visible colonies (Zitterkopf, 2008). Patients who are extremely ill need treatment immediately, and to wait for a culture could be unacceptable.

1.1.1.2. Antibody based methods (homogeneous and heterogeneous)

Antibody based methods, also called immunoassays are also commonly used as a clinical diagnostic tool (Ekins, 1998). An immunoassay is a test which uses the ability of an antibody to form a specific complex with an antigen associated with the pathogen. This complex is detected using one of a range of methods. The key to such an assay is the specificity of the antibody for the target antigen. The majority of immunoassays can be classified into one of two classes, homogeneous and heterogeneous methods. The classification is based on whether or not the immunoassay method requires physical separation of bound antibody-antigen complex from unbound material. If it does then this is defined as a heterogeneous assay, whereas if no separation step is required it is defined as a homogeneous assay. In general the lack of a separation step makes homogeneous assays easier and faster to perform, however homogenous methods are more difficult to develop (Thomas *et al.*, 2003). In the following sections the most common immunoassay formats will be discussed.

1.1.1.2.1. Agglutination assays

Agglutination is the clumping of particles to form aggregates, a phenomenon that forms the basis of this type of assay. These tests use carrier particles (also known as conjugated detection particles) e.g. latex particles, gelatin beads or colloidal particles derivatised with a pathogen specific antibody. When the specific target analyte is present an aggregate forms which can be easily visualised (figure 1.1). If the target analyte is not in the specimen then no agglutination occurs (Gella *et al.*, 1991). For example a detection system for MRSA uses monoclonal antibodies directed towards the PBP2a antigen present on MRSA (Nakatomi and Sugiyama, 1998). The presence of the pathogen was signalled by the formation of an aggregate.

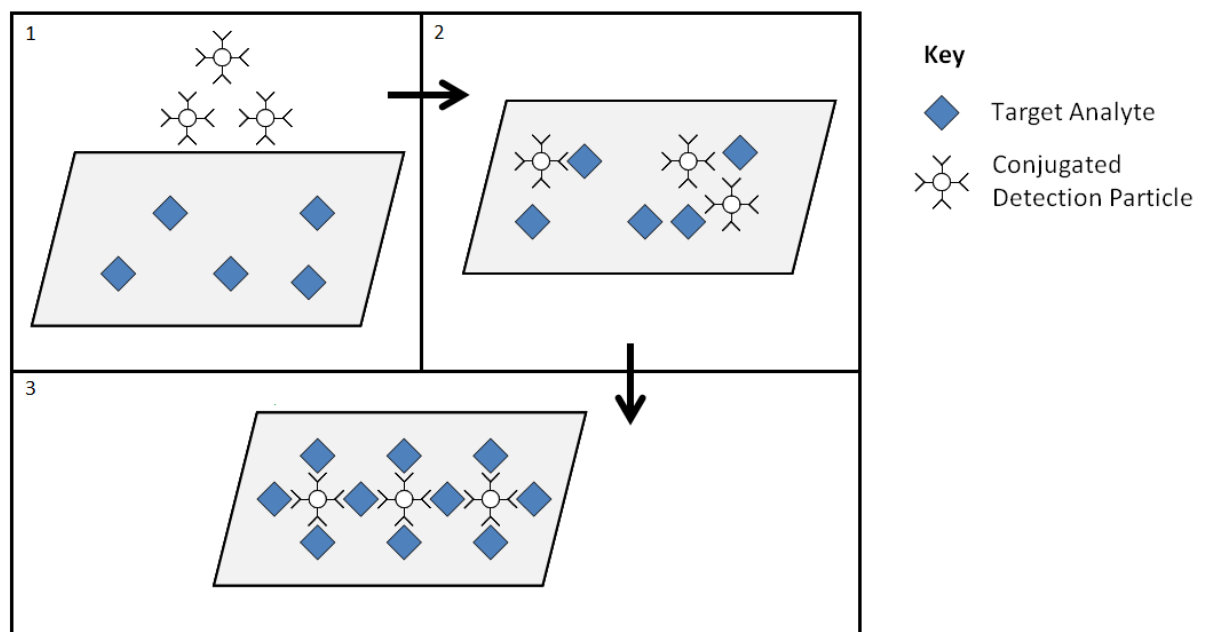


Figure 1.1 - Agglutination assay process

A schematic diagram illustrating the process of an agglutination assay. 1) A sample containing target analyte is placed onto a card followed by conjugated detection particles specific to the target analyte. 2) When agitated the target analyte molecules and conjugated detection particles begin to interact. 3) Aggregates form which result in colour changes and texture changes. If no target analyte is present in the sample then no changes are observed.

This method is elegant in its simplicity, with the method being inexpensive and rapid (Myrick and Ellner, 1982). Woods and Iwen (1991) also found that latex agglutination required fewer

reagents in comparison to dot immunobinding assays and cytotoxin assays for the diagnosis of *Clostridium difficile*-associated diarrhoea.

However, relatively high analyte concentrations (when compared to the culture method) are needed for latex agglutination, and the results are only qualitative/semiquantitative (Warsinke, 2009). The results could be improved using a spectrophotometer for readout purposes (Arsie *et al.*, 2000), but this would require an additional device. The method is also difficult to multiplex, requiring separate tests for each target.

1.1.1.2.2. Enzyme-linked immunosorbent assay

Enzyme-linked immunosorbent assay (ELISA) is the most prevalently utilised immunoassay (Smith *et al.*, 2008b) and combines the specificity of an antibody with the sensitivity of an enzyme assay. ELISAs can vary in format but always involve the formation of an antigen-antibody complex, with one of the reactants immobilised onto the surface of a plate. The addition of the specific target analyte allows for the formation of the antigen-antibody complex, and this is visualised using enzyme conjugated reagents (usually in the form of an enzyme linked secondary antibody) (Paulie *et al.*, 2005). A substrate is chosen which when added to the enzyme linked secondary antibody, changes colour. This change in colour is proportional to the amount of immobilised enzyme and hence the amount of target analyte present in the sample (Porstmann and Kiessig, 1992). Comparing the results with standard samples of known concentration can provide quantitation. ELISAs have been used to detect substances such as peptides, proteins, antibodies and hormones and as a result have commonly been used as a diagnostic tool to detect a wide array of organisms. For example this assay is used frequently to detect *Helicobacter pylori* infections (Logan and Walker, 2001), and human immunodeficiency virus (HIV) infections (von Sydow *et al.*, 1988). There are a wide

range of ELISA based methods, of which two of the most common are sandwich assays and indirect assay.

1.1.1.2.2.1. Sandwich assay

Sandwich assays work by detecting the antigen of a particular target molecule. Sandwich assays involve coating the surface of the plate with a capture antibody. The sample is then added and any antigen present will bind to the surface of the plate. Unbound antigen is removed by washing the plate. This is followed by the addition of a primary antibody which acts as a detection antibody, binding specifically to the antigen. Any unbound primary antibody is removed by washing the plate again. An enzyme linked secondary antibody is then added and binds to the primary antibody. A substrate is added, and is converted by the enzyme into a colour or fluorescent or electrochemical signal which is measured to determine the presence and quantity of antigen (figure 1.2). So the more antigens present, the greater the signal (Prescott *et al.*, 2005).

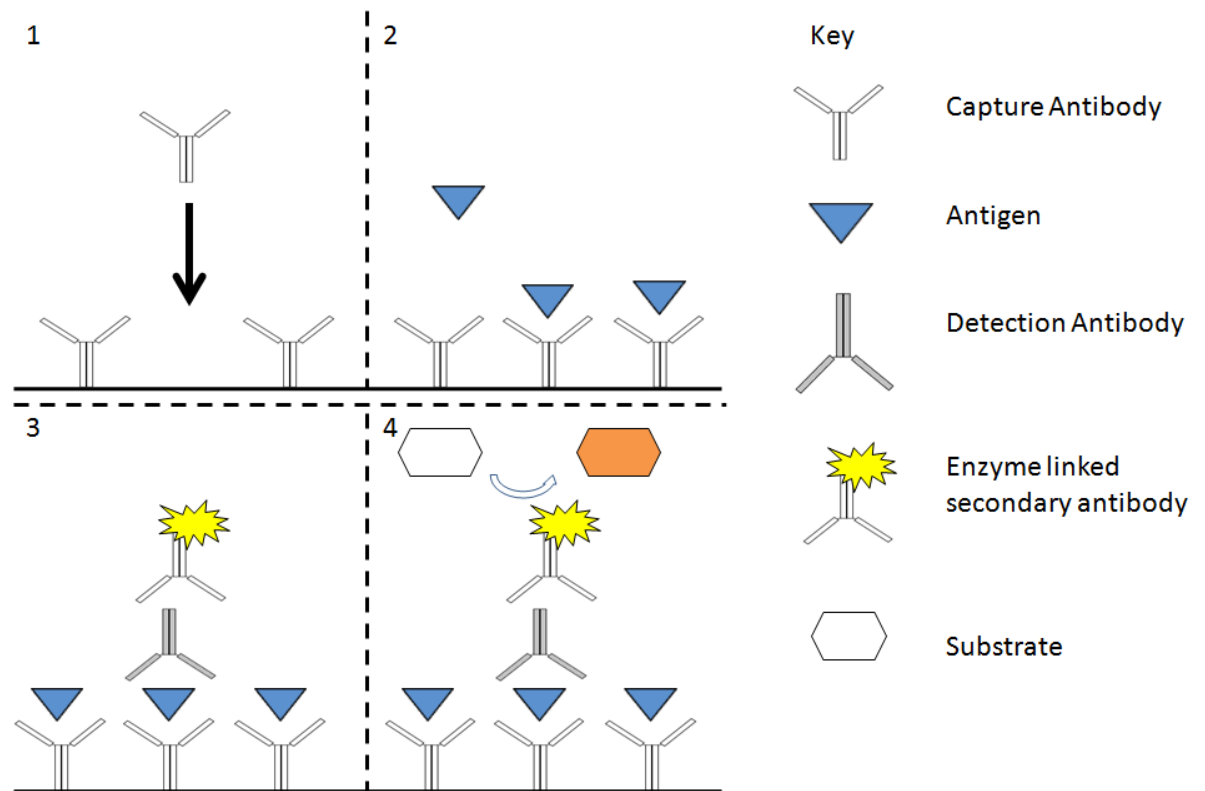


Figure 1.2 - Sandwich ELISA process

A schematic diagram illustrating how a sandwich ELISA works. 1) Within the well of a microtitre plate, capture antibodies coat the well. 2) The antigens in the sample bind to the capture antibodies. 3) The antigens are consequently detected by a detection antibody, and an enzyme linked secondary antibody is then added. 4) A substrate molecule is used to produce a signal to indicate the presence of the antigen.

1.1.1.2.2.2. Indirect assays

Often assays are developed to detect antibodies produced by the host immune system in response to infection. Using ELISAs to detect antibodies is known as an indirect immunosorbent assay and is commonly used to detect HIV (Gurtler, 1996). In this case the plate is coated with inactivated HIV antigens. The patient's sample is then added and any antibodies specific to HIV (indicative of a HIV infection) will also become immobilised on to the plate. The plate is washed to remove any unbound antibodies. The secondary enzyme linked antibody is then added and binds to the human antibodies. Any unbound secondary antibodies are again removed by washing. A substrate is finally added which changes colour in the

presence of the enzyme (figure 1.3). So the more antibodies present in the sample, the larger the change in colour, which is measured by a change in absorbance (Prescott *et al.*, 2005).

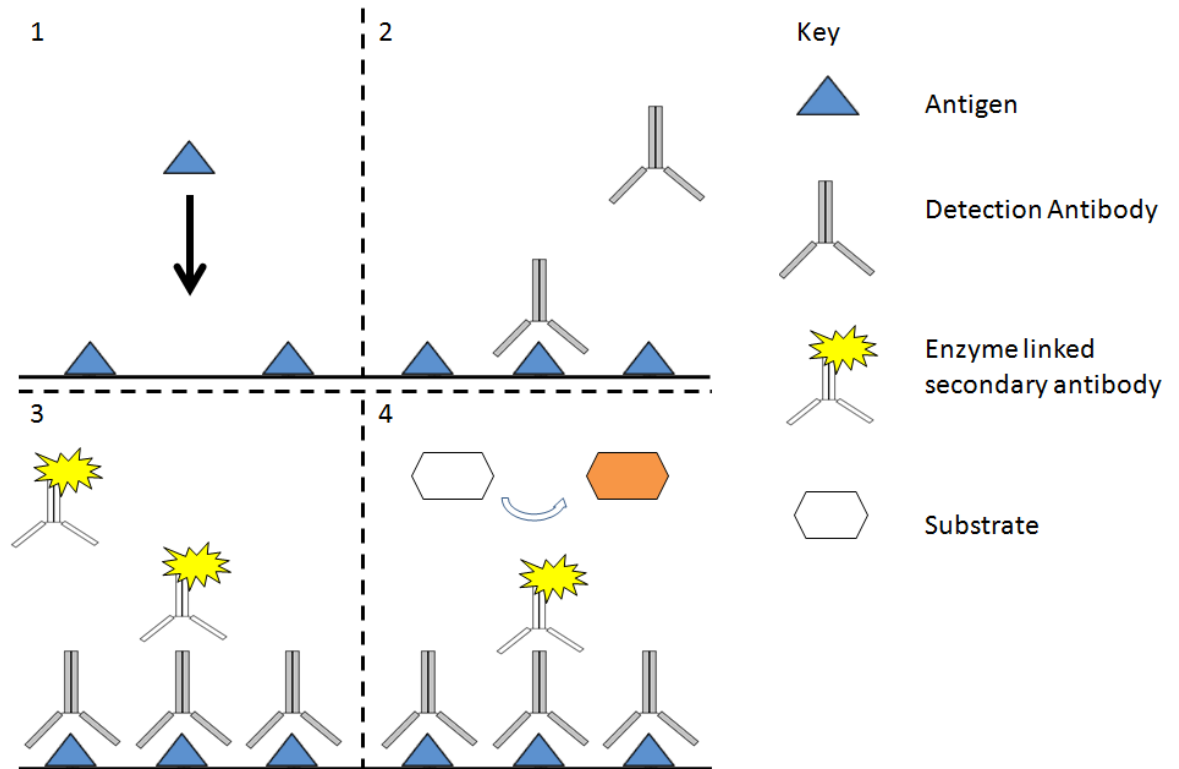


Figure 1.3 - Indirect ELISA process

A schematic diagram illustrating how an indirect ELISA works. 1) The well of a microtitre plate is coated with antigens. 2) A sample containing detection antibodies bind to the antigens. 3) The detection antibodies are consequently detected by an enzyme linked secondary antibody. 4) A substrate molecule is used to produce a signal to indicate the presence of the detection antibody.

Such tests are simple to perform, sensitive and inexpensive (Peruski and Peruski Jr, 2003). However one drawback of the indirect ELISA assay is that host antibodies (for example antibodies for HIV) only become detectable 6-8 weeks after the onset of infection (Gurtler, 1996). So an assay intended to detect these antibodies may initially give a negative signal, when indeed the patient may be infected. Moreover the antibodies can remain in the bloodstream long after an infectious disease has been resolved. False positives can also occur due to cross reactions with the antibodies.

ELISAs tend to be quite rapid in comparison to culture methods i.e. ELISAs take hours compared to days (Bacarese Hamilton *et al.*, 2004). However ELISAs also are not easily multiplexed, in general one assay can only detect one analyte at a time. However ELISAs can easily achieve high-throughput processing parallelized by using a microtitre plate to carry out multiple reactions but these have to be laboratory based.

1.1.1.2.3. Lateral flow methods

Lateral flow tests are a more recent development and represent one of the simplest diagnostic test formats currently on the market. These tests are generally still based on an antibody for primary detection but use chromatographic separation as a key part of the assay method. The detection conjugate (particle conjugated with detector molecules able to detect the target analyte) is initially static in nitrocellulose at one end of the sample pad and is solubilised with the addition of the sample. If the target analyte is present in the sample it binds to the detection conjugate molecules. This target analyte/detection conjugate complex then moves down the sample pad under capillary action, until it approaches the test line. At which point the target analytes bind the complex to the analyte capture molecules, forming a visible line and indicating a positive test result. A second capture line can be used to act as an assay control (figure 1.4). This second capture antibody will capture the detection conjugate, whether the detection conjugate is attached to the target analyte or not. If the control line is not visible then the test is invalid and needs to be repeated (Buhrer-Sekula *et al.*, 2003).

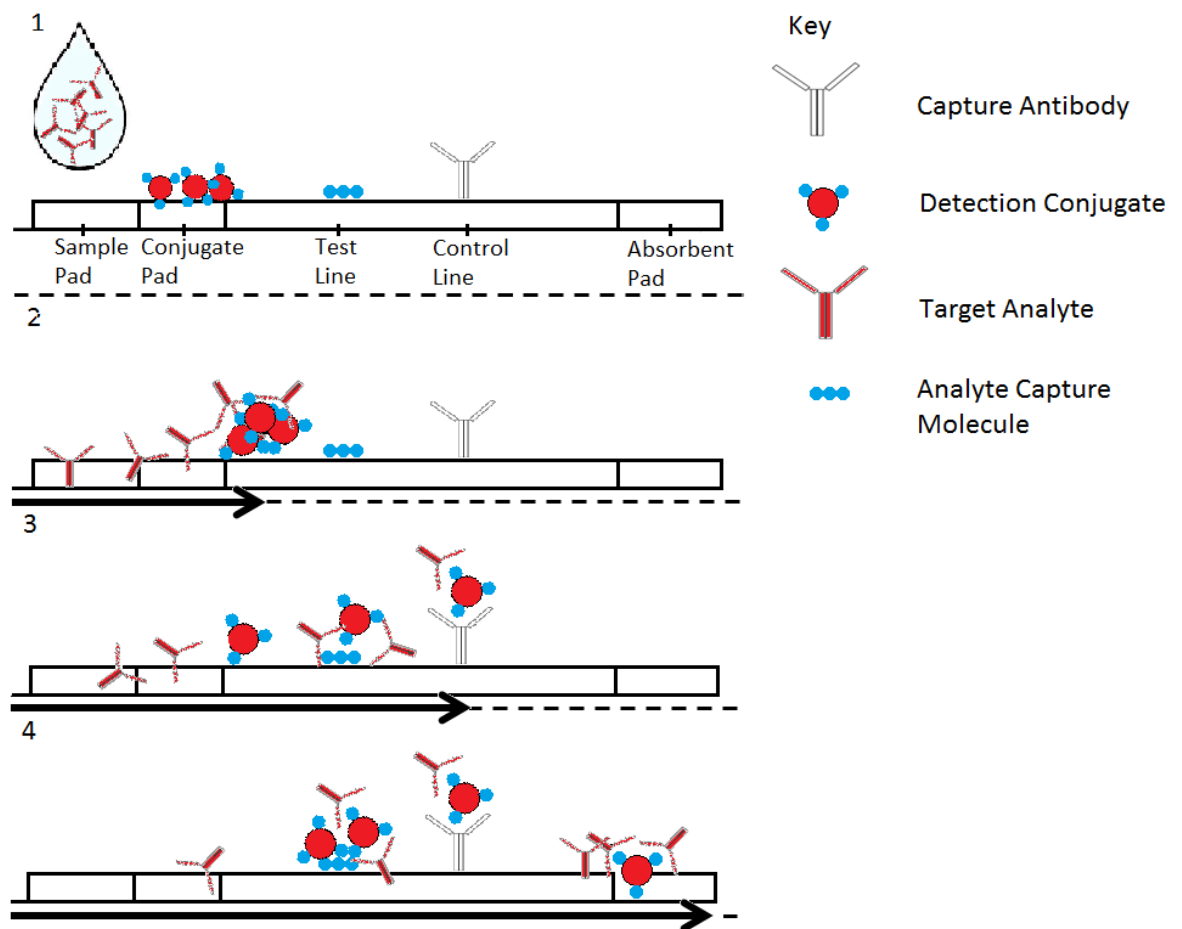


Figure 1.4 - Lateral flow process

A schematic diagram illustrating how lateral flow works. 1) A sample is added to the pad. 2) The specific antibodies within the sample form a complex with the detection conjugate. 3) The complex moves down to the test line where the complex binds to the capture molecule and causes a line to appear. 4) This complex then binds to the capture molecule on the control line forming a line which ensures the test is valid.

These tests are very simple and quick, usually taking approximately 15 minutes. However a major disadvantage of this assay is that it can only detect one agent per assay strip. So if for example, a sample is obtained with an unknown agent in it, several strips would have to be used to identify it. Additionally, the assay readout is determined by a red line created by the sample/detector conjugate binding to the capture molecule. Whether or not this red line is visible to the human eye can be the limit to the sensitivity of this assay. Sensitivity quantification is achieved using a fairly arbitrary scale, typically by assigning a number between 0 and 5, (highest intensity of the line being 5). As the scale is arbitrary the

quantification is obviously limited by the skill of the individual processing the assays (Peruski and Peruski Jr, 2003). However Cho and Paek (2001) devised a lateral flow system that exploited the use of multiple test lines allowing the user to quantify the relative concentration of the target analyte in a less subjective manner (figure 1.5). There have been recent advances with lateral flow, including the use of a silver enhancement step in the conventional gold labelled lateral flow assays. This extra step has been found to increase the sensitivity by up to one order of magnitude and in doing so, allowing the detection of lower levels of antigen (Horton *et al.*, 1991).

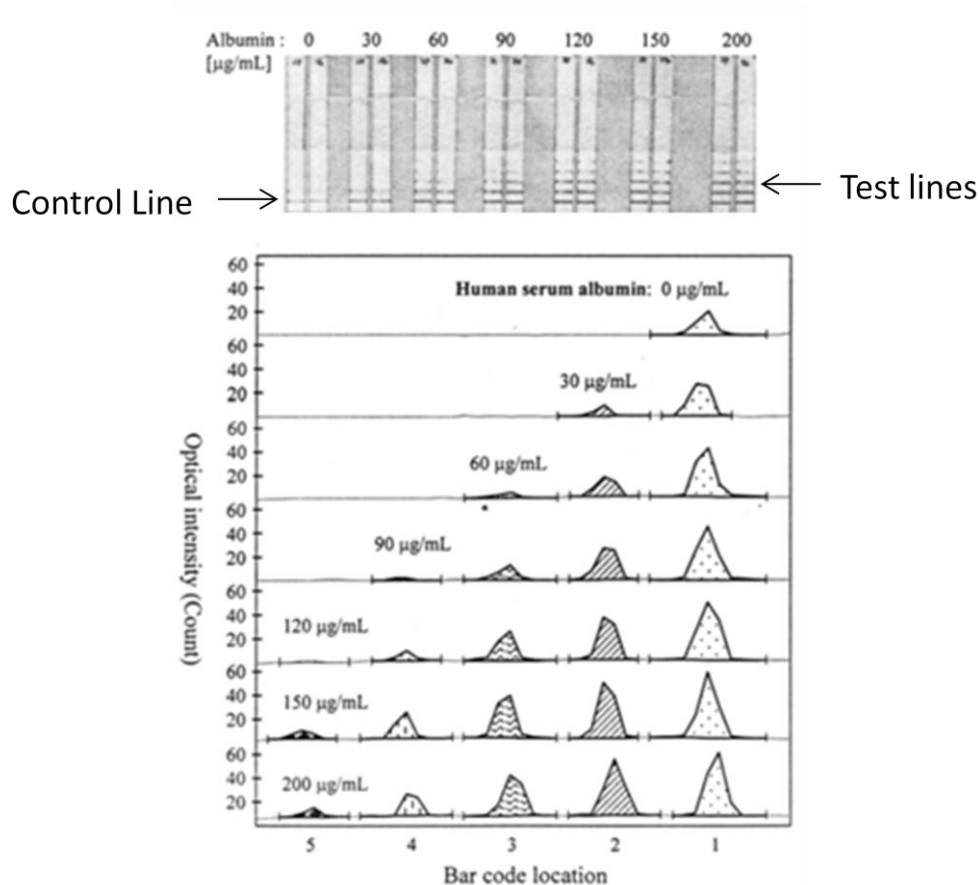


Figure 1.5 - Human serum albumin signal using a semi-quantitative lateral flow system

Patterns of signal generation when detecting increasing concentrations of human serum albumin using a semi-quantitative lateral flow system. Each strip was duplicated (top panel). Optical intensities of the coloured bars were used to demonstrate changes in signal as albumin concentration increased (bottom panel). At the detection limit of 30 µg/mL a single line is visible (in addition to the control line which appears throughout). Additional lines become visible with increasing albumin concentration and these are distributed evenly in multiples of the detection limit. Reproduced from Cho and Paek (2001).

1.1.1.2.4. Homogenous methods

The immuno-methods discussed so far have been heterogeneous assays which all require some form of separation of antibody-antigen complex from the milieu. These separations can be difficult to optimise which has meant that significant efforts have been put into developing separation-free (homogenous) assay methods. There are a wide range of homogeneous methods, the most common being enzyme multiplied immunoassay technique (EMIT) and fluorescence polarisation immunoassay (FPIA).

1.1.1.2.4.1. Enzyme multiplied immunoassay technique

EMIT is generally used to detect small molecular weight haptens including antibiotics and opiates. An EMIT assay consists of an enzyme bound to a hapten, it is bound in such a way that it does not affect the enzyme active site. An antibody specific to the hapten is added and this binds to the enzyme/hapten complex, blocking the enzyme active site.

In the absence of any free haptens the enzyme active site remains blocked and the substrate is not broken down. In the presence of free haptens the bound haptens are displaced from the antibody allowing the enzyme to catalyse the degradation of the substrate. By measuring the quantity of the substrate products (which are generally chosen to be coloured) one can infer the hapten quantity within the sample (Oellerich, 1980) (figure 1.6).

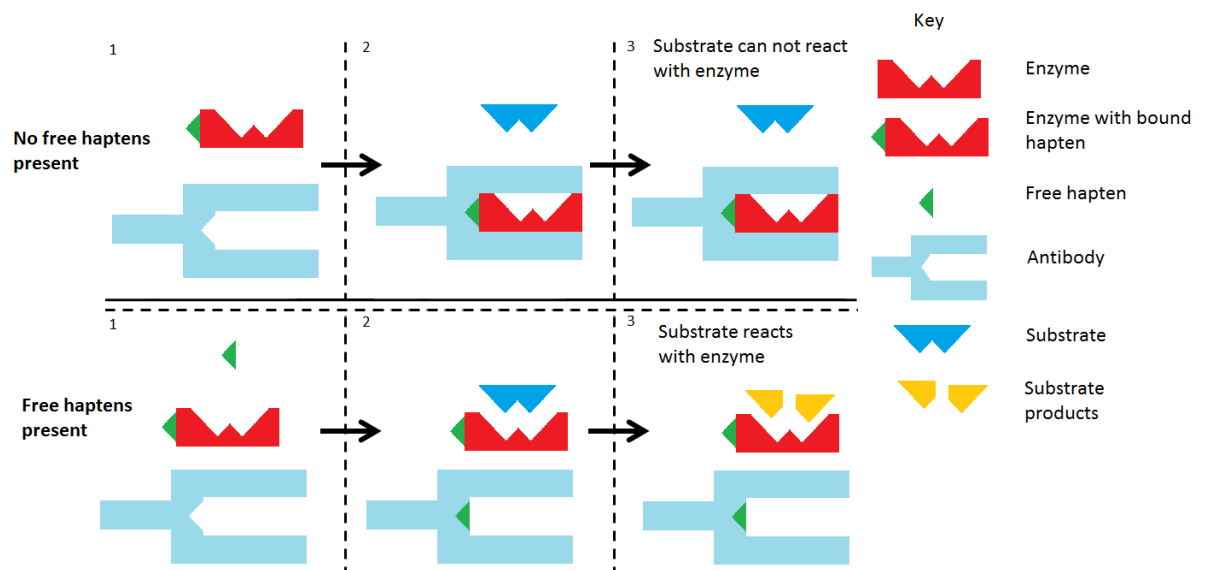


Figure 1.6 - EMIT process

A schematic diagram illustrating how EMIT works. When no free haptens are present in a sample, 1) the enzyme with bound hapten is able to bind to the antibody. 2) This prevents the substrate from reacting with the enzyme bound with hapten as it cannot reach the active site. 3) This consequently results in no degradation of substrate and no signal change. However if there are free haptens present in a sample, 1) they bind to the antibody. 2) This allows for the substrate to react with the enzyme bound with hapten. 3) This consequently results in the degradation of the substrate and a signal change.

Drug testing is a popular use for EMIT due to its rapid response time, high sensitivity and the simplicity of the assay (Scharpe *et al.*, 1976, Ullman, 1999). The EMIT assay is homogenous and as such does not require any wash steps, this is an important advantage over ELISA assays.

The assay time for a commercial EMIT system is less than 1 minute (Schneider *et al.*, 1973) which is quicker than any of the assays mentioned previously, it is also highly sensitive with a detection limit of <1 nM (Rosenthal *et al.*, 1976). However EMIT is only used for small molecules (<1000 Da), although new advances have been made to produce an EMIT assay that can detect an influenza hemagglutinin A peptide (Chiu *et al.*, 2011) in 13 minutes. This research shows that it may be possible to detect larger molecules. EMIT, like many of the other tests detailed in this review, is not multiplexed.

1.1.1.2.4.2. Fluorescence polarisation immunoassay

The fluorescence polarisation immunoassay (FPIA) was established by Dandiker *et al.* (1973), and was further developed by Abbot Diagnostics in the 1980s for commercial applications. This method utilises a fluorescent labelled antigen, which competes with an unlabelled antigen for a specific antibody. A fluorescent label is used and is excited with plane polarised light leading to the emission of a varying degree of plane polarised light. The degree of polarisation of the emitted light is determined by the tumbling time of the fluorophore e.g. a fast rotating fluorophore leads to less polarisation. In an assay, if an antibody binds to a small fluorescent antigen the antigen rotates slower, leading to an increase in polarisation. Antigen in an unknown sample competes with the known fluorophore for the antibody leading to fluorophore release and a measurable change in polarisation (Diamandis and Christopoulos, 1996) (figure 1.7 and 1.8).

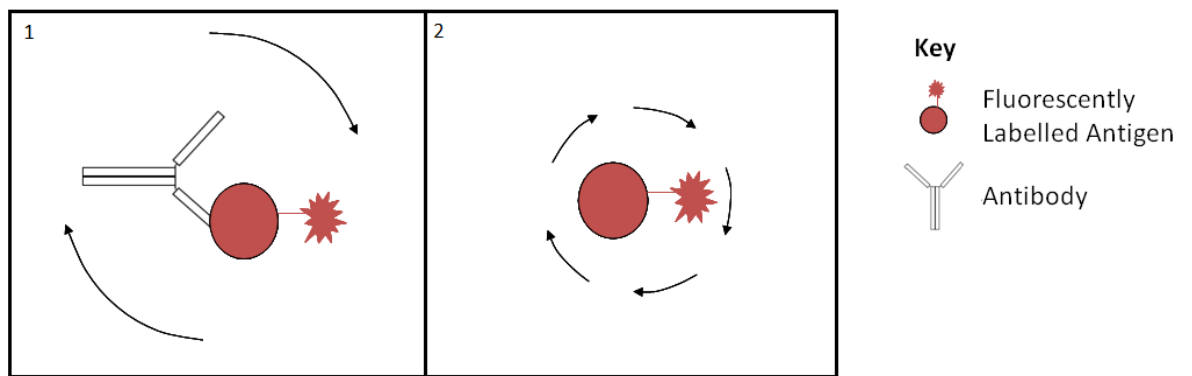


Figure 1.7 - FPIA mechanism

A schematic diagram illustrating how FPIA works. 1) Fluorescently labelled antigen-antibody complex causes slow rotation and high fluorescence polarisation. 2) Fluorescently labelled antigen enables fast rotation and low fluorescence polarisation. Adapted from Bonwick and Smith (2004).

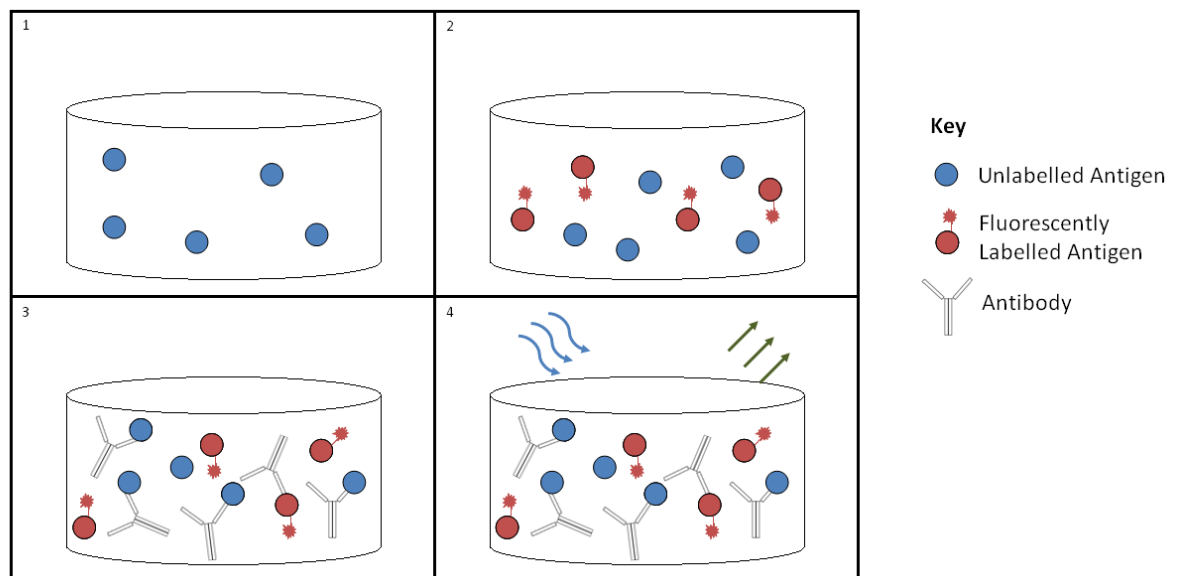


Figure 1.8 - FPIA process

A schematic diagram illustrating FPIA. 1) A sample containing unlabelled antigen is added to the assay. 2) Fluorescently labelled antigen is added to the sample and 3) both antigens compete to bind to the antibodies. 4) A large concentration of unlabelled antigen means the amount of fluorescently labelled antigen bound to antibody decreases leading to faster rotation of fluorescently labelled antigens and consequently low fluorescence polarisation.

FPIA has been successfully applied to the detection of drugs (Colbert and Chllderstone, 1987), metal ions (Johnson, 2003), mycotoxins (Maragos, 2009) and hormones (Hong and Choi, 2002). The obvious advantage of using a FPIA is that it is homogeneous and therefore does not require a separation step or washing. Another advantage is that the reaction is rapid and Hong

and Choi (2002) found that a FPIA could be carried out in one step when detecting progesterone, taking 7 minutes to carry out 10 samples. Typically FPIA only requires few reagents (Nasir and Jolley, 1999). The fluorescent labelled antigens usually use fluorescein derivatives as the label, these are stable on storage, highly fluorescent and do not affect the antigen/antibody interaction (Smith and Eremin, 2008). As FPIA is homogeneous and the reagents are stable, it serves as a simple and repeatable assay.

However a limitation of this assay is that light scattering and endogenous fluorophores can cause noise in the fluorescence polarisation signal. For example human urine contains some natural fluorophores, and this was found to be the major factor limiting assay sensitivity in Colbert and Childerstone's (1987) work on FPIA. They used a single reagent and FPIA to detect multiple drugs of abuse in one sample of urine, including benzoylecgonine (a cocaine metabolite) and amphetamine. However this assay was not multiplexed.

FPIA is also limited to being applied to the detection of small molecules as the signal depends on molecular size. However Guo *et al.* (1998) have shown that FPIA can be used for high molecular weight antigens, by using a luminescent Re(I) metal ligand complex as the FPIA probe. This method was able to detect antigens with a molecular weight between 10^5 - 10^8 Da. However they did find that this probe had a lower emission intensity compared to probes such as fluorescein, reducing sensitivity and increasing noise.

1.1.2. Summary

The bio-detection techniques discussed above represent the major methods currently employed in infection detection. The methods discussed can be compared based on criteria which are important for bio-detection i.e. assay time, detection limit and limitations of technique. Sample types can also be an important factor in detection as they may interfere with the detection technique, for example urine contains natural fluorophores which can interfere with an FPIA technique. Table 1.1 details what each technique can detect and information based on each criterion.

This section has summarised many of the current bio-detection methods and their limitations. The next section will explain how linear dichroism spectroscopy (LD) can be used in combination with a bio-nanoparticle based on M13 bacteriophage (M13) to produce a novel bio-detection system. This new system will solve many of the problems seen with existing bio-detection methods.

Table 1.1 - Brief comparative table providing examples of bio-detection methods

Detection Technique	Analytes detected	Assay Time	Detection Limit *	Limitations of Technique	Samples used	Example References
Microbiological technique	Microbes	~7 days	1-10 ⁸ CFU/mL	<ul style="list-style-type: none"> • Longer assay time • Labour intensive • Detection of only live cells • No detection of toxins or drugs • Not multiplexed 	All clinical samples can be used	(Smith <i>et al.</i> , 2008a, Villari <i>et al.</i> , 1998, Arora <i>et al.</i> , 2006, Boer and Beumer, 1999)
Agglutination assay	Microbes Toxins Antibodies	>1 hour	0.5 ng/mL 10 ⁶ -10 ⁷ CFU/mL	<ul style="list-style-type: none"> • Non-specific reactions can occur • Not multiplexed 	Whole blood, sputum, stool and urine samples	(Fujikawa and Igarashi, 1988, Hajra <i>et al.</i> , 2007, Mazumder <i>et al.</i> , 1988)
ELISA	Microbes Antibodies Toxins Drugs Hormones	>1 hour	2.0 ng/mL 10 ³ -10 ⁵ CFU/mL	<ul style="list-style-type: none"> • No information on activity of the pathogen/toxin • Not multiplexed 	Blood, stool, sputum and urine samples although not used for whole blood samples as serum is typically extracted from whole blood.	(Boer and Beumer, 1999, Kerr <i>et al.</i> , 2001, Reidy <i>et al.</i> , 2011, Venkatratnam and Lents, 2011, Kongmuang <i>et al.</i> , 1987, Drennon <i>et al.</i> , 2003)
Lateral flow	Microbes Toxins	15 minutes	2.8 ng/mL 10 ⁵ -10 ⁷ CFU/mL	<ul style="list-style-type: none"> • Developed for specific single tests and not high-throughput screening • Not multiplexed 	Whole blood, sputum, stool and urine.	(Chan <i>et al.</i> , 2003, Posthuma-Trumpie <i>et al.</i> , 2008, Fisher <i>et al.</i> , 2008)

EMIT	Drugs	10 minutes	0.5ng/mL	<ul style="list-style-type: none"> Limited to molecules of small molecular size Not multiplexed 	Urine samples	(Rosenthal <i>et al.</i> , 1976)
FPIA	Drugs Hormones	0.7 minutes	2.7 ng/mL	<ul style="list-style-type: none"> Limited to molecules of small molecular size. Not multiplexed 	Urine samples, although the results can be affected by natural fluorophores which appear in urine.	(Hong and Choi, 2002, Colbert and Chllderstone, 1987)

*in terms of colony forming units (CFU) or antigen concentration

1.2. Linear dichroism

1.2.1. Theory and instrumentation and history

1.2.1.1. Absorbance

The phenomenon of light absorbance permeates our daily life, from traffic lights to stained glass windows; each is a product of light absorbance. Absorbance occurs when an electron within a molecule absorbs energy in the form of a photon of light to jump to a higher unstable energy level. After a period of time, the “excited” electron decays back to the stable ground energy level (ground state) (Hecht, 2002). The return of the electron to the lower energy level is usually accompanied by a release of thermal energy (figure 1.9).

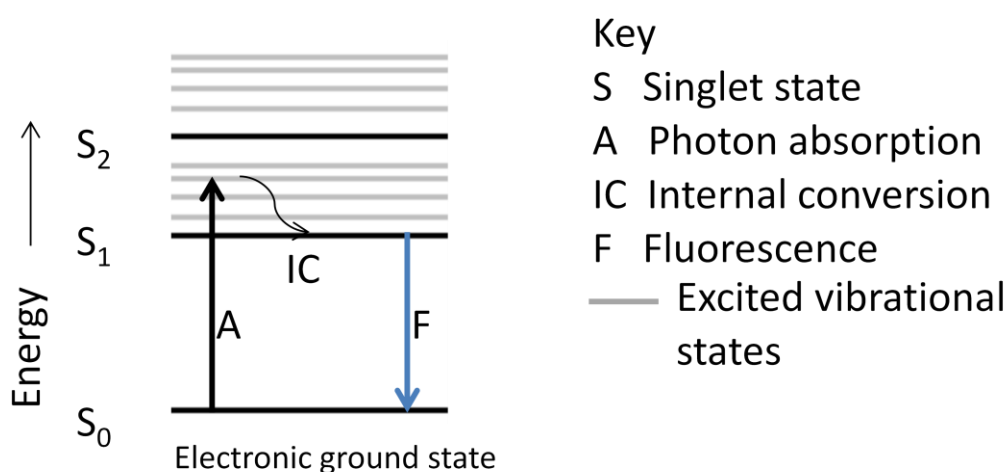


Figure 1.9 - Simple Jablonski diagram

Diagram illustrates how a molecule absorbs a photon; this causes the outer shell electron to move from the ground state to a higher energy level. The electron can lose energy as it cascades through vibrational energy levels before a photon is emitted and the electron returns to the ground state (fluorescence).

The phenomena can also be described by the Beer-Lambert Law which states that the optical absorbance in a transparent solvent is proportional to both the sample cell pathlength and the chromophore concentration. The Beer-Lambert Law follows:

Equation 1.1 - Beer-Lambert Law

$$A = \epsilon Cl$$

Where;

A is the absorbance

ϵ is the extinction coefficient

C is the concentration of the sample

l is the pathlength of the cell

Absorbance measurements are paramount to the study of biochemistry and have been used to study biological molecules, such as pigments, proteins, DNA, and many small organic molecules (Penzer, 1968). Absorbance is widely used to determine concentration, identify chromophores, examine enzyme-catalysed reactions and establish the structure of compounds (Penzer, 1968). Proteins for example absorb ultraviolet light with an absorbance maxima at 280 and 200 nm (Yanari and Bovey, 1960). This phenomenon results from proteins containing amino acids with aromatic rings (tryptophan, tyrosine and phenylalanine) which absorb around 280 nm while the absorbance at 200 nm is primarily caused by peptide bonds.

An extension of absorbance spectrometry that is often used in biology is circular dichroism (CD). CD uses circularly polarised light to determine the secondary structure of proteins as well as other macromolecules including DNA and RNA. This technique measures the difference in absorption of left-handed circularly polarised light and right-handed circularly polarised light and is able to observe conformational changes in structure (Norden *et al.*, 2010). In this project another form of absorbance spectrometry will be used as the basis of a pathogen detection system. This method uses linearly polarised light and is called linear dichroism (LD).

1.2.1.2. Theory of linear dichroism

Linear dichroism is a form of light spectroscopy that is based on the absorbance of linearly polarised light. LD is defined as “the difference in absorption, A , of light linearly polarised parallel (\parallel) and perpendicular (\perp) to an orientation axis” (Norden *et al.*, 2010) :

$$LD = A_{\parallel} - A_{\perp}$$

Linearly polarised light is a form of light in which the axis of the light wave oscillates in a single defined plane. LD uses two forms of plane polarised light, which are defined as parallel and perpendicular to a given orientation direction. An LD spectrum is only produced when the parallel polarised light is absorbed to a different degree than perpendicular polarised light. This effect is only observed when chromophores are aligned. The sign and magnitude of the LD signal indicates the extent of orientation of components within a sample with respect to the alignment axis. Figure 1.10 shows that for example, a positive LD signal implies that the orientation of the electronic transition of the sample is more parallel than perpendicular to the orientation axis (i.e. $A_{\parallel} > A_{\perp}$ and therefore, $LD > 0$). If the component of the sample is more perpendicularly aligned than parallel, the LD signal is negative (i.e. $A_{\parallel} < A_{\perp}$, therefore, $LD < 0$) as seen in figure 1.11.

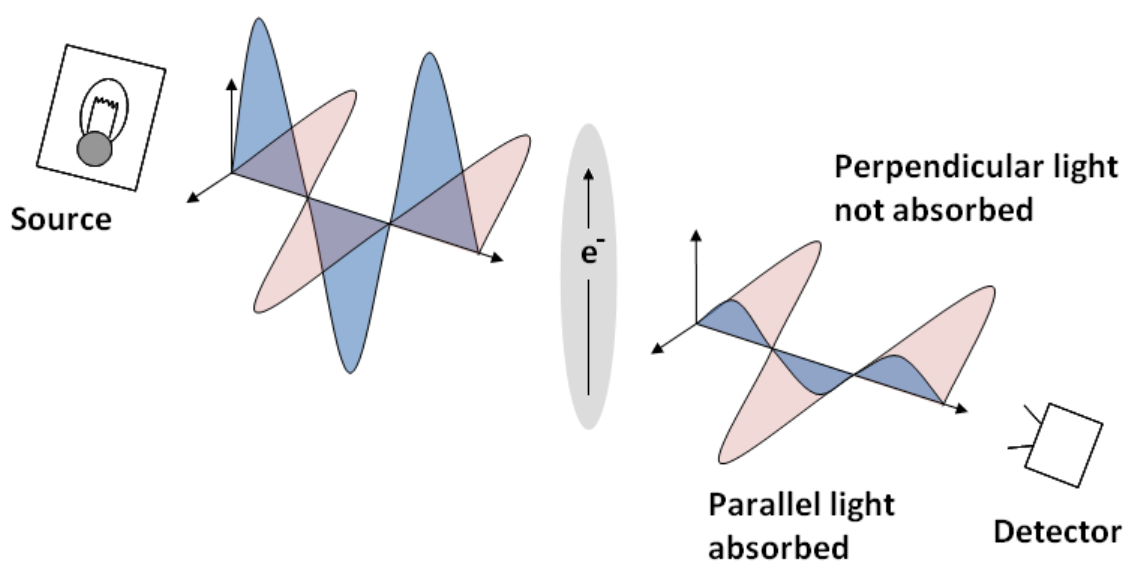


Figure 1.10 - LD schematic diagram (parallel)

A schematic diagram illustrating the principles underpinning LD. When electrons within a molecule in an oriented sample are moving parallel to the orientation axis, they will absorb the light linearly polarised parallel to the orientation axis. This will cause the electrons within the molecule to move to a higher energy state. However the electrons will not absorb the light linearly polarised perpendicular to the orientation axis. This case therefore gives a positive LD signal.

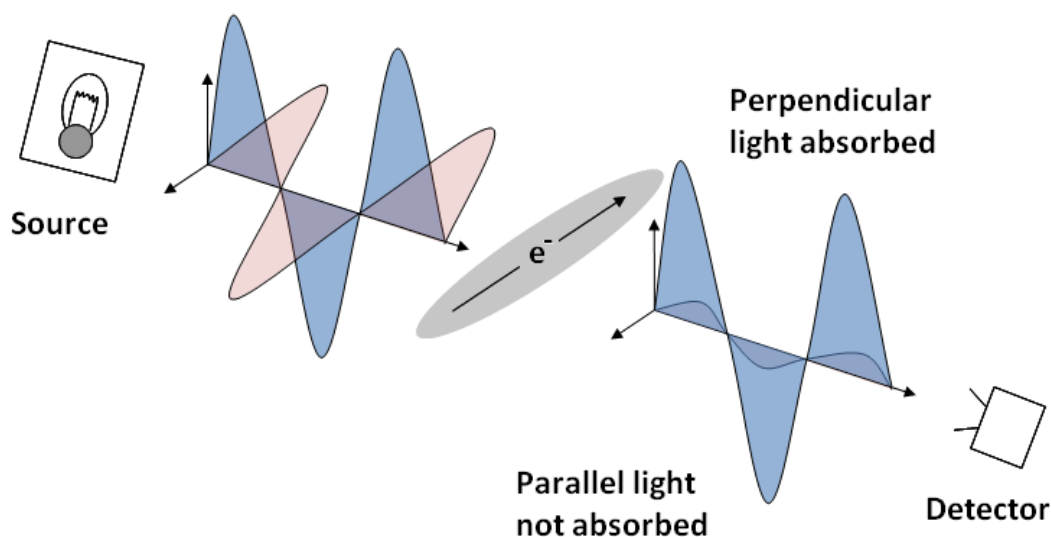


Figure 1.11 - LD schematic diagram (perpendicular)

A schematic diagram illustrating the principles underpinning LD. When electrons within a molecule in an oriented sample are moving perpendicular to the orientation axis, they will absorb the light linearly polarised perpendicular to the orientation axis. This will cause the electrons within the molecule to move to a higher energy state. However the electrons will not absorb the light linearly polarised parallel to the orientation axis. This case therefore gives a negative LD signal.

A key aspect of LD is that to produce an LD signal the molecules in the sample need to be aligned at the molecular level (figure 1.12). For non-aligned molecules the overall LD signal is zero because the molecules are all randomly positioned. It is this observation that provides the basis of the assay developed in this project where LD is used as a probe for the alignment of an assay reagent.

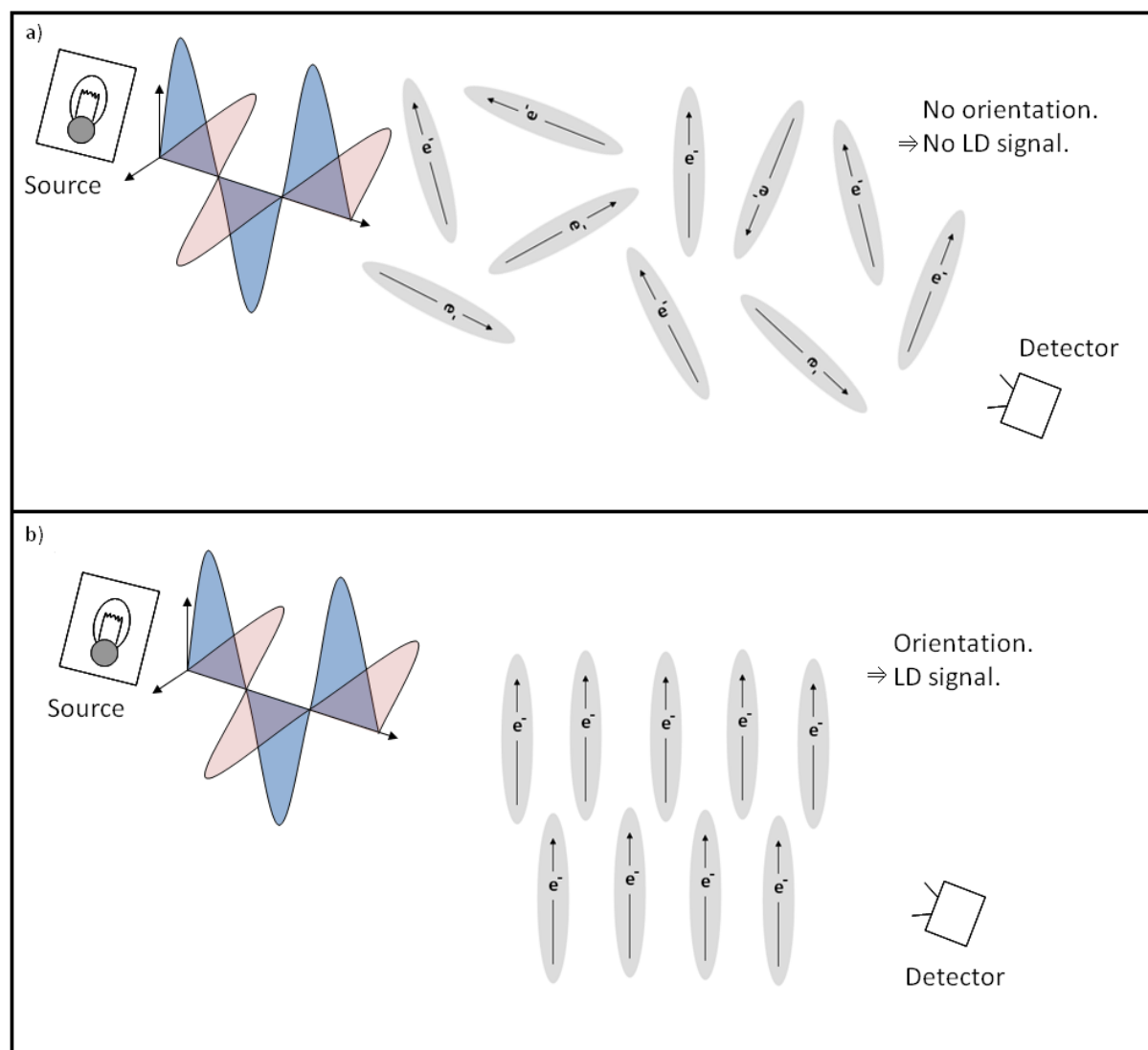


Figure 1.12 - The effect of molecular alignment on LD

a) Demonstrates that when the electronic transitions within the sample are not aligned with one of the light beams absorption cannot occur. Whereas b) shows that when they are aligned absorption can occur.

1.2.1.3. Molecular alignment methods

Alignment of molecules is essential in LD spectrometry and can be achieved using a number of different methods which are appropriate for different types of biomolecules (Rodger, 1993). These methods rely on some form of asymmetry in the molecular structure. This might include magnetic, electronic or structural asymmetry. In this project, methods are used that allow the alignment of structurally asymmetric molecules. Such molecules have a high aspect ratio (shapes with one axis much larger than the other) e.g. DNA (Dafforn and Rodger, 2004), and are commonly aligned using hydrodynamic methods which include thin film orientation (Bechinger *et al.*, 1999), squeezed gel orientation (Tapie *et al.*, 1982), and shear flow orientation (Rodger *et al.*, 2002).

The most common method for aligning structurally asymmetric molecules for LD measurements is shear flow orientation; this method also has the advantage of being ideally suited to liquid samples. Such shear alignment experiments are usually carried out in a Couette cell, in which a sample is placed between two concentric cylinders one of which is rotated with respect to the other (figure 1.14). For optical measurements in this system the cylinders are formed from a transparent material for example a quartz rod in a quartz capillary (figure 1.15) (Marrington *et al.*, 2004). Continuous flow is achieved by rotating this quartz capillary using a motor; this is typically fitted at the base of the cell (figure 1.13). The rotating capillary creates a viscous drag which causes a flow gradient in the solution flowing through the small gap between the capillary and the rod.

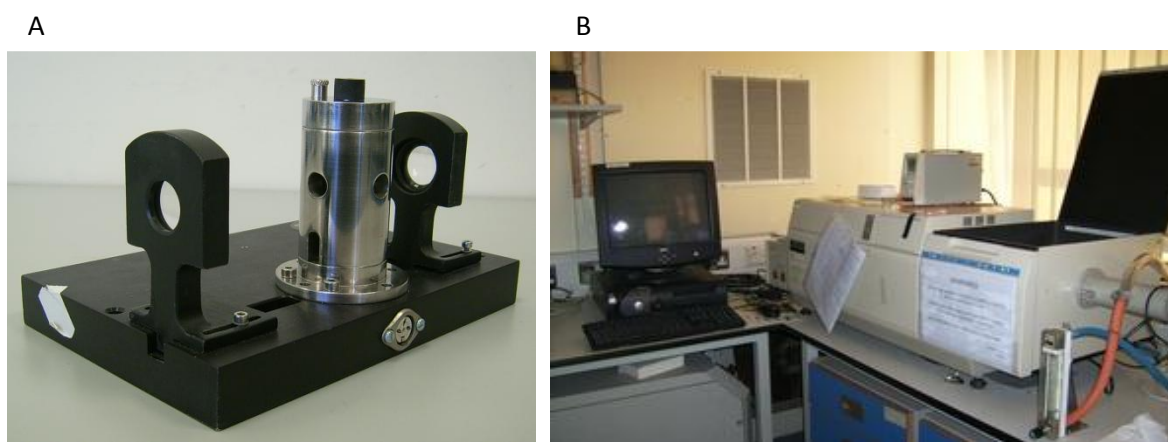


Figure 1.13 - LD instrument

A) A Couette flow cell B) A linear dichroism instrument (photographed by Julia Kraemer).

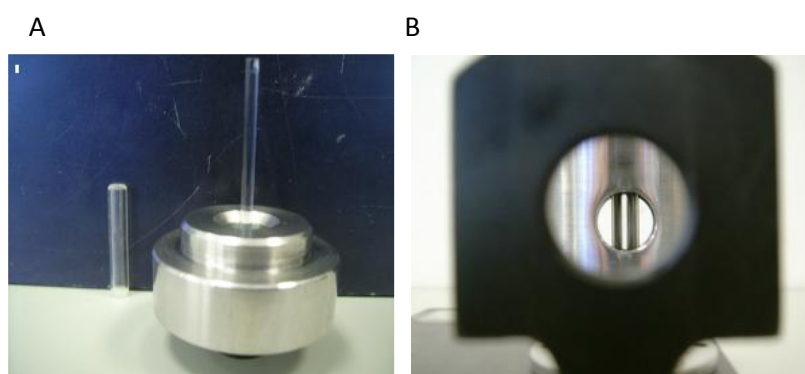


Figure 1.14 - Quartz Couette and sample chamber

A) Quartz Couette and quartz rod used in a LD instrument. B) The quartz Couette viewed through the optical lens of the LD instrument. A sample is placed into the quartz Couette and the quartz rod is placed inside before an LD measurement is made (photographed by Julia Kraemer).

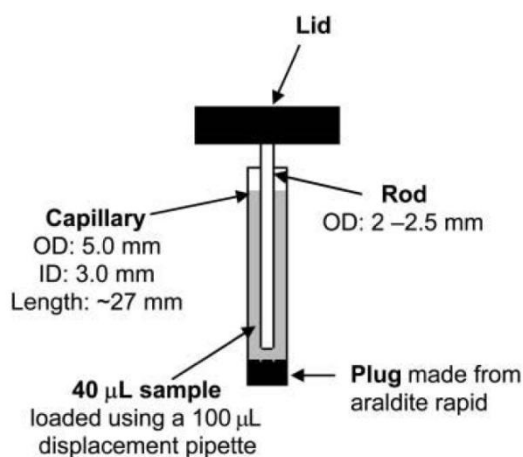


Figure 1.15 - Capillary and rod used to produce shear flow in LD

Capillary and rod used to produce shear flow in the LD instrument. Reproduced from Marrington *et al.* (2004).

1.2.2. Applications in Biology

The use of LD in biology has increased over the past 40 years; this can be seen in a survey of papers using Pubmed with Linear Dichroism in the title which shows that the number of papers increased steadily. Only one paper was published with LD in the title in the 1960s (Brahms *et al.*, 1968). Prior to this paper the technique was known as ultra violet (UV) dichroism (Bendet and Mayfield, 1967, Higashi *et al.*, 1963, Ruch, 1957). Between 1960 and 1980 there were 54 papers published with LD in the title. Between 1980 and 2014, 236 papers have been published with LD in the title, demonstrating a steady growth of LD as a spectroscopic technique.

1.2.2.1. LD and structural studies of DNA

Part of the growth in publications using LD has been an increasing application of the technique to the study of a wide range of biomolecules that can be aligned. Perhaps the most important of these being DNA, which probably represents the system with the largest accumulation of LD data. For example LD has been used to examine the interactions between DNA and DNA-bound ligands, where LD is able to probe the orientation of the ligand. This does not show where the particular ligand binds to the DNA, but determines the orientation of the ligand

providing insights into the binding mode (Rodger *et al.*, 2006). LD Studies have shown that ligands are capable of intercalating between the DNA bases, for example in the case of the binding properties of potential anti-tumour agents (Dalla Via *et al.*, 2002). LD has also been used to show ligands can be oriented by binding along the minor (Nguyen *et al.*, 2004) and major groove (Lee *et al.*, 2002) of DNA.

The ability of LD to detect the alignment of a sample was first used as the basis of an assay when it was applied to the detection of DNA mutations (Halsall *et al.*, 2001). Halsall *et al.* (2001) used LD to study the β -glucocerebrosidase gene which is linked to Gaucher disease. Polymerase chain reaction (PCR) amplimers were prepared from exon 10 in the β -glucocerebrosidase gene in patients known to have compound heterozygous (h1/h2) and heterozygous (h1/wt and h2/wt) mutations. A control PCR amplimer was also prepared from patients with no mutations (wt/wt). The LD spectra of these samples are shown in figure 1.16. At 260 nm all samples exhibit a negative LD signal of similar magnitude, corresponding to the base pairs being oriented perpendicular to the DNA helix axis. At 230 nm the peak is positive for all samples corresponding to a greater parallel alignment. Crucially, the LD signal is related to the number of mismatched pairs, with the sample containing no mutations (wt/wt) producing the highest LD signal, whilst the compound heterozygous sample (h1/h2) produces the lowest LD signal. The LD signals from the different PCR amplimers can be discriminated and hence the change to the DNA structure caused by the mutations can be detected. This demonstrates that LD is capable of detecting mismatched base pairs in a PCR amplimer greater than a kilobase in length.

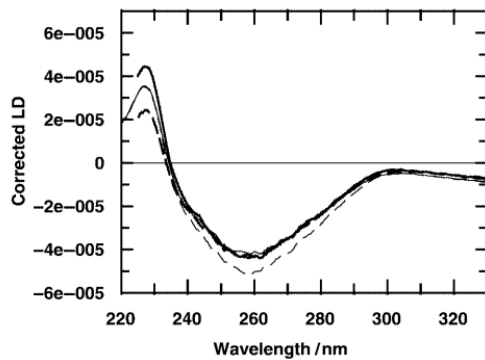


Figure 1.16 - Flow LD spectra of PCR amplimers

Flow LD spectra of PCR amplimers prepared from patients confirmed to be a control without any mutation for the β -glucocerebrosidase gene (wt/wt) (thick solid line), patients who were heterozygous for one mutation (h1/wt) (thin solid line), (h2/wt) (thin dashed line), and patients who were compound heterozygote (h1/h2) (thick dashed line). The maximum at 230 nm is related to the number of mis-matched base pairs. Reproduced from Halsall *et al.* (2001).

1.2.2.2. Protein fibres

LD has not only been used to study aligned DNA, but can also be applied to the study of aligned protein fibres. In the 1960s and 1970s LD was used to gain new insights into the orientation of secondary structure elements, aromatic amino acids and bound nucleotide within F-actin (Higashi *et al.*, 1963 ; Miki and Mihashi, 1976). These experiments were limited by the large amounts of samples required to make a measurement. More recently an improved capillary Couette cell has been developed (Dafforn *et al.*, 2004) and was used with two medically important protein fibres (the all- β -sheet amyloid fibres of the Alzheimer's derived protein A β and the long-chain assemblies of α_1 -antitrypsin polymers). This data provided information on the fibre structures (Dafforn *et al.*, 2004). The development of a temperature controlled micro volume Couette LD cell also allowed the analysis of tubulin microtubules. This study probed the structural reorientations of tubulin chromophores which occur during polymerisation and determined the effect of ligand binding on fibre structure (Marrington *et al.*, 2006). Adachi *et al.* (2007) also successfully utilised LD to detect and characterise fibril formation by amyloid peptides. In addition, LD has been used to carry out structural analysis of molecules within linear polymers. For example Small *et al.* (2007) used LD

to investigate a specific conformational change in guanosine-5'-triphosphate (GTP) bound to filamenting temperature-sensitive mutant Z (FtsZ) polymers (which are found in the cytoskeleton of bacterial cells) upon bundling by an accessory cell division protein. They found that the conformational change seen in bound GTP revealed a general mechanism of FtsZ bundling. To further explore the impact of protein conformation on LD spectra, Bulheller *et al.* (2009) constructed a model to calculate the electronic structure directly. They investigated prototypical proteins including a self-assembling fibre and tropomyosin (all- α -helical), FtsZ (an $\alpha\beta$ protein), an amyloid fibril (β -sheet), and collagen (poly(proline)-II helices). They found that combining experiment with calculation clarified the protein orientation and the orientation of the chromophores within the protein fibres.

1.2.2.3. Bacteriophage

In 1967 LD spectroscopy was first used in the study of filamentous bacteriophage (Bendet and Mayfield, 1967). Using LD, the internal structure of the fd bacteriophage (a type of filamentous bacteriophage known to infect *E. coli*) was studied providing insights into the orientation of structural elements within the bacteriophage (Bendet and Mayfield, 1967) (figure 1.17). These results showed that the DNA within the fd bacteriophage produced a negative LD signal, whilst the proteins within the fd bacteriophage gave a positive LD signal. From this they could conclude that molecules within the same bacteriophage have a different orientation. The study was further extended to show that the base pairs of tobacco mosaic virus genome are orientated more or less parallel to the longitudinal axis of the virus (Schachter *et al.*, 1966).

Clack and Gray (1992) built on these studies, measuring LD of other filamentous bacteriophages, Pf1, Pf3 and Ike as well as fd filamentous bacteriophages. They found that these filamentous bacteriophages produced similar protein and DNA LD spectra.

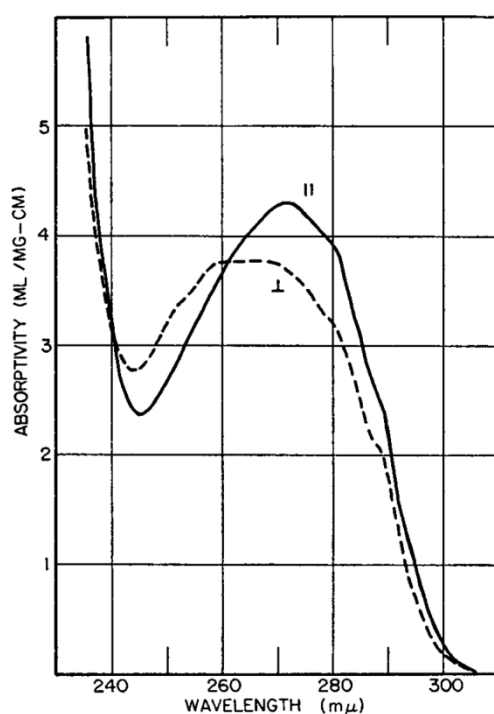


Figure 1.17 - Difference in absorbance of perpendicular and parallel light by bacteriophage

The first measurements of the difference in absorbance of perpendicular and parallel light by bacteriophage. The LD spectra indicates that the DNA and protein are aligned differently. Reproduced from Bendet and Mayfield (1967).

It is interesting to compare the instrumentation used in these studies. Bendet and Mayfield (1967) used a flow cell which required 10 mL of 1.5 mg/mL of bacteriophage solution per experiment, which was constantly flowed through a 1 mm² cross-section quartz capillary to achieve alignment. In contrast, Clack and Gray (1992) required 30 mL of 3.4 mg/mL bacteriophage solution for each LD experiment. This highlights large sample requirement as a limitation for LD in the early days. To address this, Marrington *et al.* (2004) developed a Couette cell format in which the sample requirement is reduced to 25 μL and 200 μM concentrations. The micro-volume LD cell uses a quartz capillary which rotates around a mounted rod (figure 1.15). In this project a capillary cell that requires as little as 80 μL is used, which is a significant decrease compared to other laboratories.

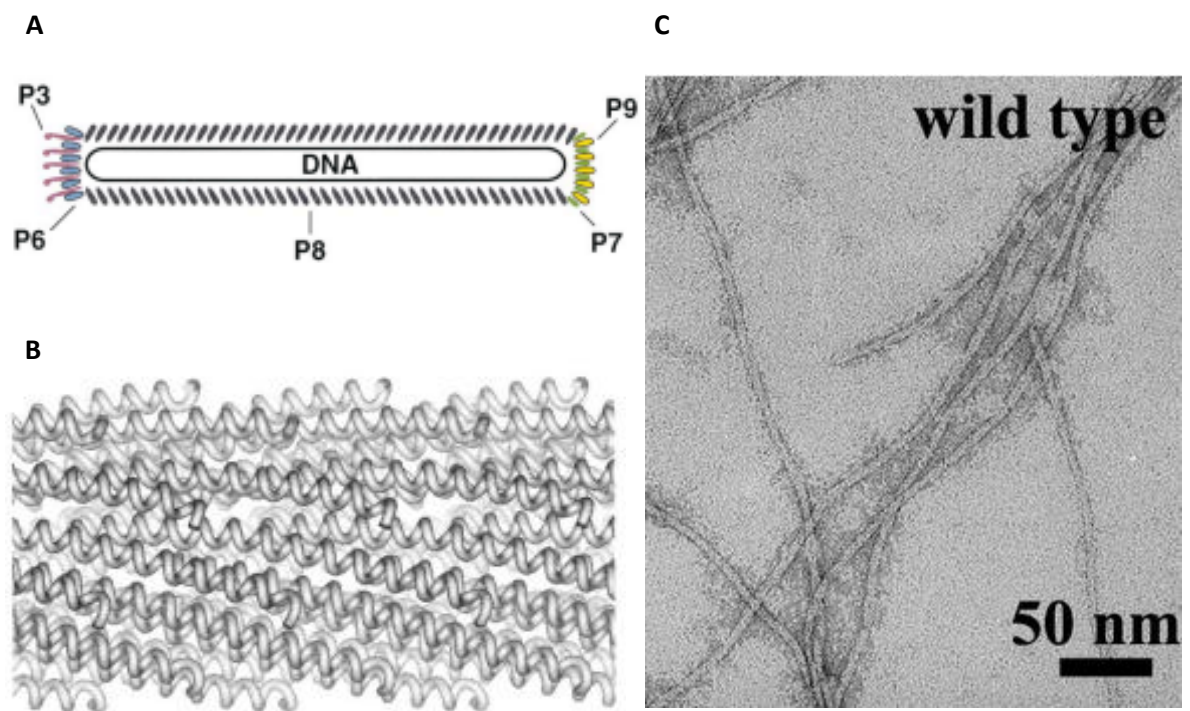


Figure 1.18 - Structure of M13 bacteriophage

The structure of M13 bacteriophage is displayed in image A. Reproduced from Sidhu (2001). Image B is a model of the M13 coat reconstructed from fiber X-ray data of M13. This image reveals how the p8 coat proteins form an organised structure. The C termini are buried inwards, while the N termini are facing outwards on the surface of the particle. Reproduced from Sidhu (2001). Image C is a transmission electron microscope (TEM) image of wild type (wt) M13 bacteriophage. Reproduced from Murugesan *et al.* (2013).

These early studies also show that the bacteriophage particle has a high enough aspect ratio to align in shear flow. Electron microscopy studies confirmed this, showing that M13 bacteriophage has a diameter of approximately 6.5 nm and a length of 900 nm (Murugesan *et al.*, 2013) (figure 1.18).

In this project M13 bacteriophage will be used extensively as a scaffold for development of a novel assay. It is therefore important that the M13 structure is described in greater detail than the other fibres in this section. M13 consists of single stranded DNA encapsulated by a protein coat. The protein coat is made up of one major coat protein known as p8 and there are approximately 2700 copies of p8 along the coat. There are 5 copies of each of the minor coat proteins known as p3, p6, p7 and p9, which are situated at the ends of the bacteriophage

(Sidhu, 2001). All 5 of the coat proteins provide structural properties to the M13 bacteriophage, however only p3 is utilised for host cell infection. The major coat protein p8 is positioned such that its C-terminus associates with the internalised DNA. Association of the hydrophobic regions of adjacent p8 proteins stabilises their interaction with one another, and the particle itself. The N-terminus of the protein is situated externally and plays a key role in facilitating the bioengineering potential of the M13 bacteriophage (Sidhu, 2001).

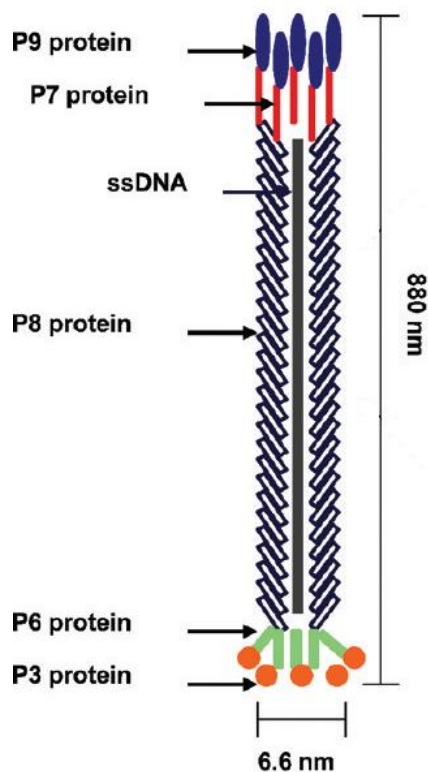


Figure 1.19 - Schematic diagram of M13 bacteriophage

M13 bacteriophage consists of approximately 2700 copies of coat protein p8 which surrounds the internal single stranded DNA. There are also 5 copies of each of the minor coat proteins (p3, p6, p7 and p9), which are located at the ends of the bacteriophage. Reproduced from Li *et al.* (2010).

M13 is a filamentous bacteriophage and infects *E. coli* cells which present F pili on their surface. Infection commences when the p3 coat protein attaches to the F pilus. This is followed by the insertion of the M13 single stranded DNA into the cytoplasm of the cell. In order to produce M13 bacteriophage proteins within the cell, the single stranded DNA is transformed

into double stranded DNA and is then replicated. Single stranded DNA is then produced through a rolling circle replication process. The coat proteins are embedded into the membrane of the host cell and other proteins form gated pores to allow the viral DNA to be extruded through the pore with its coat proteins assembling on to it (figure 1.20). The M13 bacteriophage particles are released and this is a non-lytic process as the *E. coli* cells continue to grow and divide, but at a much slower rate (Sidhu, 2001).

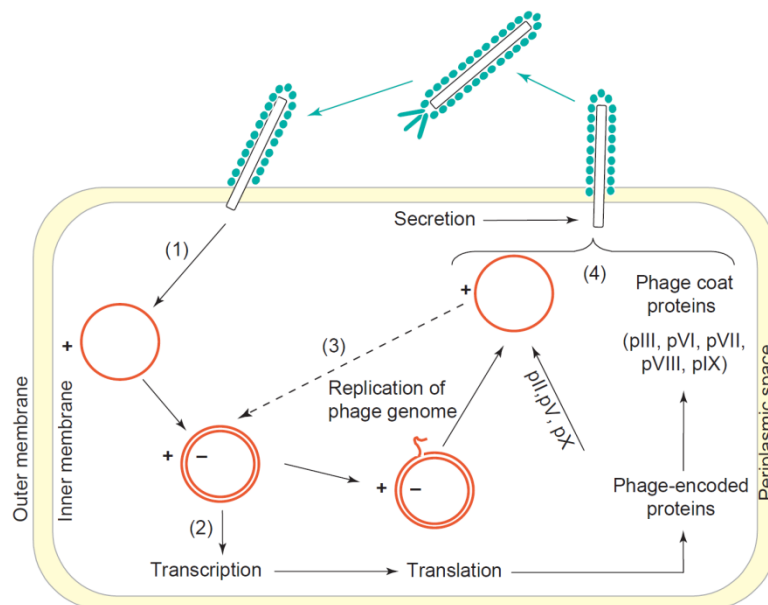


Figure 1.20 - M13 bacteriophage lifecycle

A diagram illustrating the lifecycle of M13 bacteriophage. (1) Infection of *E. coli* cell by M13 bacteriophage via the p3 coat protein. The single stranded viral DNA is injected into the cell and this is used as a template to produce double stranded DNA. (2) This results in host-mediated protein synthesis, producing the M13 bacteriophage proteins. (3) The viral DNA is replicated and (4) the M13 bacteriophages are assembled and released from the *E. coli* cell. Reproduced from Mullen *et al.* (2006).

Examination of the LD spectrum of M13 shows positive peaks between 200-240 nm which arise from peptide backbone transitions. A negative band between 240 nm and 260 nm arises from DNA transitions indicating that the base pairs are perpendicular to the long axis of the bacteriophage. A positive peak between 260 nm and 300 nm is due to aromatic transitions of Tyrosine, Tryptophan (maximum at 280 nm) and Phenylalanine (Clack and Gray, 1992, Pacheco-Gomez *et al.*, 2012). These observations of aligned bacteriophage and resulting LD signals have provided the basis for the LD based assay method detailed in this project.

However it is clear that bacteriophage alone will not function as an assay reagent. To work with such a reagent, the bacteriophage has to be engineered in order to allow it to interact with the assay target. Engineering a biological molecule to function in a new system is one of the underlying principles of a new area of science, synthetic biology.

1.3. Synthetic biology

Synthetic biology is the construction of biological systems and re-construction using engineering principles of existing natural biological systems, for useful purposes (Khalil and Collins, 2010).

Synthetic biologists can be said to come in two classes. One uses elements from natural biology to form an unnatural structure or systems. Whereas the other uses unnatural elements to recreate naturally occurring systems (Benner and Sismour, 2005). Synthetic biology first appeared in the scientific literature in 1980 in an article titled “Gene surgery: on the threshold of synthetic biology” by Barbara Hobom (Hobom, 1980). She used the term synthetic biology to describe genetically engineered bacteria using recombinant DNA technology; here the term was synonymous with bioengineering. Synthetic biology was later mentioned in 2003 as a means to re-construct life which is an extension of biomimetic chemistry (Benner, 2003), where artificial molecules are synthesised and mimic natural molecules e.g. enzymes. Synthetic biology therefore attracts engineers who want to extract parts from living systems and test them as structural units and re-build them in a way to mimic living systems (Benner and Sismour, 2005). It is expected that the outputs of synthetic biology will be cheaper drugs, greener fuels and targeted therapies (Khalil and Collins, 2010).

1.3.1. Synthetic biology and detection

Synthetic biology has also provided new approaches to detection. Saeidi *et al.* (2011) engineered *E. coli* to detect and eradicate *Pseudomonas aeruginosa* (*P. aeruginosa*). They developed a synthetic genetic system which comprised of quorum sensing, killing and lysing devices to enable *E. coli* to detect and kill a strain of *P. aeruginosa*. The *E. coli* was engineered to firstly detect the *P. aeruginosa* using quorum sensing, and then to produce and release pyocin (an antimicrobial peptide) by lysing the *E. coli* chassis. They found that the engineered

E. coli cells were successful in detecting and killing the *P. aeruginosa* cells as there was a 99% drop in viable *P. aeruginosa* cells and a 90% drop in the formation of biofilms (Saeidi *et al.*, 2011). Similarly Ghosh *et al.* (2012) utilised synthetic biology in detection by using modified M13 bacteriophage. They were able to highlight cancer cells and tumours in mice for magnetic resonance imaging. Iron oxide magnetic nanoparticles were assembled along the M13 coat and the M13 was engineered to display the target ligand at the distal end which detects a glycoprotein over expressed in cancer cells (Ghosh *et al.*, 2012). M13 bacteriophage also appears in another detection system where it was engineered to act as a scaffold (Lee *et al.*, 2012). These scientists used DNA-conjugated M13 to detect an antigen where a colour change occurred in the presence of the specific antigen. DNA-conjugated M13 was able to hybridise with DNA-conjugated gold nanoparticles in the presence of the antigen and this led to a colour change. The antigen was then identified using a microarray. These studies demonstrate how synthetic biology is advancing and that organisms can be manipulated to execute specific tasks, in this case detect particular target molecules.

1.4. LD in immune detection

Using a combination of synthetic biology and LD, a new assay has been developed in the laboratory of Professor Dafforn to detect specific target molecules (Pacheco-Gomez *et al.*, 2012).

1.4.1. Theory

As discussed earlier, LD requires sample alignment at the molecular level; this means that the amplitude of an LD signal is related to the alignment of a sample. The sensitivity of LD to the alignment of a biomolecular assembly in shear flow has already been used as the basis of a genetic assay (Halsall *et al.*, 2001).

In its most basic sense any LD assay is made up of a minimum of two components, an LD spectrometer and a reagent. The reagent must have an LD signal which can be detected by the spectrometer. That signal must then be perturbed by an interaction between the reagent and the target, resulting in a change in the LD signal that can be measured. Crucial to a successful assay is the choice of reagent as the reagent has to be:

- A long rigid rod that aligns under shear flow.
- Biochemically flexible in order to attach chromophores and moieties which will ensure the specificity for the target molecule.
- Stable.

One such reagent is M13.

The rigid nature of M13 allows easy alignment which produces a distinct and robust LD signal (Clack and Gray, 1992), making it potentially a good scaffold for an LD based assay. M13 is also genetically and biochemically flexible. The flexibility has been exploited for many years with the most common modification being the fusing of exogenous proteins to the capsid. The most famous example of this is the fusion of antibodies to p3 for antibody engineering (Barbas *et al.*, 1991). Barbas *et al.* (1991) demonstrated the versatility of M13 bacteriophage by producing M13 displaying combinatorial antibody Fab libraries. The carboxyl-terminal domain of the p3 coat protein was fused with Fab fragments that bound to tetanus toxin. Usefully, M13 bacteriophage also demonstrates a high degree of stability (Branston *et al.*, 2013) with it being resistant to heat (Holliger *et al.*, 1999), various organic solvents (Olofsson *et al.*, 2001), urea, acid, alkali and other stresses, (Petrenko and Vodyanoy, 2003).

Given all of these characteristics, recent work by Pacheco-Gomez *et al.* (2012) has demonstrated that M13 could be functionalised to detect *E. coli* O157 in conjunction with LD (as described below).

1.4.2. Previous work on an M13/LD based assay

Pacheco-Gomez *et al.* (2012) developed an assay capable of detecting *E. coli* O157 using M13 and LD. They achieved this by fusing an FB domain (derived from protein A) on to the p3 coat protein of M13 (FB-M13). The FB domain was able to bind specifically to the secondary antibody forming a complex which aligned in a flow cell producing a characteristic M13 signal. The secondary antibody was able to interact with the constant region of the pathogen specific antibody (primary antibody). The primary antibody that was used in this study was raised to bind specifically to an antigen on the surface of *E. coli* O157 and was therefore used to detect *E. coli* O157. When the anti-*E. coli* O157 and *E. coli* O157 were added to the conjugated FB-M13 the LD signal dropped significantly (figure 1.21 and 1.22). The concentration of primary and secondary antibody was also reduced 10-fold and increased 2-fold to observe the sensitivity of the assay to antibody concentration. The results demonstrated that reducing the antibody concentration 10-fold limited the sensitivity of the assay, but increasing it 2-fold did not significantly improve the LD signal (figure 1.22B). Pacheco-Gomez *et al.* (2012) therefore confirmed that M13 coupled with LD could provide a promising new method of detection for bacteria based on immune techniques.

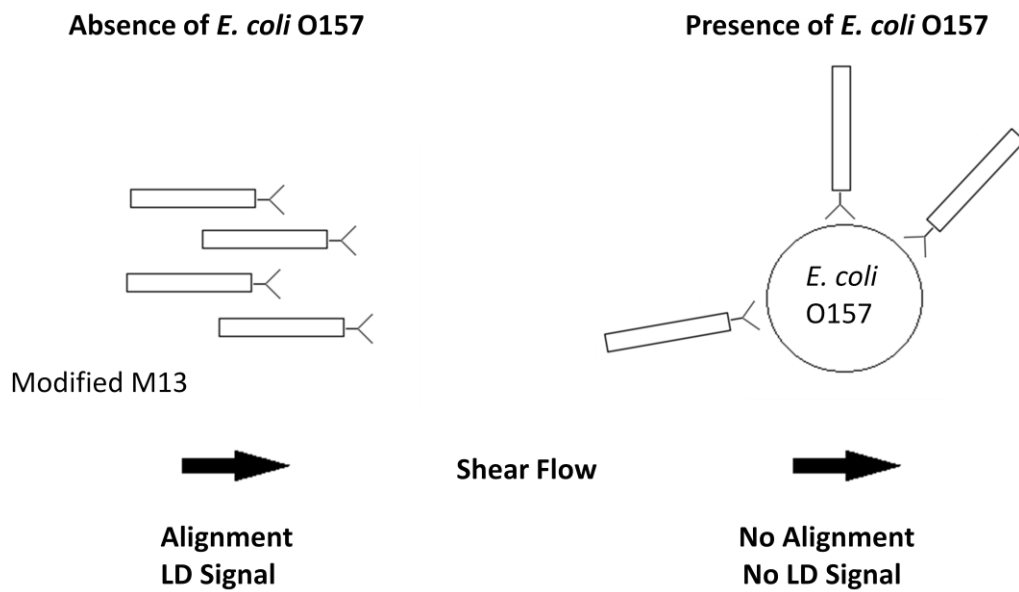


Figure 1.21 - Principle behind an existing M13/LD based assay

A schematic diagram illustrating the principle behind the pathogen detection assay used by Pacheco Gomez *et al.* (2012) which utilised LD and M13 bacteriophage. M13 bacteriophage labelled with anti-*E. coli* O157 antibody (via the p3 coat protein) aligns under shear flow, thus a LD signal is seen. If a sample containing *E. coli* O157 is added to the M13 reagent, alignment is disrupted due to the formation of bonds between the antibody labelled M13 and the *E. coli* O157. Therefore a reduction in the LD signal is observed.

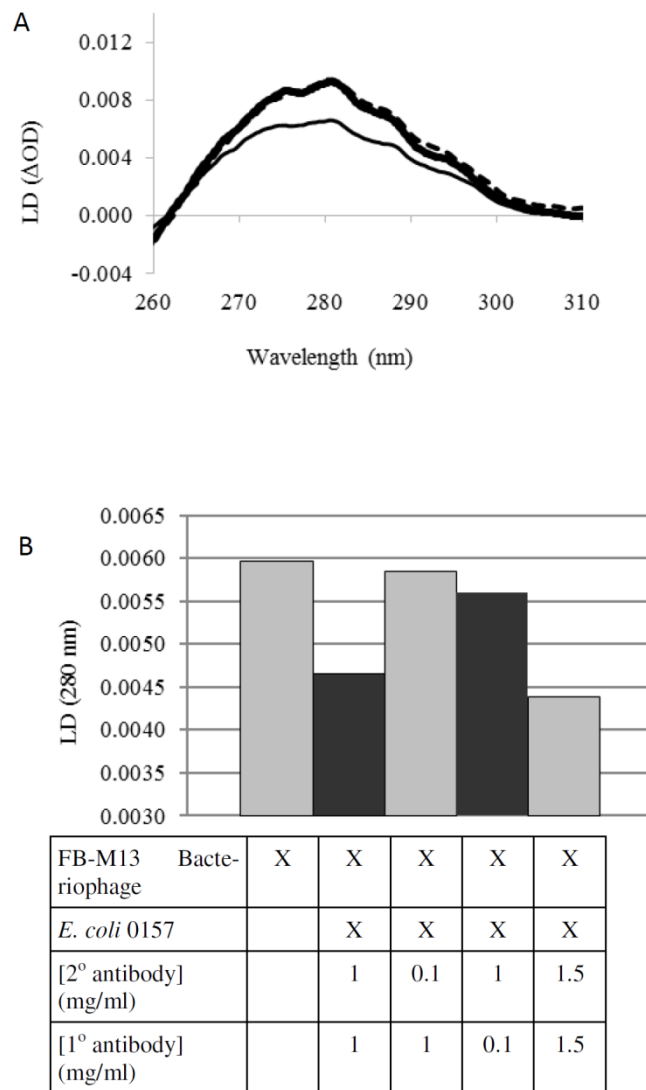


Figure 1.22 - *E. coli* O157 detection using an existing M13/LD based assay

A) The effect of various protein complexes with FB-M13 on the bacteriophage LD spectrum. Thick dark line is FB-M13 + *E. coli* 0157 (10^7 cells/mL final concentration). Dotted line is FB-M13 + primary antibody (1 mg/mL) + secondary antibody (1 mg/mL) + *E. coli* BL21 (10^7 cells/mL final concentration). Thin line is FB-M13 + primary antibody (1 mg/mL) + secondary antibody (1 mg/mL) + *E. coli* 0157 (10^7 cells/mL final concentration). The LD signal only drops when the target bacterium is present. B) The effect of varying concentrations of primary and secondary antibodies on the assay signal. Reproduced from Pacheco-Gomez *et al.* (2012).

1.5. Aims

Taken together there is a clear need for new assay methods and in this project we explore the use of M13 bacteriophage coupled with LD in a range of different assay types. The project is broken down into a number of aims and these are:

- To increase M13 bacteriophage production to meet the requirements for the assay.
- To covalently attach various chromophores onto M13 bacteriophage in preparation for a multiplexed assay and multimodal assay.
- To increase the sensitivity of pathogen detection using LD and M13 bacteriophage.
- To develop a method to detect small molecules using LD and M13 bacteriophage.

CHAPTER 2

- MATERIALS AND METHODS

2.1. Materials

A stock of wild-type (wt) M13 bacteriophage was provided by Professor John Ward (University College, London). Heat-killed *E. coli* O157:H7 was provided from KPL (Maryland, USA). The quartz cuvette (0.3 cm pathlength) used to obtain the absorbance spectra, was provided by Starna (Essex, UK).

2.2. Methods

2.2.1. Production of M13 bacteriophage

There are currently two commonly used methods for the production of wt M13. One method is based on Sambrook and Russell (2001), while the other is based on New England Biolabs (2011).

2.2.1.1. Method based on Sambrook and Russell (2001)

Four hundred mL of autoclaved Luria Broth (LB) medium in a 2.5 L flask containing tetracycline to a final concentration of 5 µg/mL was inoculated with 500 µL of (glycerol stock of log phase) Top10F' *E. coli* (Invitrogen, California, USA) (F'[lacI^q Tn10(tet^R)] mcrA Δ(mrr-hsdRMS-mcrBC) φ80lacZΔM15 ΔlacX74 deoR nupG recA1 araD139 Δ(ara-leu)7697 galU galK rpsL(Str^R) endA1 λ⁻) and 5 µL of 13 mg/mL wt M13 bacteriophage. The culture was then incubated overnight at 37 °C at 180 rpm. The culture was then decanted into 450 mL centrifuge tubes and centrifuged at 11000 rpm for 15 minutes at 4°C in a fiberlite F10B 6X500 rotor. The supernatant was mixed with 20% v/v of 25% w/v PEG (polyethylene glycol) 6000/2.5 M NaCl and left on ice for 15

minutes. The precipitated M13 particles were then recovered by centrifugation of the samples at 11000 rpm for 15 minutes at 4°C in a fiberlite F10B 6X500 rotor. The supernatant was removed and the pellet was resuspended in 50 mM phosphate buffer, pH 8.0. The M13 was passed through a 0.22 µm membrane filter twice (Millipore, Massachusetts, USA) to remove any *E. coli* cells.

2.2.1.2. Method from New England Biolabs (2011)

Two hundred and fifty mL of autoclaved LB containing tetracycline (a final concentration of 5 µg/mL) was inoculated with 500 µL of Top10F' *E. coli* (Invitrogen, California, USA) and incubated overnight at 37 °C, 180 rpm. The culture was diluted by transferring 40 mL of the overnight culture to 360 mL LB, and tetracycline was added again to provide a final concentration of 5 µg/mL. Five µL of 13 mg/mL wt M13 stock was added and was incubated for 4.5-5 hours at 37 °C, 180 rpm. The culture was decanted into 500 mL centrifuge tubes and centrifuged at 11000 rpm for 15 minutes at 4°C in a fiberlite F10B 6X500 rotor. The supernatant was transferred into new 500 mL centrifuge tubes and centrifuged again at 11000 rpm for 15 minutes at 4°C in a fiberlite F10B 6X500 rotor. The upper 80 % of the supernatant was taken and mixed with 20% v/v of 25 % w/v PEG6000/2.5 M NaCl in a new tube and, left to precipitate overnight at 4 °C. The tubes were then centrifuged at 11000 rpm for 15 minutes at 4 °C in a fiberlite F10B 6X500 rotor, the supernatant was discarded and the pellet was resuspended in 1 mL 50 mM phosphate buffer pH 8 and transferred into a 1.5 mL eppendorf tube. This was then centrifuged in a bench top centrifuge (Spectrafuge 16M, Labnet) at 14000 rpm for 5 minutes at 4 °C, to pellet the remaining cells. The supernatant was transferred into a new tube and precipitated with 20% v/v of 25 % w/v PEG6000/2.5 M NaCl for 1 hour at 4 °C. These were centrifuged at 14000 rpm for 10 minutes at 4 °C in a bench top centrifuge (Spectrafuge 16M, Labnet). The supernatant was discarded and the pellet was resuspended in 100 µL of 50 mM phosphate buffer pH 8.

2.2.1.3. New method for M13 bacteriophage production

Four hundred mL of autoclaved LB medium in a 2.5 L flask containing tetracycline to a final concentration of 5 µg/mL was inoculated with 500 µL of (glycerol stock of log phase) Top10F' *E. coli* (Invitrogen, California, USA) and 5 µL of 13 mg/mL wt M13. The culture was then incubated overnight at 37 °C at 180 rpm. The culture was decanted into 450 mL centrifuge tubes and centrifuged at 11000 rpm for 15 minutes at 4°C in a fiberlite F10B 6X500 rotor. The supernatant was then transferred into new tubes and centrifuged for 15 minutes at 11000 rpm at 4°C in a fiberlite F10B 6X500 rotor. The upper 80 % of the supernatant was mixed with 20% v/v of 25 % w/v PEG6000/2.5 M NaCl in a new tube and left to precipitate for 15 minutes at 4 °C. They were then centrifuged for 15 minutes at 11000 rpm at 4 °C in a fiberlite F10B 6X500 rotor. The supernatant was discarded and the pellet was resuspended in 1 mL 50 mM phosphate buffer pH 8 and transferred into 1.5 mL eppendorf tubes. These were centrifuged at 14000 rpm for 5 minutes at 4 °C in a bench top centrifuge (Spectrafuge 16M, Labnet) to pellet the remaining cells. The supernatant was transferred into a new tube and precipitated with 20% v/v of 25 % w/v PEG6000/2.5 M NaCl for 15 minutes at 4 °C. These were then centrifuged at 14000 rpm for 10 minutes at 4 °C in a bench top centrifuge (Spectrafuge 16M, Labnet) and the supernatant discarded. The pellet was resuspended in 100 µL 50 mM phosphate buffer pH 8.

2.2.1.4. Optimising precipitation time for M13 bacteriophage production

Four hundred mL of autoclaved LB medium in a 2.5 L flask containing tetracycline to a final concentration of 5 µg/mL was inoculated with 500 µL of Top10F' *E. coli* and 5 µL of 13 mg/mL wt M13. The culture was then incubated overnight at 37 °C at 180 rpm. The culture was decanted into 450 mL centrifuge tubes and centrifuged at 11000 rpm for 15 minutes at 4 °C in a fiberlite F10B 6X500 rotor. The supernatant was then transferred into new tubes and centrifuged for 15 minutes at 11000 rpm at 4 °C in a fiberlite F10B 6X500 rotor. The upper

80 % of the supernatant was mixed with 20% v/v of 25 % w/v PEG6000/2.5 M NaCl in a new tube and left to precipitate for 5/30/45/60/120 minutes at 4 °C. These samples were then centrifuged for 15 minutes at 11000 rpm at 4 °C in a fiberlite F10B 6X500 rotor. The supernatant was discarded and the pellet was resuspended in 1 mL 50 mM phosphate buffer pH 8 and transferred into 1.5 mL eppendorf tubes. These were centrifuged at 14000 rpm for 5 minutes at 4 °C in a bench top centrifuge (Spectrafuge 16M, Labnet) to pellet the remaining cells. The supernatant was transferred into a new tube and precipitated with 20% v/v of 25 % w/v PEG6000/2.5 M NaCl for 5/30/45/60/120 minutes at 4 °C. These were then centrifuged at 14000 rpm for 10 minutes at 4 °C in a bench top centrifuge (Spectrafuge 16M, Labnet) and the supernatant discarded. The pellet was resuspend in 100 µL 50 mM phosphate buffer pH 8.

2.2.1.5. Measurement of M13 bacteriophage concentration

A Jasco (Japan) V550 UV/Vis-Spectrophotometer was used to measure the concentration of the M13 bacteriophage and a 0.3 cm pathlength quartz cuvette (Starna, Essex, UK) was used. The parameters used can be seen in table 2.1.

Table 2.1 - UV/Vis-Spectrophotometer (Jasco V550 UV/Vis spectrophotometer) parameters

Parametric mode	Abs
Response	Medium
Band width	1 nm
Scanning speed	200 nm/min
Start	800 nm
End	200 nm
Data pitch	0.5 nm

The extinction coefficient of M13 bacteriophage is $3.84 \text{ cm}^{-2}/\text{mg}$ at 269 nm (Niu *et al.*, 2008). The M13 sample was diluted using 50 mM phosphate buffer (pH 8.0) and the concentration was determined using the Beer Lambert's Law (see Equation 1.1) which was rearranged to provide the concentration of the M13 bacteriophage:

Equation 2.1 - Rearranged Beer-Lambert law

$$C = \frac{A}{\epsilon l}$$

2.2.1.6. Collection of LD data

After each M13 bacteriophage culture, the LD spectra of the purified bacteriophage was recorded using Jasco (Japan) J715 spectropolarimeter and a Couette flow cell. This ensured that bacteriophage was present in the sample and that the correct LD signal was produced.

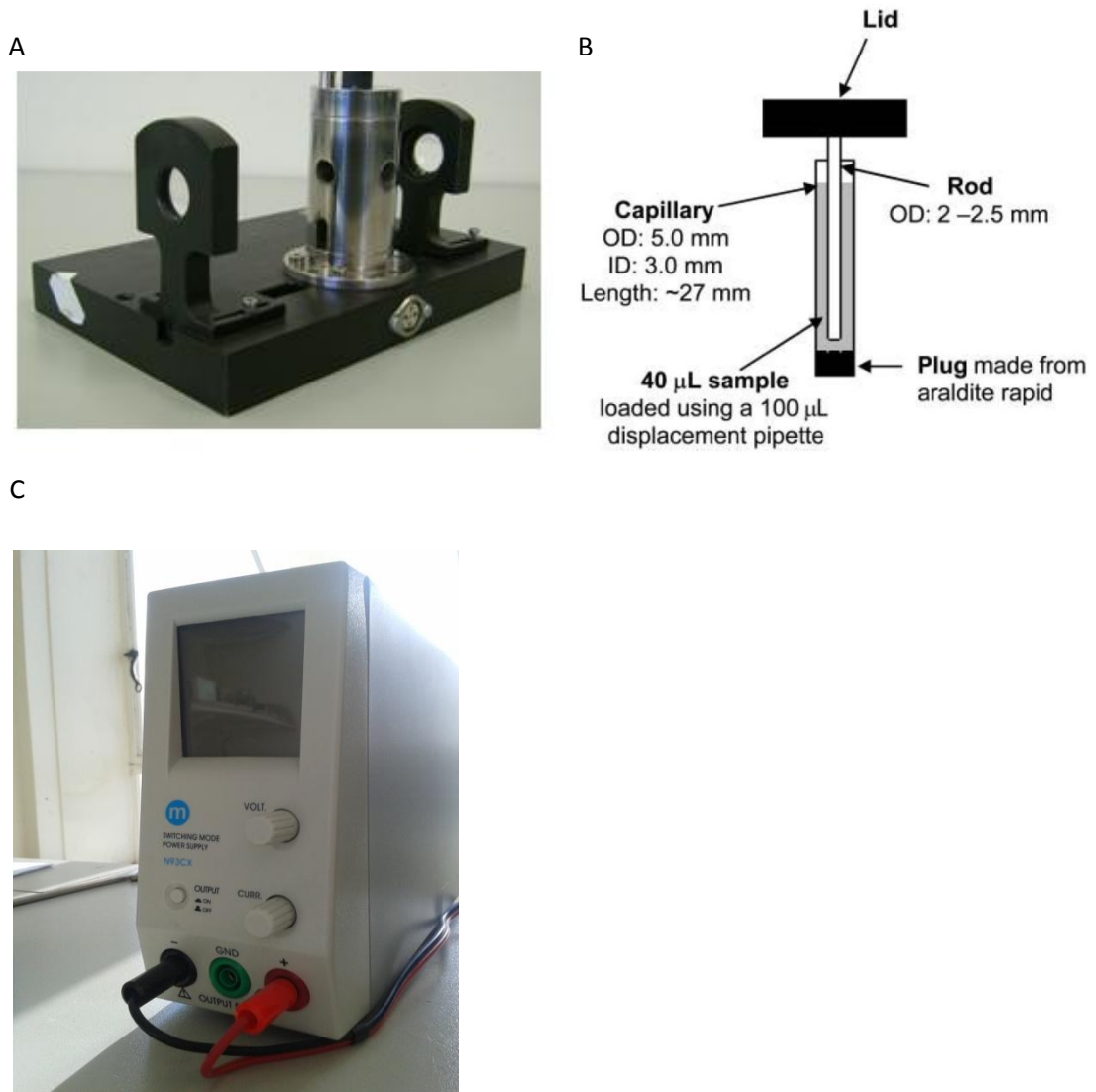


Figure 2.1 - Components of the LD instrument

A) Is a Couette Flow Cell (photographed by Julia Kraemer). B) Capillary and rod used to produce shear flow in the LD. Reproduced from Marrington *et al.* (2004). C) The power supply is provided by 'm', switching mode power supply, model N93CX (photographed by Julia Kraemer).

A Couette containing the sample was placed into the spectropolarimeter and a quartz rod placed inside (figure 2.1 A and B). A motor is attached to the Couette and rotates the Couette, causing a state of continuous flow. The power supply is provided by 'm', switching mode power supply, model N93CX (figure 2.1 C). For each experiment, a baseline (non-rotating capillary) was collected and then subtracted from the signal and the signal was zeroed at 350 nm. All of the rotating signals were recorded at 3V. The parameters used can be seen in table 2.2 (see figure 2.2 for LD spectra). All LD data was processed using the Spectra Analysis program (version 1.53.04 Build 1).

Table 2.2 - Jasco (Japan) J-715 spectropolarimeter parameters used to gather LD spectra.

Sensitivity	Standard (0.1 Δ OD)
Start	350 nm
End	190 nm
Data pitch	1 nm
Scanning mode	Continuous
Scanning speed	200 nm/min
Response	1 second
Band width	2 nm
Accumulation	1

2.2.1.7. Calibration of LD instrument

Obtaining an LD signal is an essential part of the assay and hence it was important to determine the dynamic range of the instrument. Similarly high concentrations can cause interference by background emissions resulting in a distorted spectrum. Different dilutions from the same M13 stock were made and their LD spectrum was measured with 5 V applied to the motor of the LD Couette.

The results were compiled (figure 2.2) and analysed to find out the optimum concentration at which characteristic M13 peaks could be visualised in the LD signal. The parameters used were the same as those used in table 2.2. The LD signal produced from 0.373 mg/mL was the optimal concentration for obtaining LD data because all of the peaks can be seen clearly. At

high concentrations the second peak is lost due to the high tension being so high, and this happens when there is too much absorbance and scattering. Figure 2.3 also shows that there is a strong linear relationship between the M13 concentration and LD signal at 280 nm.

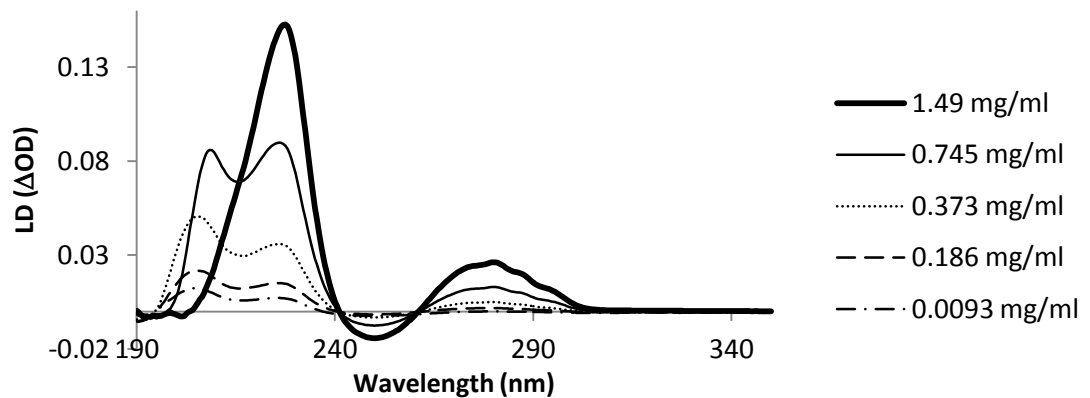


Figure 2.2 - LD spectra of various dilutions of M13 bacteriophage

Graph shows the LD signals of various dilutions from the same M13 bacteriophage stock.

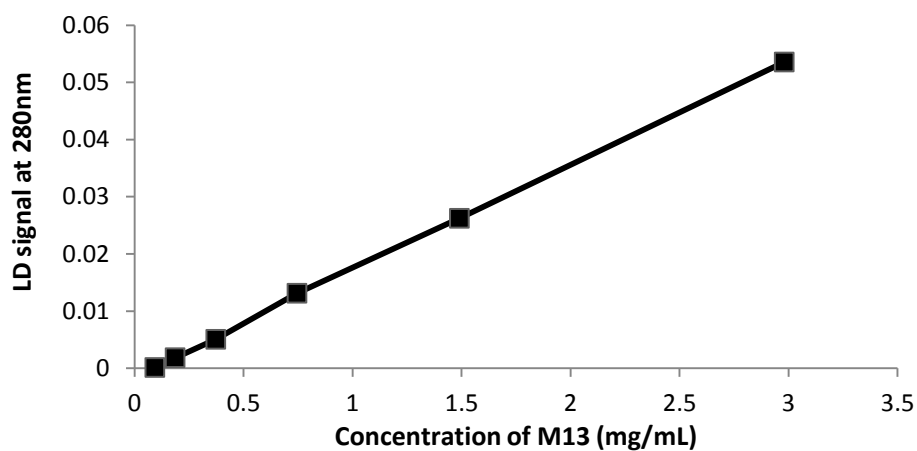


Figure 2.3 - LD signal at 280 nm for various dilutions of M13 bacteriophage

Plot showing change in LD signal with change in concentration of wt M13.

When the LD readings at 280 nm for different concentrations were plotted, these data showed a linear relationship (figure 2.3). This indicates that LD could be used to determine the concentration of M13 bacteriophage in a sample.

2.2.2. Labelling of M13 bacteriophage with extrinsic chromophores

2.2.2.1. Labelling M13 bacteriophage with fluorescamine

A 10 mg/mL fluorescamine (Invitrogen, California USA) solution was freshly prepared by dissolving 10 mg of fluorescamine in 1 mL of DMSO (Fisher Scientific, New Hampshire, USA). A volume of 20 μ L of fluorescamine solution was mixed with 0.8 mL of 2.5 mg/mL wt M13 in a test tube. The mixture was then incubated for 1 hour at room temperature with continuous mixing. The reaction mixture was then dialysed using 3,500 molecular weight cut off (MWCO) dialysis tubing (Sigma-Aldrich, Missouri, USA) in the presence of 50 mM phosphate buffer (pH 8), to remove unbound dye. Dialysis was firstly carried out for 1 hour, followed by repeating it overnight and replacing the 50 mM phosphate buffer pH 8 with 250 mL of fresh buffer. The dialysed solution was stored in the absence of light at 4°C.

2.2.2.2. Labelling M13 bacteriophage with rhodamine B isothiocyanate

A 10 mg/mL stock of rhodamine B isothiocyanate (rhodamine) (Invitrogen, California, USA) was made in DMSO (Fisher Scientific, New Hampshire, USA). A volume of 20 μ L of the dye was added to 0.8 mL of 2.5 mg/mL wt M13. This was incubated for 1 hour at room temperature with continuous mixing in the absence of light. This was then dialysed for 1 hour using 3,500 KDa MWCO dialysis tubing (Sigma-Aldrich, Missouri, USA) in 250 mL of 50 mM phosphate buffer pH 8 at 4°C, and then repeated overnight after replacing the buffer.

2.2.2.3. Labelling M13 bacteriophage with fluorescein isothiocyanate isomer 1

A 10 mg/mL stock of fluorescein isothiocyanate isomer 1 (FITC) (Sigma-Aldrich, Missouri, USA) was made in DMSO (Fisher Scientific, New Hampshire, USA). A volume of 100 μ L of the dye was added to 1 mL of 2 mg/mL wt M13. This was incubated for 1 hour at room temperature in the absence of light with continuous mixing. The solution was then dialysed for 1 hour using 3

500 KDa MWCO dialysis tubing (Sigma-Aldrich, Missouri, USA) in 250 mL of 50 mM phosphate buffer pH 8 at 4°C. The dialysis was repeated overnight after replacing the buffer.

2.2.2.4. Labelling M13 bacteriophage with 4-chloro-7-nitrobenzofurazan

A 10 mg/mL stock of 4-chloro-7-nitrobenzofurazan (NBD chloride) (Invitrogen, California, USA) was made in DMSO (Fisher Scientific, New Hampshire, USA). A volume of 20 µL of the dye was added to 0.8 mL of 2.5 mg/mL wt M13. This was incubated for 1 hour at room temperature in the absence of light with continuous mixing. Following this, the solution was dialysed for 1 hour using 3,500 MWCO dialysis tubing (Sigma-Aldrich, Missouri, USA) in 250 mL of 50 mM phosphate buffer pH 8 at 4°C and this was repeated overnight after replacing the buffer.

2.2.2.5. Labelling M13 bacteriophage with black hole quencher-10

A 10 mg/mL stock of black hole quencher-10 (BHQ-10) (Biosearch Technologies, California, USA) was made in DMSO (Fisher Scientific, New Hampshire, USA). A volume of 20 µL of the dye was added to 0.8 mL of 2.5 mg/mL wt M13. This was incubated for 1 hour at room temperature in the absence of light with continuous mixing. Following this, the solution was dialysed for 1 hour using 3,500 MWCO dialysis tubing (Sigma-Aldrich, Missouri, USA) in 250 mL of 50 mM phosphate buffer pH 8 at 4°C and this was repeated overnight after replacing the buffer.

2.2.2.6. Labelling M13 bacteriophage with eosin-5-maleimide

A starting material of 2 mg of wt M13 was mixed with 0.1 M phosphate buffer, pH 7.5 to give a volume of 400 µL. A 1 mg/mL stock concentration of N-succinimidyl-S-acetyl thioacetate (SATA) (Fisher Scientific, New Hampshire, USA) was made using DMSO (Fisher Scientific, New Hampshire, USA), and a 0.3:1 molar ratio of SATA (Fisher Scientific, New Hampshire, USA) to p8 coat protein was added to the wt M13 and incubated for 1 hour at room temperature. The reaction was quenched by adding 10 % v/v of 50 mM ethylene diamine tetra acetic acid

(EDTA)/2.5 M Hydroxylamine solution pH 7.0 and left to incubate for another 15 minutes. To separate the M13 bacteriophage from the SATA, 100% v/v of 25 % w/v PEG6000/2.5 M NaCl was added and left on ice. After 15 minutes the M13 solution was centrifuged in a bench top centrifuge (Spectrafuge 16M, Labnet) for 10 minutes at 14000 rpm. The pellet was resuspended in 200 μ L conjugation buffer, (50 mM phosphate buffer, 150 mM NaCl, 5 mM EDTA, pH 7) and the supernatant was discarded.

A 10 mg/mL solution of eosin-5-maleimide (Invitrogen, California, USA) was freshly prepared by dissolving 1 mg of eosin-5-maleimide in 100 μ L of DMSO. Of this 10 mg/mL stock of eosin-5-maleimide solution, 100 μ L was taken and mixed with 200 μ L of M13 bacteriophage which had been modified using SATA. The mixture was then incubated overnight at 4°C. A 1 mg/mL solution of N-ethylmaleimide (NEM) (Thermo Scientific, New Hampshire, USA) was added to the M13 and dye solution to provide a 0.3:1 molar ratio of NEM to p8 coat protein, and left to incubate at room temperature for 15 minutes. 100% v/v of 25 % w/v PEG6000/2.5 M NaCl was added to the M13 solution and left on ice. After 15 minutes the M13 and dye solution was centrifuged in a bench top centrifuge (Spectrafuge 16M, Labnet) for 10 minutes at 14000 rpm. The pellet was resuspended in 500 μ L 50 mM phosphate buffer, pH 8 and the supernatant was discarded.

2.2.2.7. Measurement of labelling efficiency

To measure the absorbance of the chromophores as well as the concentration of the M13, a Jasco (Japan) V-550 spectrophotometer was used.

UV/Vis absorption spectra were measured at room temperature in a 0.3 cm pathlength quartz cuvette (Starna, Essex, UK). The parameters used are shown in table 2.3. Spectra of 50 mM phosphate buffer, pH 8 was also collected and used as the baseline for each experiment.

Table 2.3 - UV/Vis-Spectrophotometer (Jasco V550 UV/Vis spectrophotometer) parameters

Parametric mode	Abs
Response	Medium
Band width	1 nm
Scanning speed	200 nm/min
Start	800 nm
End	200 nm
Data pitch	0.5 nm

To measure the labelling efficiency, firstly the concentration of M13 was calculated and this was done by taking the absorbance value at 269 nm and inserting it into the Beer Lambert Law equation(see Equation 1.1), which was rearranged to provide the concentration (see Equation 2.1). It is assumed that the binding of the dye does not change the extinction coefficient.

The p8 concentration and the label concentration were calculated for each sample with extinction coefficients for the labels given in table 4.2. The labelling efficiency was calculated assuming 2700 p8 coat proteins on each M13 bacteriophage are available for reacting with the chromophores. This could then be expressed as a percentage of available p8 coat protein.

Equation 2.2 - Labelling efficiency of M13

$$Labelling\ Efficiency = \left(\frac{C\ label}{C\ M13 \times 27} \right) \%$$

Where;

C label is the concentration of label

C M13 is the-concentration of M13

2.2.2.8. LD measurements of chromophore labelled M13

The LD experiments were carried out using a Jasco (Japan) J-715 (LD) spectropolarimeter and processed using the Spectra Analysis program (version 1.53.04 Build 1). LD spectral data were recorded at room temperature with the parameters in table 2.4. For each experiment, a baseline (non-rotating capillary) was collected and then subtracted from the signal and the signal was zeroed at 800 nm. All of the rotating signals were recorded at 3V.

Table 2.4 - Jasco (Japan) J-715 spectropolarimeter parameters used to record LD spectra

The parameters used when using the Jasco (Japan) J-715 (LD) spectropolarimeter to measure the M13 labelled with chromophores.

Sensitivity	Standard (0.1 ΔOD)
Start	800 nm
End	190 nm
Data pitch	1 nm
Scanning mode	Continuous
Scanning speed	200 nm/min
Response	1 second
Band width	2 nm
Accumulation	3

2.2.2.9. Fluorescence measurements

Fluorescence was measured using a luminescence spectrometer (Perkin Elmer Instruments LS 55). The sample was placed into a 0.3 cm pathlength cuvette and the fluorescence was measured. The parameters used differed depending on which chromophore was used (table 2.5).

Table 2.5 - Fluorescence parameters

	Parameters					
Sample	Start (nm)	End (nm)	Ex Slit (nm)	Em Slit (nm)	Excitation (nm)	Scan speed (nm/min)
wt M13	290	500	2.5	2.5	280	100
M13+fluorescamine	385	650	5	5	381	200
Fluorescamine	385	650	5	5	381	200
M13+rhodamine	500	900	5	5	556	200
Rhodamine	500	900	5	5	556	200
M13+NBD chloride	340	650	5	5	337	200
NBD chloride	340	650	5	5	337	200
M13+eosin-5-	525	650	2.5	2.5	520	100
Eosin-5-maleimide	525	650	2.5	2.5	520	100

2.2.3. Conjugation of wt M13 with purified goat-anti-mouse

The assay requires M13 to detect specific targets, to achieve this, the p8 coat proteins on M13 bacteriophage need to be covalently linked to antibodies. In a realistic setting this antibody would be one raised to an antigen on a pathogen such as *E. coli* O157. But to simply show proof of concept goat anti-mouse (GAM) was used as the antibody. Heterobifunctional

crosslinkers (such as SATA and succinimidyl-4-(N-maleimidomethyl)cyclohexane-1-carboxylate (SMCC)) are used to introduce reactive groups to p8 and the GAM, which will result in the formation of a covalent bond between the two molecules.

2.2.3.1. Thiolation of wt M13 bacteriophage (method 1)

The method for thiolation was a modified protocol of Aslam and Dent (1998). A starting sample of 2 mg of wt M13 was mixed with 0.1 M phosphate buffer, pH 7.5 to give a volume of 400 μ L. A 0.3:1 molar ratio of SATA (Fisher Scientific, New Hampshire, USA) to p8 coat protein was added to the wt M13 and incubated for 1 hour at room temperature. The SATA introduces a thiol group to the p8 coat protein on the bacteriophage. The reaction was quenched by adding 10 % v/v of 50 mM EDTA/ 2.5 M Hydroxylamine solution pH 7 and left to incubate for another 15 minutes. To separate the bacteriophage from the SATA, the sample was mixed with conjugation buffer (50 mM phosphate buffer, 150 mM NaCl, 5 mM EDTA, pH 7) to make a volume of 20 mL and then concentrated in a centrifugal tube (Vivaspin centrifugal concentrator from Sigma-Aldrich, Missouri, USA) in a Beckman GS-6R centrifuge, using a GH3.8 rotor at 3750 rpm at 4°C. When the M13 solution was reduced in volume to 5 mL, another 15 mL of conjugation buffer was added and concentrated again until the volume reached 1 mL. The absorbance of the sample was measured to calculate the concentration of recovered M13.

2.2.3.2. Maleimide derivatisation of affinity purified goat anti-mouse antibody

The GAM antibody (Abcam, Cambridge, UK) is provided as a lyophilized powder. 1 mg of the powder was dissolved in 1 mL distilled water. The antibody was then desalted using a PD-10 desalting column (GE Healthcare, Buckinghamshire, UK), which was first equilibrated with 25 mL of 0.1 M phosphate buffer pH 7.5. The 1 mL GAM sample and 1.5 mL 0.1 M phosphate buffer pH 7.5 were applied and allowed to enter the packed bed completely. The GAM sample was eluted with 2.5 mL 0.1 M phosphate buffer pH 7.5.

The absorbance of the eluted GAM sample was measured to calculate the GAM starting concentration ($\epsilon_{280\text{nm}}$, GAM = 1.4 mg⁻¹ mL cm⁻¹ (information provided by Abcam, Cambridge, UK)). This was used to calculate the required amount of SMCC (Merck Millipore, Darmstadt, Germany) in DMSO (Fisher Scientific, New Hampshire, USA) solution to provide a 10x molar excess to GAM. The SMCC reacts with amine groups to introduce a maleimide group on to the antibody. After 1 hour incubation at room temperature the solution was quenched with 1 % v/v of 10 mg/mL glycine (Fisher Scientific, New Hampshire, USA) made in conjugation buffer and left for 15 minutes.

A PD-10 column (GE Healthcare, Buckinghamshire, UK) was used to separate the maleimide-derivatised GAM from the SMCC after first being equilibrated with 25 mL of conjugation buffer. After the sample was eluted its absorbance was measured at 280 nm to calculate the recovered concentration of GAM.

2.2.3.3. Bioconjugation

The wt M13 and GAM were mixed together and left to incubate overnight at 4 °C. A 1 mg/mL solution of NEM (Thermo Scientific, New Hampshire, USA) was prepared and a 0.3:1 molar ratio of NEM was added per mole of p8 coat protein on the M13 to the overnight mixture containing the M13 conjugate with GAM. The sample was then concentrated in a centrifugal concentrator (Vivaspin centrifugal concentrator from Sigma-Aldrich, Missouri, USA) in a Beckman GS-6R centrifuge, using a GH3.8 rotor at 3750 rpm at 4°C until only 2 mL remained. The conjugated wt M13 was then precipitated by adding an autoclaved 20% v/v PEG6000/2.5 M NaCl solution until a visible precipitate formed (approx. 320 µL). Finally, the sample was centrifuged for 5 minutes at 14000 rpm in a bench top centrifuge (Spectrafuge 16M, Labnet). The supernatant was discarded and the pellet was resuspended in phosphate buffer pH 8. The

obtained sample contained M13 bacteriophage with GAM antibodies covalently attached to it. This was stored at 4°C, no preservatives were added.

2.2.4. Electron microscopy

Electron microscopes use a beam of highly energetic electrons to observe samples and create an enlarged image. The image is formed by the use of electrostatic and electromagnetic lenses which control the electron beam to focus it at a specific plane. One of the most prevalent forms of electron microscopy is transmission electron microscopy (TEM). An electron beam is focussed upon the sample and many of the electrons pass through the sample. These electrons are gathered by a series of electromagnetic lenses and focussed onto a screen. The screen can comprise of a fluorescent screen or photographic plate or, as is common in modern applications, a charge-coupled device (CCD) camera. A major advantage of using CCDs is that the image can be displayed in real time.

2.2.4.1. Sample preparation

In order to scatter imaging electrons and achieve a good contrast, the samples were stained. Staining the samples with aqueous or alcoholic solutions of heavy metals is a common practice for biological specimens since many biological samples are nearly transparent to electrons.

2.2.4.2. Preparation of carbon-coated grids for electron microscopy

2.2.4.2.1. Glow discharge of the carbon-coated copper grids

The carbon-coated grids were glow discharged prior to negative staining. Glow discharge is formed by applying a potential difference between two electrodes that are inserted in a cell that is filled with an inert gas at a certain pressure. Glow discharge makes the carbon coated electron microscopy grids hydrophilic in preparation for the negative staining since the sample will be applied onto the grids. In order to glow discharge the carbon coated grids, the grids

were placed carbon side up onto a glass slide and inserted in the glow discharge instrument for 20 seconds at lower settings (10 mA, pale purple glow).

2.2.4.2.2. Staining and visualisation

A 1% uranyl acetate stock solution (UA) was prepared and stored at 4 °C in the dark when the solution was not used. The stock was prepared by diluting a 4% UA solution. UA contains insoluble salts and consequently 1 mL of the 1% stock solution was filtered using a 0.2 µm filter and kept in a 1.5 mL eppendorf. There are several methods for negative staining the sample. The method used in this study is described below.

Firstly a 50 µL sample of 0.3 mg/mL of M13 conjugated with GAM was prepared. A filter paper was then placed in a petri dish, a grid was carefully taken by the rim edge of the copper mesh using a pair of tweezers provided with a rubber ring which ensured that the grid was not moving while the sample was being applied and the sample was applied onto the carbon side of the grid. Five µL of the sample mixture was then placed onto the carbon side for 1 minute and the sample was immediately stained by washing with three drops of the 1% UA solution. The grid was oriented 45° with respect to the surface as the wash should be gentle. The last drop of the 1% UA solution was left for 45 seconds before the excess liquid was blotted from the sample by gently touching/dragging the grid parallel or perpendicular to the filter paper. The grid was then released from the tweezers and the tip of the tweezers were dried with filter paper. Samples were stored in a cool dry place, in the absence of light. The grids were then viewed in a (Joel JEM-2010, Tokyo, Japan) TEM at 15,000X, 25,000X, 30,000X and 40,000X objective magnification.

2.2.5. Conjugation of wt M13 with goat anti-*E. coli* O157 and BHQ-10

To detect *E. coli* O157 in this current assay a goat anti-*E.coli* O157 antibody (GAE) (Thermo Scientific, New Hampshire, USA) was required and was conjugated on to the M13

bacteriophage. For a multiplexed assay various chromophores would be enlisted to detect different pathogens, and in this case BHQ-10 dye was chosen as the chromophore.

2.2.5.1. Thiolation of wt M13 bacteriophage (method 2)

This thiolation method differs from the one described in section 2.2.3.1; it uses a much larger molar ratio of SATA and a PD-10 desalting column was employed. A starting material of 2 mg of wt M13 was prepared with 0.1 M phosphate buffer, pH 7.5 to gain a volume of 1 mL. A volume of 50 μ L of 1% v/v tween 20 was added to give a final concentration of 0.05%. A 50 mg/mL stock concentration of SATA (Fisher Scientific, New Hampshire, USA) was made using DMSO (Fisher Scientific, New Hampshire, USA) and a 50:1 molar ratio of SATA to p8 coat protein was added to the M13 solution and incubated for 1 hour at room temperature. The reaction was quenched by adding 10 % v/v of 50 mM EDTA/ 2.5 M Hydroxylamine solution pH 7 and left to incubate for another 15 minutes.

To separate the thiolated M13 from the SATA a PD-10 desalting column (GE Healthcare, Buckinghamshire, UK) was used. The PD-10 desalting column was firstly equilibrated with 25 mL of conjugation buffer (50 mM phosphate buffer, 150 mM NaCl, 5 mM EDTA, pH 7) and secondly the M13 solution was added with the volume made up to 2.5 mL with conjugation buffer. M13 was eluted with 3.5 mL conjugation buffer.

2.2.5.2. Maleimide derivatisation of goat anti-*E. coli* O157

A 5.5 mg/mL stock of GAE antibody (Thermo Scientific, New Hampshire, USA) was diluted in 0.1 M phosphate buffer pH 7.5 to provide a final concentration of 0.5 mg/mL. The antibody was desalted using a PD-10 desalting column (GE Healthcare, Buckinghamshire, UK), which was first equilibrated with 25 mL of 0.1 M phosphate buffer pH 7.5. The 1 mL GAE sample was made up to 2.5 mL with 0.1 M phosphate buffer pH 7.5 and applied to the PD-10 desalting column (GE Healthcare, Buckinghamshire, UK). The GAE sample was eluted with 3.5 mL 0.1 M

phosphate buffer pH 7.5. A 1 mg/mL stock concentration of SMCC (Merck Millipore, Darmstadt, Germany) was made in DMSO (Fisher Scientific, New Hampshire, USA), and a 10:1 molar ratio of SMCC to GAE was added to the GAE solution. This solution was left to incubate for 1 hour at room temperature. The SMCC reacts with amine groups to introduce a maleimide group on to the antibody. The solution was quenched with a 1 % v/v solution of glycine (Fisher Scientific, New Hampshire, USA) in conjugation buffer (10 mg/mL) and left for 15 minutes. A PD-10 column (GE Healthcare, Buckinghamshire, UK) was then used to separate the maleimide-derivatised GAE from the SMCC after first being equilibrated with 25 mL of conjugation buffer. The GAE solution was made up to 2.5 mL with conjugation buffer and added to the column and eluted in 3.5 mL conjugation buffer.

2.2.5.3. Bioconjugation and labelling with BHQ-10

The eluted M13 solution was mixed with the eluted GAE solution and incubated overnight at 4°C.

A mass of 0.5 mg BHQ-10 (Biosearch Technologies, California, USA) was dissolved in 180 µL N-(2-aminoethyl) maleimide (AEM) (Sigma-Aldrich, Missouri, USA) solution (1 mg/mL stock solution made in 0.1 M phosphate buffer pH 7.5). This was incubated at room temperature for 1 hour in the absence of light.

This BHQ-10 solution was added to the M13-GAE solution and incubated at room temperature for 1 hour in the absence of light with continuous mixing. Following this, 100% v/v of 25 % w/v PEG6000/2.5 M NaCl was added to the M13 conjugated with GAE and BHQ-10 solution and kept in the absence of light at 4°C for 1 hour. The solution was aliquoted into 1.5 mL eppendorf tubes and centrifuged in a bench top centrifuge (Spectrafuge 16M, Labnet) for 10 minutes at 14000 rpm. The pellets were resuspended in a total volume of 1 mL of 50 mM phosphate buffer, pH 8 and the supernatant was discarded.

2.2.6. Detection of *E. coli* O157 using M13 bacteriophage and LD

To detect the heat-killed *E. coli* O157 (KPL, Maryland, USA), M13 conjugated with GAE and BHQ-10 (double labelled M13) was used as the reagent and LD was used as the spectroscopic technique to detect the bacteria.

2.2.6.1. *E. coli* O157 preparation

The heat-killed *E. coli* O157 (KPL, Maryland, USA) was provided in a lyophilized form and contained 1.15×10^9 cells/mL. To prepare the *E. coli* O157 it was dissolved in 1.15 mL of water and aliquoted into separate eppendorfs ready for storage at -18°C . When required an aliquot was thawed at room temperature ready for use. A 0.8 μL volume of heat-killed *E. coli* O157 from the stock provided 10^7 cells/mL. To provide 10^6 and 10^5 cells/mL a 1 in 10 and 1 in 100 dilution was made respectively with water.

2.2.6.2. *E. coli* XL10 preparation

For a control, *E. coli* XL10 cells were used in the assay. A 100 μL culture was provided from Dr Mohammed Jamshad at the University of Birmingham. The 100 μL culture was thawed at room temperature, centrifuged at 14000 rpm for 1 minute in a bench top centrifuge (Spectrafuge 16M, Labnet). The supernatant was discarded and the pellet was resuspended in 100 μL of 50 mM phosphate buffer pH 8. This solution was centrifuged again at 14000 rpm for 1 minute and the supernatant was discarded and the pellet was resuspended in 100 μL of 50 mM phosphate buffer pH 8. The absorbance of the *E. coli* XL10 cells was measured using a Jasco (Japan) V-550 spectrophotometer at 600 nm to calculate the number of cells per mL. An absorbance of 1.0 at 600 nm is equal to approximately 8.8×10^8 cells/mL (Brown, 2010). An absorbance of 0.13 was measured at 600 nm in a cuvette with a pathlength of 0.3 cm.

Therefore using the Beer-Lambert law;

$$C_2 = C_1 \left(\frac{A_2}{A_1} \right) \left(\frac{l_1}{l_2} \right) = \left(\frac{0.13}{1.0} \right) \times \left(\frac{1.0 \text{ cm}}{0.3 \text{ cm}} \right) \times 8.8 \times 10^8 \text{ cells/mL} = 3.8 \times 10^8 \text{ cells/mL}$$

Where;

C_2 is the *E. coli* concentration,

$A_2 = 0.13$ is the measured absorbance,

$l_2 = 0.3 \text{ cm}$ is the measured pathlength

$C_1 = 8.8 \times 10^8 \text{ cells/mL}$, $A_1 = 1.0$, $l_1 = 1.0 \text{ cm}$

A total volume of 80 μL was required for the LD measurements, therefore:

$$\left(\frac{1 \times 10^7}{3.8 \times 10^8} \right) \times 80 \mu\text{L} = 2.1 \mu\text{L of } E. coli \text{ XL10 cells was required to provide } 10^7 \text{ cells/mL}$$

2.2.6.3. Sample preparation

Each sample was made in triplicate and can be seen in table 2.6.

Table 2.6 - Assay constituents for the detection of *E. coli* O157

Samples	Reagents			<i>E. coli</i> O157 (μL)			<i>E. coli</i> XL10 10^7 cells/mL (μL)
	Double labelled M13 (M13-GAE-BHQ- 10) (3.6 mg/mL) (μL)	0.1M phosphate buffer pH 7.5 + tween (0.05%) (μL)		10^7 cells/mL	10^6 cells/mL	10^5 cells/mL	
Control 1	20	60					
Control 2	20	57.9					2.1
1	20	59.2	0.8				
2	20	59.2			0.8		
3	20	59.2				0.8	

2.2.6.4. LD measurements

The LD experiments were carried out using a Jasco (Japan) J-715 (LD) spectropolarimeter and processed using the Spectra Analysis program (version 1.53.04 Build 1). LD spectral data were recorded at room temperature with the parameters in table 2.7. For each experiment, a

baseline (non-rotating capillary) was collected and then subtracted from the signal and the signal was zeroed at 800 nm. All of the rotating signals were recorded at 3V.

Table 2.7 - Jasco (Japan) J-715 spectropolarimeter parameters used to gather LD spectra

The parameters used when using the Jasco (Japan) J-715 (LD) spectropolarimeter as part of a detection system to detect *E. coli* O157.

Sensitivity	Standard (0.1 ΔOD)
Start	800 nm
End	190 nm
Data pitch	0.5 nm
Scanning mode	Continuous
Scanning speed	500 nm/min
Response	1 second
Band width	5 nm
Accumulation	1

2.2.7. Conjugation of wt M13 with anti-FITC antibody

The M13 aggregation assay was utilised for the detection of small molecules. Two reagents were required for this assay; M13 conjugated with target molecule and M13 conjugated with anti-target antibody. To show proof of concept the target antigen used in this assay was fluorescein. This meant that one reagent required would be M13 labelled with fluorescein and another was M13 conjugated with anti-fluorescein. Fluorescein isothiocyanate isomer 1 (FITC) (Invitrogen, California, USA) was used to label M13 (see section 2.2.2.3. for method) and anti-FITC antibody (Invitrogen, California, USA) was used to conjugate another sample of M13.

2.2.7.1. Thiolation of wt M13 bacteriophage (method 2)

This method is the same as described in section 2.2.5.1. A starting material of 2 mg of wt M13 was prepared with 0.1 M phosphate buffer, pH 7.5 to gain a volume of 400 μL. A 50 mg/mL stock concentration of SATA (Fisher Scientific, New Hampshire, USA) was made using DMSO (Fisher Scientific, New Hampshire, USA) and a 50:1 molar ratio of SATA to p8 coat protein was added to the M13 solution and incubated for 1 hour at room temperature. The reaction was

quenched by adding 10 % v/v of 50 mM EDTA/ 2.5 M Hydroxylamine solution pH 7.0 and left to incubate for another 15 minutes at room temperature.

To separate the thiolated M13 from the SATA a PD-10 desalting column (GE Healthcare, Buckinghamshire, UK) was used. The PD-10 desalting column was firstly equilibrated with 25 mL of conjugation buffer and secondly the M13 solution was added with the volume made up to 2.5 mL with conjugation buffer. The M13 was eluted with 3.5 mL conjugation buffer.

2.2.7.2. Maleimide derivatisation of anti-FITC antibody

In an attempt to conjugate each M13 bacteriophage with 20 rabbit (polyclonal) anti-FITC antibodies (Invitrogen, California, USA), 351 μ L of 1 mg/mL anti-FITC antibody was initially added to 649 μ L 0.1 M phosphate buffer pH 7.5. A 1 mg/mL stock concentration of SMCC (Merck Millipore, Darmstadt, Germany) was made in DMSO (Fisher Scientific, New Hampshire, USA), and a 10:1 molar ratio of SMCC to anti-FITC antibody was added to the anti-FITC antibody solution. This solution was left to incubate for 1 hour at room temperature. The SMCC reacts with amine groups to introduce a maleimide group on to the antibody. The solution was quenched with a 1 % v/v solution of glycine (Fisher Scientific, New Hampshire, USA) in conjugation buffer (10 mg/mL) and left for 15 minutes at room temperature. A PD-10 column (GE Healthcare, Buckinghamshire, UK) was then used to separate the maleimide-derivatised anti-FITC antibodies from the SMCC after first being equilibrated with 25 mL of conjugation buffer. The anti-FITC antibody solution was made up to 2.5 mL with conjugation buffer and added to the column and eluted in 3.5 mL conjugation buffer.

2.2.7.3. Bioconjugation

The eluted M13 solution was mixed with the eluted anti-FITC antibody solution and incubated overnight at 4°C. A 1 mg/mL solution of NEM (Thermo Scientific, New Hampshire, USA) was made in conjugation buffer and a 10:1 molar ratio of NEM to p8 coat protein was added to the

M13 and anti-FITC antibody solution and incubated at room temperature for 15 minutes. This solution was then concentrated in a centrifugal tube (Vivaspin centrifugal concentrator, Sigma-Aldrich, Missouri, USA) in a Beckman GS-6R centrifuge, using a GH3.8 rotor at 3750 rpm at 4°C until the volume was reduced to 3 mL. This volume was required in order to put the solution through a size exclusion chromatography (SEC) column (HiLoad™ 16/60 Superdex™ 200 Prep grade). This was done to remove any unreacted molecules and free antibodies from the solution. The detectors were set to 269 nm and 280 nm and the flow rate was ~1.0 mL/min. The column was equilibrated overnight in 50 mM phosphate buffer pH 8 with 150 mM NaCl to prevent non-specific binding. The fraction collector was set to collect the appropriate fractions and 3 mL of the sample was injected and ran for several column volumes (~3 hours). The column was then equilibrated in storage buffer before being switched off. A pure sample of M13 conjugated with anti-FITC was then generated as this procedure ensured all contaminants had been removed.

2.2.8. Detection of fluorescein using the M13 bacteriophage aggregation assay

The M13 aggregation assay was utilised for small molecule detection and was used to detect fluorescein. M13 conjugated with anti-FITC antibodies and M13 conjugated with FITC were used as the reagents and LD was used as the spectroscopic technique to detect fluorescein. Varying concentrations of fluorescein were added to the assay to establish the sensitivity of the assay.

2.2.8.1. Fluorescein preparation

A 10 mM stock of fluorescein (Invitrogen, California, USA) was prepared in water for the samples requiring a larger concentration of fluorescein (1 mM, 0.5 mM and 0.2 mM) and was diluted 10 fold to provide lower concentrations (0.1 mM, 0.04 mM, 0.02 mM and 0.01 mM).

2.2.8.2. Rhodamine 6G preparation

A stock of 20 mM rhodamine 6G (Invitrogen, California, USA) was made up in ethanol (70%) and this was diluted 100 fold to 0.2 mM for the assay to provide a final concentration of 0.02 mM.

2.2.8.3. Sample Preparation

For each of the experimental samples the specific volume of 50 mM phosphate buffer pH 8 and 10 mM or 1mM fluorescein (Invitrogen, California, USA) was added to 30 μ L of 0.07 mg/mL M13 conjugated with anti-FITC and left to incubate overnight at 4°C in the absence of light. The following day 30 μ L of 0.08 mg/mL M13 labelled with FITC was added to compete with the free fluorescein and the LD measurements were taken immediately.

The mixture sample consisted of 30 μ L of 0.07 mg/mL M13 conjugated with anti-FITC antibody and 30 μ L of 0.08 mg/mL M13 labelled with FITC and had no fluorescein added.

The rhodamine 6G sample had the addition of 8 μ L of 0.2 mM rhodamine 6G (to provide a final concentration of 0.02 mM) and 12 μ L of 50 mM phosphate buffer pH 8 to 30 μ L of 0.07 mg/mL M13 conjugated with anti-FITC antibody and left to incubate overnight at 4°C in the absence of light. The following day 30 μ L of 0.08 mg/mL M13 labelled with FITC was added and the LD measurements were taken immediately. Each sample was made up 3 times and the LD signal was measured.

Table 2.8 - Assay constituents for the detection of fluorescein

Sample	Reagents				
	0.08 mg/mL M13-FITC (μL)	0.07 mg/mL M13-anti-FITC antibody (μL)	Fluorescein (μL)		0.2 mM Rhodamine 6G (μL)
			10 mM	1 mM	50 mM Phosphate buffer pH 8 (μL)
Mixture	30	30			20
0.02 mM	30	30			8
1 mM	30	30	8		12
0.5 mM	30	30	4		16
0.2 mM	30	30	1.6		18.4
0.1 mM	30	30		8	12
0.04 mM	30	30		3.2	16.8
0.02 mM	30	30		1.6	18.4
0.01 mM	30	30		0.8	19.2

2.2.8.4. LD measurements

The LD experiments were carried out using a Jasco (Japan) J-715 (LD) spectropolarimeter and processed using the Spectra Analysis program (version 1.53.04 Build 1). LD spectral data were recorded at room temperature with the parameters in table 2.9. For each experiment, a baseline (non-rotating capillary) was collected and then subtracted from the signal and the signal was zeroed at 600 nm. All of the rotating signals were recorded at 3V.

Table 2.9 - Jasco (Japan) J-715 spectropolarimeter parameters used to gather LD spectra

The parameters used when using the JASCO J-715 (LD) spectropolarimeter as part of a detection system to detect fluorescein.

Sensitivity	Standard (0.1 ΔOD)
Start	600 nm
End	200 nm
Data pitch	1 nm
Scanning mode	Continuous
Scanning speed	200 nm/min
Response	1 second
Band width	2 nm
Accumulation	6

CHAPTER 3

- OPTIMISATION OF M13

PRODUCTION

3.1. Production of M13 bacteriophage

This project involves the production of a reagent using M13 as a starting point for a number of chemical modification steps. Given that the yields for such reactions are significantly less than 100%, it is clear that the production of sufficient quantities of M13 during the project will be important. In this chapter a number of parameters within the M13 production process are varied to enhance the yield of material and the specific activity.

There are currently two established methods for the production of M13, one method based on the work of Sambrook and Russell (2001) and another method from New England Biolabs (2011). This chapter describes how these two methods were assessed in terms of speed, ease of use, purity, yield of product and its specific activity. It should be noted that previous uses of M13 bacteriophage have been restricted to the area of Molecular Biology where it has been used for things such as bacteriophage display; however in these areas M13 is not required in large quantities (0.1-20 μg) (Kunkel *et al.*, 1986, Liu *et al.*, 2001, Sung and Stratton, 1996). In this project, M13 was required in larger quantities as sufficient functionalised M13 is required to produce an LD signal. To produce a reasonable LD signal approximately 0.4 mg is required; any less than this and not all of the peaks in the LD signal can be identified. If we assume that to get a suitable dose response curve we need 10 points with 3 repetitions, this means 30

separate reactions, which would require 12 mg of M13 bacteriophage. The quantity of M13 bacteriophage produced therefore needed to meet the high demand required for this project.

In this study the yields produced from the method based on Sambrook and Russell (2001) and from the New England Biolabs (2011) method were initially assessed. These two methods each have different limitations. The method based on Sambrook and Russell (2001) requires a filter to remove *E. coli* cells, whereas the New England Biolabs (2011) method uses various centrifugation steps to remove any *E. coli* cells. The method based on Sambrook and Russell (2001) has the benefit of only requiring 2 days in comparison to the New England Biolabs (2011) method, which requires 3 days.

To assess which method was best, a number of parameters were measured. These included the yield and purity of M13 bacteriophage produced in each method. Conventionally M13 concentrations were determined by measuring plaque forming units. This is a very time consuming method, and in this context, we are only interested in whether the M13 aligns and produces an LD signal, not whether it can replicate. We therefore used the inherent LD signal of M13 as a measure of the yield. The LD spectrum produced from M13 has 3 clear peaks, a positive peak between 200-240 nm which arises from peptide backbone transitions, a negative peak between 240-260 nm which arises from DNA transitions and another positive peak between 260-300 nm which is due to the aromatic transitions of Tyrosine, Tryptophan (maximum at 280 nm) and Phenylalanine. The presence of these peaks indicates that the M13 is intact and the structure is not damaged and therefore reveals the quality of the M13. To produce an LD signal, M13 needs to be able to align, and for this to happen, M13 has to retain its long, thin structure. If the structure of the M13 is damaged it will no longer produce its distinctive LD signal. This makes LD a good technique to measure the amount of M13 in the samples produced during these methods. The LD signal is only produced by the aligned M13

and is not affected by the presence of any non-aligned impurities. However, the presence of such impurities (e.g. DNA, protein and cells) has the potential to disrupt the conjugation reactions which are essential to developing M13 as an assay reagent.

To assess purity we measure the absorbance of the sample at 269 nm. This provides a measure of the amount of material that absorbs at this wavelength. This includes DNA and protein, both of which are likely to be common contaminants of the solution.

The average UV absorbance at 269 nm and LD signal at 220 nm were also used to determine the specific activity of the M13 product from each method. Specific activity in this case can be defined as the LD signal produced from the M13 per milligram of protein produced from each method. Our aim is to create a method which produces a high M13 yield which has a high specific activity.

The ease of use of each method was also taken into consideration as well the time required for each method because a fast and simple method was desired.

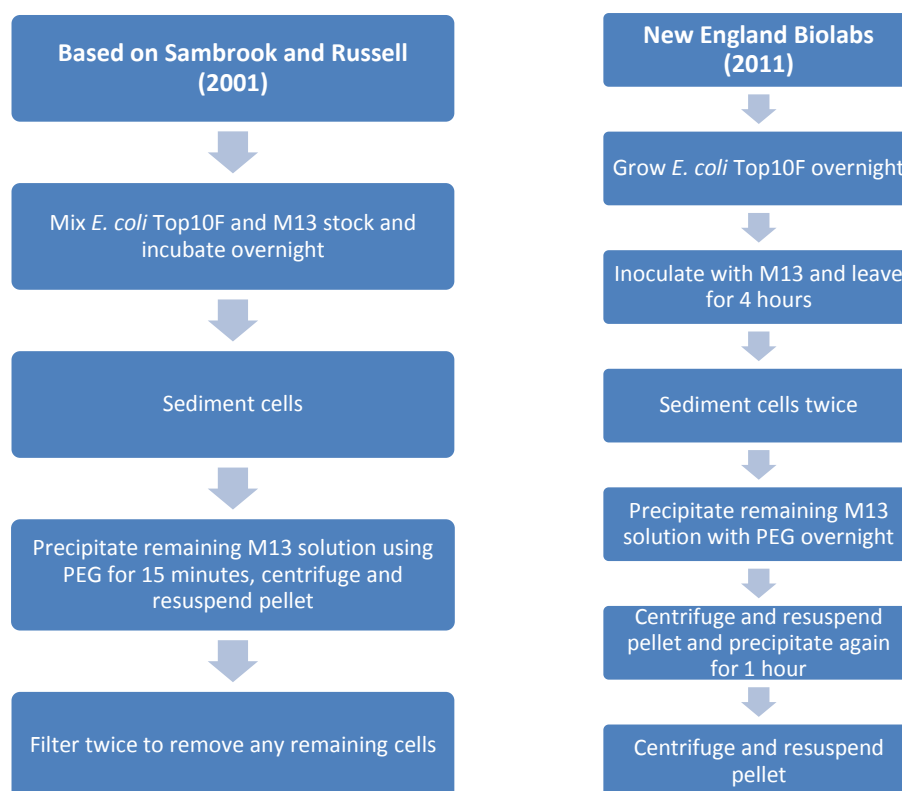


Figure 3.1 - Comparison of two existing M13 production methods

A comparison of the two current methods used to produce M13 bacteriophage; one is based on Sambrook and Russell (2001) and the other is based on New England Biolabs (2011).

3.1.1. Production of M13 bacteriophage using the method based on Sambrook and Russell (2001)

This method of making bacteriophage was based on Sambrook and Russell's (2001) method (figure 3.1) and produced an average yield of 3.24 mg (+/-0.2) of M13 per Litre of culture based on the absorbance at 269 nm (table 3.1) (extinction coefficient of M13 bacteriophage is 3.84 cm⁻²/mg at 269 nm (Niu *et al.*, 2008)). The yield based on LD at 220 nm shows that a yield of 0.0084 (+/-0.001) ΔOD (The units of LD are delta optical density, abbreviated to ΔOD) per Litre of culture was produced (table 3.2). The filtering step in this method proved to be very challenging with continuous blockages increasing the time taken to carry out the method. The final M13 sample was also usually still contaminated with *E. coli* cells and the results show that the final M13 solution is not concentrated. Overall this method took 2 days to produce M13

bacteriophage, this is mainly because the M13 bacteriophage and *E. coli* Top10F' cells were added together and left to incubate overnight without initially allowing the *E. coli* Top10F' cells to grow.

Table 3.1 - M13 yield based on UV absorbance

This table shows 3 repeats and the average yield of M13 produced based on UV absorbance from the method based on Sambrook and Russell (2001). To determine the yield of the final M13 solution, the absorbance was measured at 269 nm, the starting volume of LB was required and the volume of phosphate buffer used to resuspend the M13 pellet was required. This method of calculation was repeated for all of the M13 production methods.

A₂₆₉(M13)	0.51	0.57	0.42		
dilution factor	2	2	2		
V(LB) [L]	2.4	2.4	2.4		
V(M13) [mL]	8	9	10		
c(M13) [mg/mL]	0.88	1.00	0.73		
m(M13) [mg]	7.0	9.0	7.3	Average	Standard deviation
Y(m(M13)/V(LB))	2.94	3.7	3.1	3.24	0.43

Table 3.2 - M13 yield based on LD absorbance

This table shows 3 repeats and the average yield of M13 produced based on LD spectra from the method based on Sambrook and Russell (2001). To determine the yield of the final M13 solution, the LD signal was measured at 220 nm, the starting volume of LB was required and the volume of phosphate buffer used to resuspend the M13 pellet was required. This method of calculation was repeated for all of the M13 production methods.

LD₂₂₀(M13)	0.0031	0.0017	0.0020		
V(LB) [L]	2.4	2.4	2.4		
V(M13) [mL]	8	9	10	Average	Standard deviation
Y(V(M13)*LD₂₂₀)/V(LB)	0.01	0.0064	0.0084	0.0084	0.002

The specific activity is used to determine how much of the M13 present in the yield calculated from the absorbance at 269 nm actually produces an LD signal at 220 nm. As the absorbance signal can be affected by impurities, the specific activity can be thought of as a pseudo purity measure. To calculate the specific activity, equation 3.1 was used:

Equation 3.1 - Specific activity definition

$$\text{Specific Activity} = \text{Total LD Yield} \div \text{Total OD Yield}$$

The specific activity for the M13 solution produced from the method based on Sambrook and Russell (2001) was 0.0026 ΔOD/mg (figure 3.3C).

3.1.2. Production of M13 bacteriophage using the New England Biolabs method (2011)

This method of making M13 was appealing because it lacked the filtration step which was very time consuming. Instead it used two centrifugation steps to sediment any unwanted *E. coli* cells and also used repeated precipitation steps to produce the end sample. However this method required 3 days compared to the 2 days required for the Sambrook and Russell method. The extra day was because the protocol initially involved growing *E. coli* Top10F' cells overnight and then inoculating with M13. This is to allow the M13 bacteriophage to infect the *E. coli* Top10F' cells during their exponential phase. The method was carried out on 3 separate occasions and the yield based on the absorbance at 269 nm produced a yield of 0.91 mg (+/- 0.18) of M13 per Litre of culture (figure 3.3A). This is 3.5 times smaller than the average yield of M13 produced from the Sambrook and Russell method. However the final M13 solution was more concentrated than those produced from the Sambrook and Russell method. The yield based on the LD signal at 220 nm produced a yield of 0.0072 (+/-0.00155) Δ OD per Litre of culture (figure 3.3B). This is similar to that produced by the Sambrook and Russell method.

The specific activity for the M13 solution produced from the New England Biolabs (2011) was 0.0079 Δ OD/mg (figure 3.3C). This specific activity is larger than that produced by the method based on Sambrook and Russell (2001). However if a greater specific activity can be achieved it would greatly satisfy the needs of this assay.

3.1.3. New method of M13 bacteriophage production

As a result of a limited amount of M13 being produced from the current methods, it was necessary to try to optimise the yield produced. As well as optimising the yield, a protocol that was quick, not labour intensive and would produce a cell free yield of M13 with a good LD signal was desired. For example the method based on Sambrook and Russell (2001) used a

filtering step which was found to be labour intensive and unreliable. As a starting point for optimisation of the protocol, a method was developed that combined aspects of both established protocols (figure 3.2). For example instead of using a filter to remove the cells, the centrifugation and precipitation steps from the New England Biolabs protocol were used. To shorten the protocol both the M13 and Top 10F *E. coli* cells were added together as was done previously with the method based on Sambrook and Russell (table 3.3). This new method was assessed in the same way as the two established methods, and the results were compared.

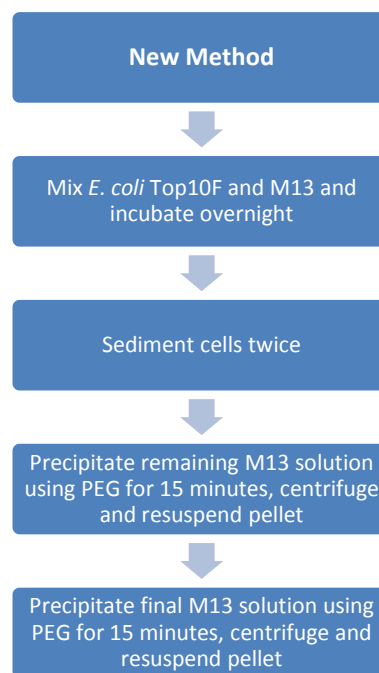


Figure 3.2 - New M13 production method

The new method proposed to optimise the production of M13 bacteriophage after combining aspects of two established methods; Sambrook and Russell (2001) and New England Biolabs (2011).

Table 3.3 - Comparison of M13 production methods

Table describes the steps from the current M13 production methods which have been modified to produce the new method and a justification for the changes.

Steps changed in method	Methods			Justification
	Sambrook and Russell (2001)	New England Biolabs (2011)	New Method	
Growth of <i>E. coli</i> Top10F' cells and M13 inoculation time	<i>E. coli</i> Top10F' and M13 added together and incubated overnight	<i>E. coli</i> Top10F' grown overnight, and then inoculated with M13 and incubated for 4 hours.	<i>E. coli</i> Top10F' and M13 added together and incubated overnight	Quicker
Number of times the cells are sedimented	Once	Twice	Twice	Ensures removal of <i>E. coli</i> cells
Precipitation time with PEG	15 minutes	Overnight	15 minutes	Quicker
Final M13 purification step	Filter M13 twice	Precipitate with PEG for 1 hour	Precipitate with PEG for 15 minutes	Less labour intensive and quicker

The average yield produced based on the LD signal was in line with those produced by the existing methods (at 220 nm the LD per Litre of culture was 0.008 Δ OD (+/-0.003)) (figure 3.3B). This material also had a much lower OD signal at 269 nm, suggesting a purer sample (0.55 mg (+/-0.14) per Litre of culture) (figure 3.3A).

The specific activity for the M13 solution produced from the new method was 0.015 Δ OD/mg (figure 3.3C).

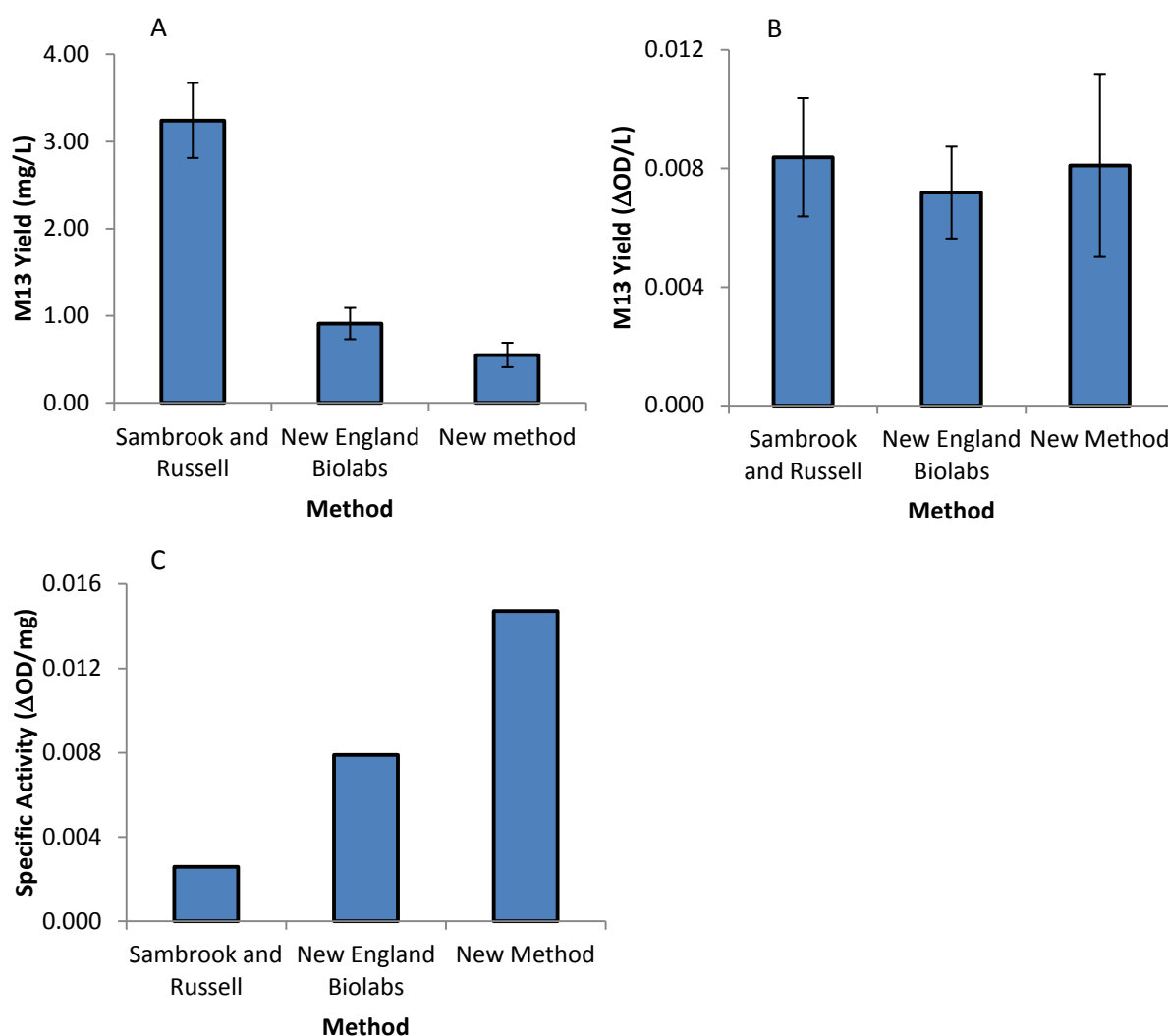


Figure 3.3 - Comparison of M13 production yields and specific activities

A) Comparison of the M13 yield produced from 2 current established methods and a new method which combines the two together to form an easier method. The yield was calculated from the UV absorbance at 269 nm. The error bars show standard deviation. B) Comparison of the M13 yield produced from the 3 methods, the yield was calculated from the LD signal at 220 nm. The error bars show standard deviation. C) Comparison of the specific activity of the final M13 solution produced from the 3 methods investigated.

As the main aim of this project is to use M13 in an LD based assay, it is essential that the material produced using the new method still maintains the LD signals required for the assay. The M13 yield based on the LD signal at 220 nm, produced from all three methods (figure 3.3B) were all very similar. This therefore proves that the yield produced from the UV absorbance was affected by other contaminants that may have been present in the M13 solutions. The Sambrook and Russell method produced the largest UV signal, followed by the

New England Biolabs method and finally the new method. This indicates that despite the new method producing a similar LD yield to the other methods, the new method produced a solution of M13 which was of higher quality containing fewer contaminants and more concentrated. In addition, the new method is also much easier, quick and less labour intensive.

The specific activity was calculated from the UV absorbance yield and the LD signal yield (equation 4), and provides a measure of the amount of M13 in each solution that was actually providing an LD signal per milligram of total protein. Figure 3.3C clearly indicates that the new method produced a specific activity which was approximately 5 times larger ($0.015 \Delta OD/mg$) than the specific activity produced from the M13 solution from the Sambrook and Russell method ($0.0026 \Delta OD/mg$) and twice as large than the specific activity produced from the M13 solution from the New England Biolabs method ($0.0079 \Delta OD/mg$). Thus it can be concluded that the new method produced better quality M13 than the other methods.

The final check of the material produced using this method involved the collection of an LD spectrum of the sample. As mentioned earlier M13 has a particular LD spectrum that includes signals from proteins and DNA in the particle. Figure 3.4 is an LD spectrum from the M13 produced using this new method and it shows the presence of all the characteristic peaks of M13, demonstrating that the M13 is viable for further work.

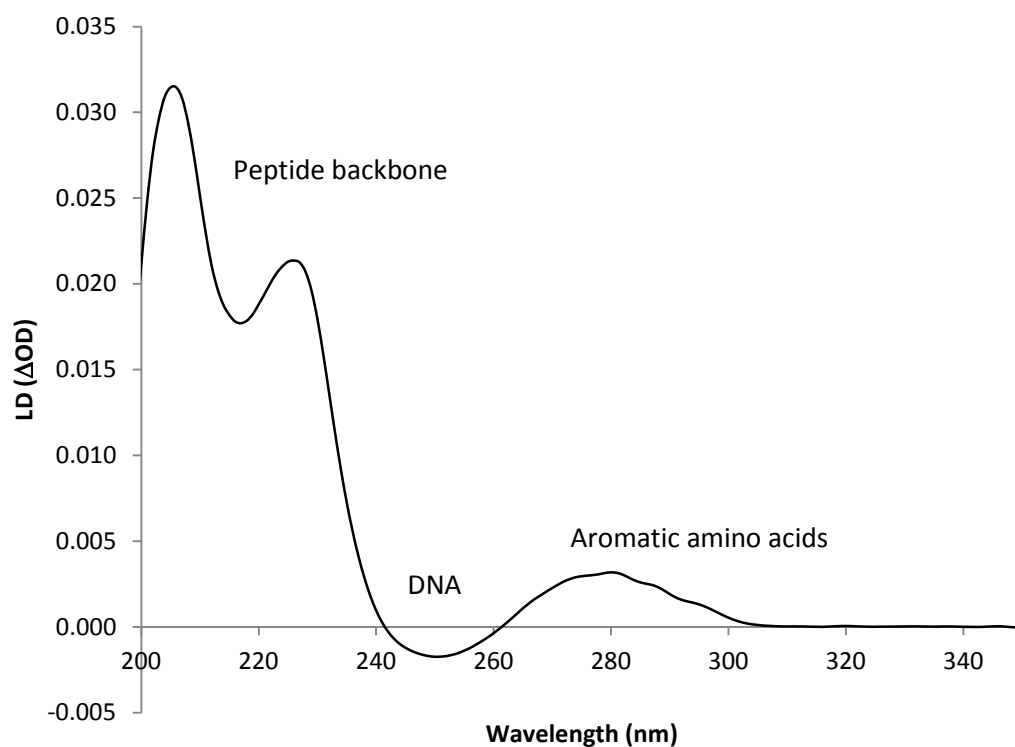


Figure 3.4 - LD spectrum of M13 bacteriophage generated from the new method

LD spectrum of M13 bacteriophage (0.04 mg/mL) generated from the new method, with peaks labelled.

Overall the new method has provided the easiest and quickest method to produce M13 and the final M13 solution has the highest specific activity.

3.1.4. Optimisation of precipitation time in M13 production

The new method is a much easier and quicker method to use and produces a more concentrated and higher quality stock of M13 which has a larger specific activity. However the yield is still not sufficient to carry out an assay. One of the essential steps in bacteriophage production is the precipitation step as the PEG/NaCl solution acts to sediment the M13 (Yamamoto *et al.*, 1970). Work published after the development of the new method for producing M13 (shown in the preceding section) showed that PEG based precipitations could be optimised to result in bacteriophage purity and yield improvements (Branston *et al.*, 2011a). This observation was used as a basis to further optimise the new method by examining the effect of precipitation times on the M13 yield.

The New England Biolabs (2011) method precipitated the M13 with the PEG/NaCl solution overnight, whereas the M13 method based on Sambrook and Russell (2001) used only 15 minutes to precipitate the M13 with the PEG/NaCl solution. The new method developed in the preceding section similarly used only 15 minutes to precipitate the M13 with the PEG/NaCl solution. To investigate whether, as shown by Branston *et al.* (2011), precipitation time affects the yield (according to UV absorbance at 269 nm and LD signal at 220 nm) of M13 and the specific activity of the final M13 solution, the precipitation times of the new method were varied to 5, 30, 45, 60 and 120 minutes and compared to the original 15 minute precipitation time.

Table 3.4 - Comparison of M13 yields and specific activities

Compares the yield (both based on LD and UV absorbance) and specific activity of M13 produced from two established methods (Sambrook and Russell (2001) and New England Biolabs (2011)) for producing M13 bacteriophage and a newly developed method. The new method is further modified by varying precipitation times.

Method	M13 Yield mg/L	M13 Yield $\Delta OD/L$	Specific Activity $\Delta OD/mg$
Sambrook and Russell (2001)	3.24	0.0084	0.0026
New England Biolabs (2011)	0.91	0.0072	0.0079
New Method Precipitation Time (min)	M13 Yield mg/L	M13 Yield $\Delta OD/L$	Specific Activity $\Delta OD/mg$
5	0.1	0.00092	0.0092
15	0.55	0.0081	0.015
30	5.84	0.11	0.018
45	8.02	0.073	0.0091
60	24.6	0.25	0.0095
120	36.65	0.44	0.012

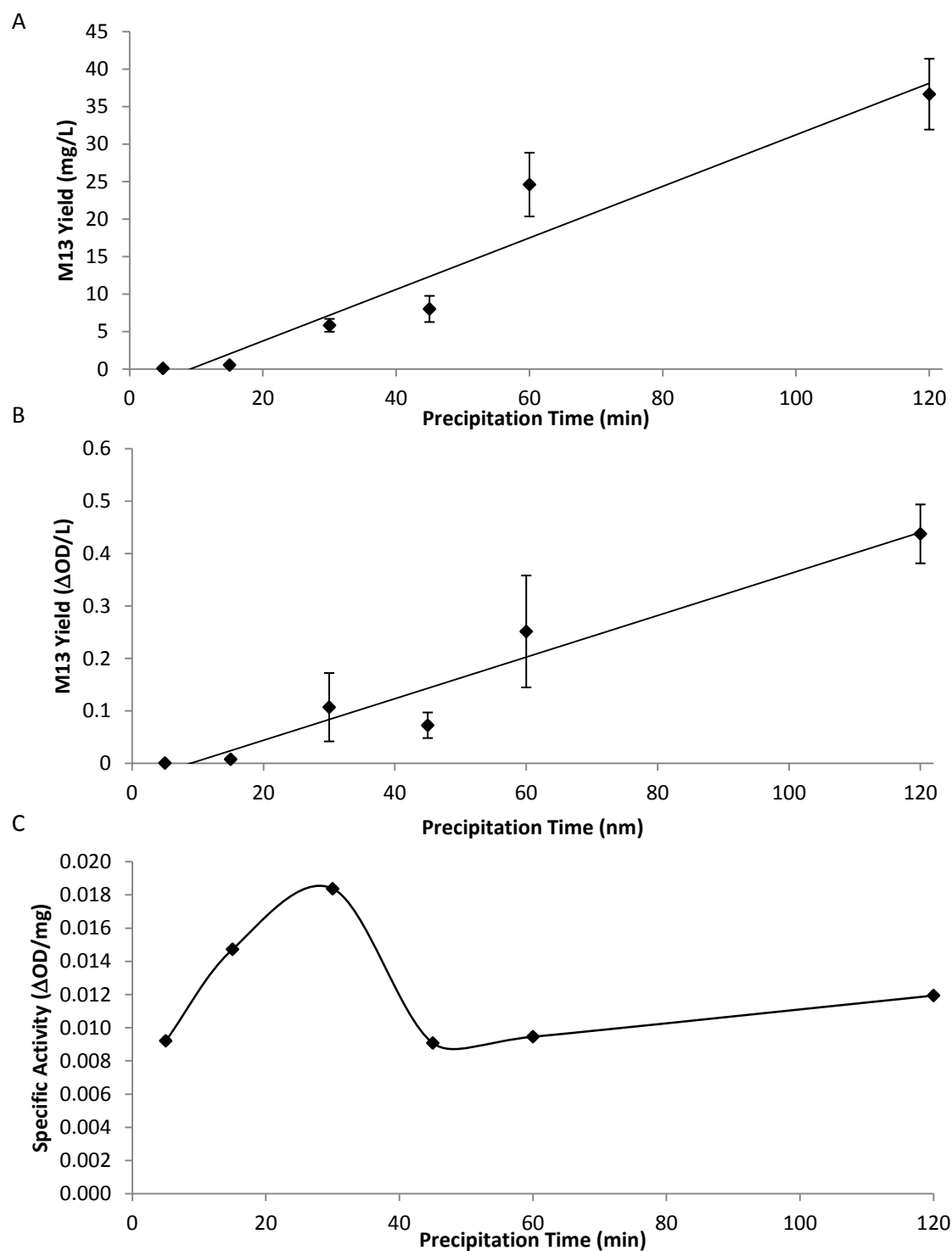


Figure 3.5 - The effect of precipitation time on M13 production yield and specific activity

A) Comparison of the M13 yield produced from a newly developed method where the precipitation time has been varied from 5, 15, 30, 45, 60 and 120 minutes to investigate whether this affects the M13 yield. The yield was calculated from the UV absorbance at 269 nm. The error bars show standard deviation. B) Comparison of M13 yield calculated from the LD signal produced at 220 nm. This graph displays the differing precipitation times used within the method and the effect on the yield. The error bars show standard deviation. C) Comparison of the specific activity of the final M13 solution produced from the new method when the precipitation times have been varied.

The current two established methods produce very low M13 yields according to their UV absorbance at 269 and their LD signal at 220 nm. The new method, although considerably easier and quicker to carry out and producing a much larger specific activity, also produces a low yield. This led to varying the precipitation times within the new method to investigate if this affects the M13 yield and specific activity.

Lengthening the precipitation time from 5 minutes to 120 minutes had a profound effect on the yield of M13. Figure 3.5A demonstrates that there is a linear rise in M13 yield based on UV absorbance at 269 nm as the precipitation time increases to 120 minutes. The yield increased approximately 360 times as the precipitation time increased from 5 minutes to 120 minutes. However UV absorbance also measures contaminants which may be present in the solution. To therefore measure the quality of each sample, LD was used.

Similarly, the LD data from 220 nm revealed a linear rise in M13 yield as the precipitation time increased. The M13 yield increased approximately 400 times as the precipitation time increased from 5 minutes to 120 minutes (figure 3.5B). This data indicates that increasing the precipitation time not only increases the number of M13 bacteriophages present in the final sample, but it also improves the quality of the M13 produced. The M13 solutions produced large LD signals, confirming the intact and well assembled structure of the M13.

The specific activity was measured using the yield from the UV absorbance at 269 nm and LD signal at 220 nm. The specific activity of the M13 bacteriophage produced from the new method initially doubled as the precipitation time increased from 5 minutes to 30 minutes (figure 3.5C and table 3.4). However when the precipitation time further increased to 45, 60 and 120 minutes, the specific activity decreased by a half. This could be due to the fact that the yield based on the UV absorbance was increasing at a faster rate than the yield based on the LD signal. The yield based on the UV absorbance may be increasing at a faster rate because

when precipitating for a longer time, it may be precipitating contaminants as well as the M13. This may lead to a larger absorbance at 269 nm. So although the yield from both the UV absorbance and LD signal is larger when precipitated for longer, it may lead to more contaminants being present. It could therefore be concluded that precipitating for 30 minutes would be more advantageous. As precipitating for 30 minutes produces the largest specific activity, which indicates that there is more M13 producing an LD signal per milligram of total protein. In addition the contaminants could interfere with conjugation processes occurring in later stages; this could lead to conjugating specific molecules (e.g. antibodies) to contaminants rather than M13 bacteriophages. It would therefore be more beneficial to remove the contaminants in the first instance. Not only this but precipitating for 30 minutes rather than 2 hours makes the method much quicker and achieves an M13 yield suitable for assay development.

3.1.5. Conclusion

Developing an assay where M13 bacteriophage is the key reagent requires an enhanced M13 production process. We assessed the speed, ease of use, purity, specific activity and yield of M13 of two established methods based on Sambrook and Russell (2001) and New England Biolabs (2011). The results show that although both produced samples with high absorbance (potentially indicating the presence of M13) the amount of M13 as measured by LD was low, indicating a low specific activity. In addition the work identified inherent limitations to both methods. The Sambrook and Russell method required the use of a filter to remove the *E. coli* cells which proved extremely difficult and resulted in a less concentrated sample of M13 which was also still contaminated with *E. coli* cells. The New England Biolabs method required 3 days rather than 2 days to produce M13 bacteriophage because it involved incubating *E. coli* Top10F' cells overnight before inoculating them with M13 bacteriophage and also at a later stage precipitating the M13 solution with PEG/NaCl overnight. These limitations collectively

provided the impetus to develop a new method to produce M13 bacteriophage and took aspects from both established methods. In particular the new method added both the M13 and *E. coli* Top10F' together to incubate overnight, as was done in the Sambrook and Russell method. This new method also used various centrifugation steps to remove the *E. coli* cells and various PEG/NaCl precipitation steps to concentrate the sample as was done in the New England Biolabs method. However the new method only required 15 minutes to precipitate the M13 solution as was used in the Sambrook and Russell method. This new method had the benefit of being quick, easy, not labour intensive and resulted in a clean, concentrated and cell free solution of M13. The yield produced by the new method, as measured by LD, was on parity with the original methods and encouragingly, the specific activity and hence purity was significantly improved.

Work done by Branston *et al.* (2011) highlighted the importance of the PEG precipitation step on final M13 purity and yield. In an effort to further optimise the new method and produce a larger yield of M13 which would be sufficient for use in an assay, the precipitation time with PEG was varied. The original precipitation time used in the new method was 15 minutes and this was altered to 5, 30, 45, 60 and 120 minutes. The results indicate that extending the precipitation time from 5 minutes to 120 minutes significantly increase the yield based on LD and UV spectra. Interestingly the specific activity initially increases significantly from 5 to 30 minutes, after which it declines. This could be due to the precipitation time being too long as it starts precipitating more contaminants. Given that the presence of contaminants is not ideal for downstream conjugation experiments, the decision was taken to precipitate the M13 for 30 minutes which provides a sufficient yield for this assay and a high specific activity. This precipitation time also provides a method which is less time consuming. When comparing this new method with a precipitation time of 30 minutes to the two established methods that were originally used, the yield and specific activity has significantly improved. The M13 yield based

on UV spectra increased by approximately 5 times when compared to the yield produced from the New England Biolabs method and doubled when compared to the yield of the Sambrook and Russell method. The yield based on the LD signal has improved approximately 10 times when compared to the two established methods and the specific activity has increased 7 times when compared back to the Sambrook and Russell method and has doubled when compared back to the New England Biolabs method. These significant improvements have established a method which is quick, easy, produces a large yield and a large specific activity.

CHAPTER 4

- FLUORESCENT LABELLING OF M13 FOR USE IN ASSAYS

The previous chapter described a method that was developed to produce an increased quantity of M13 for subsequent conjugation reactions. The next stage in the development of an assay is the production of M13 derivatised with coloured dyes (figure 4.1). These dyes allow different antibody conjugated M13 bacteriophages in the same test to be detected independently using LD (figure 4.2) as each dye will produce an individual LD signal related to its spectroscopic characteristics. This offers the exciting prospect of being able to:

1. Detect more than one type of pathogen in a sample (multiplexing)
2. Detect one pathogen using more than one method (multimodality)
3. Embed control reactions in one assay

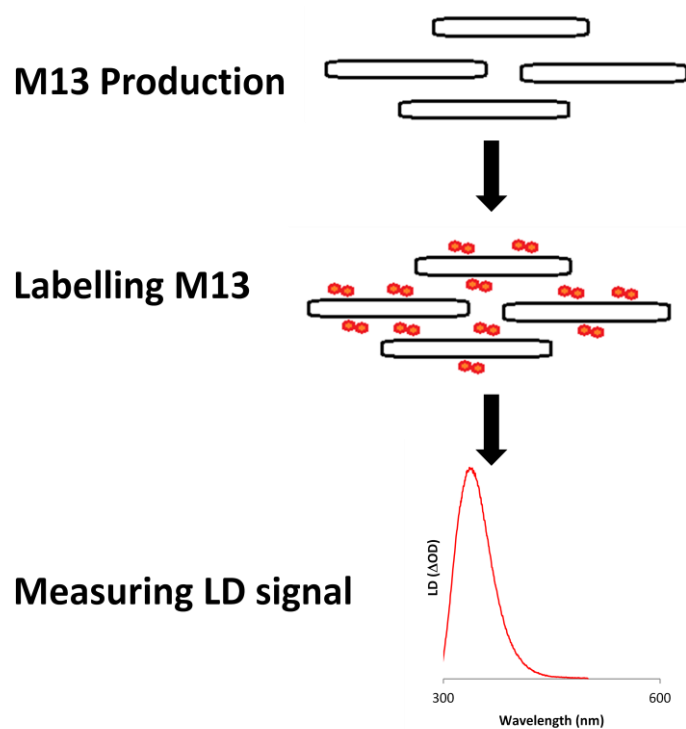


Figure 4.1 - M13 production, labelling and LD measurement process

Demonstration of the process of making M13 bacteriophage, labelling M13 bacteriophage with dyes and measuring the LD signal of the label once attached to the M13 bacteriophage.

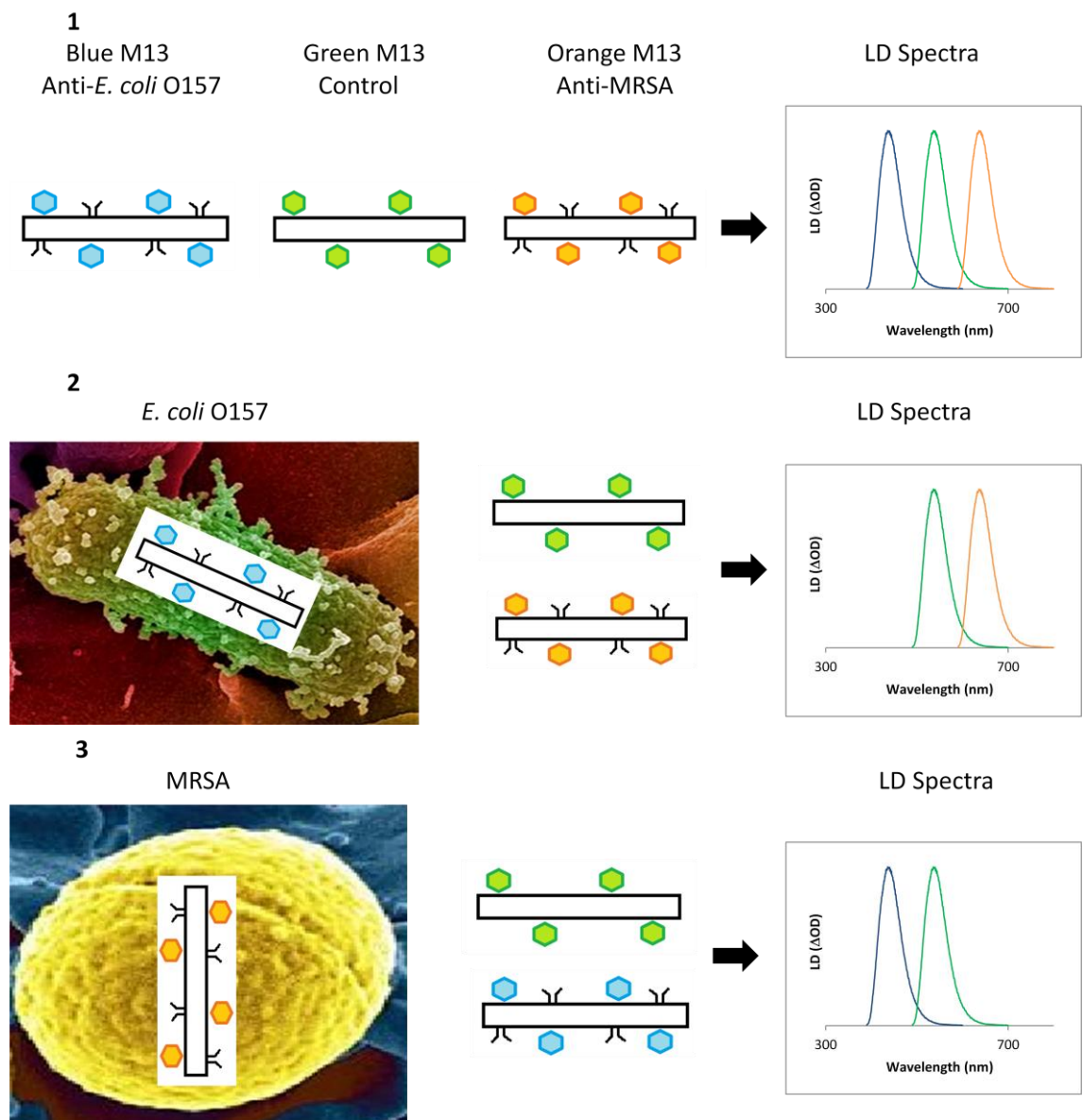


Figure 4.2 - Schematic illustrating the principle behind an M13/LD assay capable of multiplexing

Schematic diagram illustrating how M13 bacteriophage conjugated with antibodies and dyes (double labelled M13) can be used to detect different targets simultaneously using LD. In this figure there are 3 types of M13 bacteriophage. Green M13 is M13 bacteriophage labelled with green dye and is a control and therefore always produces an LD signal. Blue M13 is M13 conjugated with blue dye and antibodies specific to *E. coli* O157. Orange M13 is M13 conjugated with orange dye and antibodies specific to MRSA. In the absence of any pathogens all 3 types of M13 bacteriophage align and produce an LD signal corresponding to the dye attached. However if *E. coli* O157 is present in a sample, the blue M13 binds to the pathogen and stops aligning, this causes a drop in LD signal for that particular M13 bacteriophage. However the other bacteriophages are still able to align and produce LD signals corresponding to their dye. When MRSA is present, the orange M13 is able to detect it and this prevents it from aligning, causing a drop in LD signal. However the other bacteriophages are again still able to align and hence produce LD signals corresponding to the dyes attached. This illustration demonstrates that this assay is capable of detecting more than one pathogen simultaneously.

Currently the pathogen detection system relies on the LD signal produced from M13, which occurs in the near UV region of the electromagnetic spectrum. This necessitates the use of large complex instrumentation limiting the use of M13 and LD as a detection assay.

The conjugation of dyes to the M13 protein coat provides a route to shift the LD signal into the visible region of the electromagnetic spectrum. Thus offering the potential to develop an economical, hand held, portable detection device. Furthermore, the addition of dyes could be used to develop a multimodal and multiplexed detection assay.

In this chapter methods are developed to introduce coloured dyes into the M13 structure. To achieve this, a dye with a reactive chemical group that can form a covalent bond with a residue on the surface of M13 was added to the virus. Once reacted, a dialysis step is used to remove the free, unbound dye. Dyes were chosen to label the M13 on the basis of cost, spectroscopic characteristics and linkage chemistry. The dyes used to label M13 in this chapter include fluorescamine, rhodamine B isothiocyanate (rhodamine), 4-chloro-7-nitrobenzofurazan (NBD chloride) and black hole quencher-10 (BHQ-10). Fluorescamine forms an imine bond, NBD chloride forms an amine bond and BHQ-10 forms an amide bond with the free amine groups on the p8 coat protein. Rhodamine forms a thiourea bond with the free amine groups on the p8 coat protein.

There are two possible reactive amine groups on the p8, one is located on the N-terminus and the other is located on an accessible lysine residue (Lys-8 (Niu *et al.*, 2008)) (figure 4.3). The amines of the p8 protein of wild type (wt) M13 have been shown to be amenable to chemical modification without damaging the M13 structure and its infectivity (Muzard *et al.*, 2012). Muzard *et al.* (2012) highlight the easy accessibility of Lys-8 on p8 of the virus and describe methods to modify M13 bacteriophage for use in affinity separation. Similarly Lee *et al.* (2012) chemically modified M13 without disrupting its ability to bind to a particular antigen. They

modified the M13 bacteriophage by incorporating thiol groups on to the accessible amine groups and allowed them to react with maleimide-derivatised DNA to form reagents for their assay.

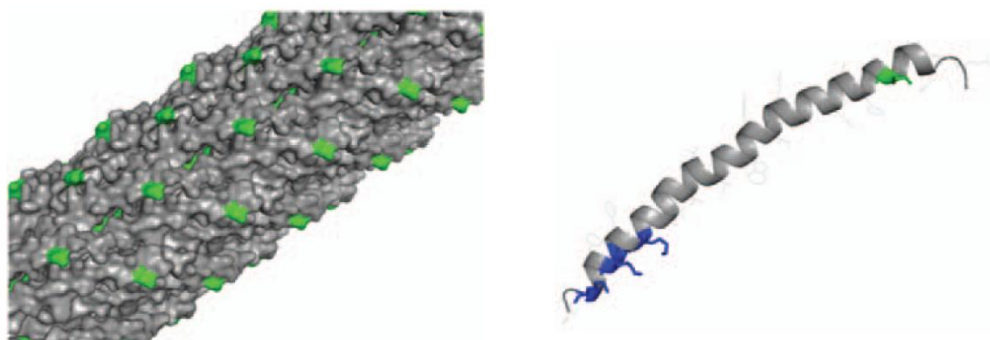


Figure 4.3 - Images illustrating the location of the p8 coat proteins within M13

The image on the left displays the helical organisation of M13 major coat proteins p8. The second image is a ribbon diagram of a single subunit of p8 with the lysines being highlighted. Lys-8 is easily accessible and is shown in green, whereas the other 4 lysines are buried in the coat protein and shown in blue. Reproduced from Niu *et al.* (2008).

Table 4.1 - The dyes proposed to label M13 bacteriophage.

Dye	Conjugation Method	Mr	Absorbance	Extinction Coefficient of dye ($M^{-1} cm^{-1}$)
Fluorescamine	Aniline linkage	278	381	7600 (Haugland, 1996)
Rhodamine	Thiourea linkage	536	556	87000 (Ma <i>et al.</i> , 2008)
NBD chloride	Amine linkage	200	337	9800 (Haugland, 1996)
BHQ-10	Amide linkage	703	516	28700 (Biosearch Technologies, 2010)

Various methods were used to confirm that the dye had labelled the M13. The labelled M13 was first tested using UV/Vis spectroscopy to determine if an absorbance peak corresponding to the dye was present. If a peak was observed this indicated dye was present in the sample with the M13 as well as providing a measure of the amount of dye attached to the M13. The labelling efficiency was calculated using equation 2.2. For example, a labelling efficiency of 20% indicates that ~540 of the 2700 p8 coat proteins have been labelled. LD was then used to determine if the dye covalently linked to the M13 was able to align. If the dye was bound and

aligned then a LD peak would be expected where the dye absorbs (NB: free dye cannot align and hence is unable to produce an LD signal as the dye is very small and lacks sufficient aspect ratio). Fluorescence of the dye labelled M13 was also measured to examine whether conjugation had altered the fluorescent characteristics of the dyes.

4.1. Labelling M13 bacteriophage with fluorescamine

Unconjugated fluorescamine is not a fluorescent compound, but produces fluorescent products on reaction with primary amine groups (De Bernardo *et al.*, 1974). Conveniently this means that a coloured solution after a reaction indicates the covalent linking of fluorescamine to a primary amine group (figure 4.4). Fluorescamine also has a low molecular weight (278.26 g/mol), meaning it should not affect the alignment of the M13 in an LD experiment. For these reasons fluorescamine was chosen as one of the labelling dyes.

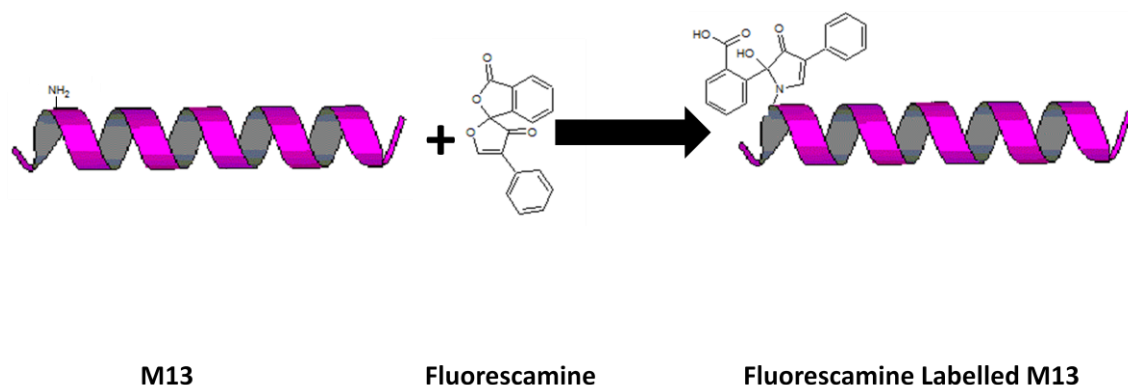


Figure 4.4 - Labelling M13 with fluorescamine

It should also be noted that fluorescamine is a light sensitive molecule, so all labelling reactions were carried out in the absence of light.

Fluorescamine was added to the M13 and after incubation, the sample was dialysed. To test if fluorescamine had labelled the M13, the UV/Vis absorbance, LD and fluorescence were measured.

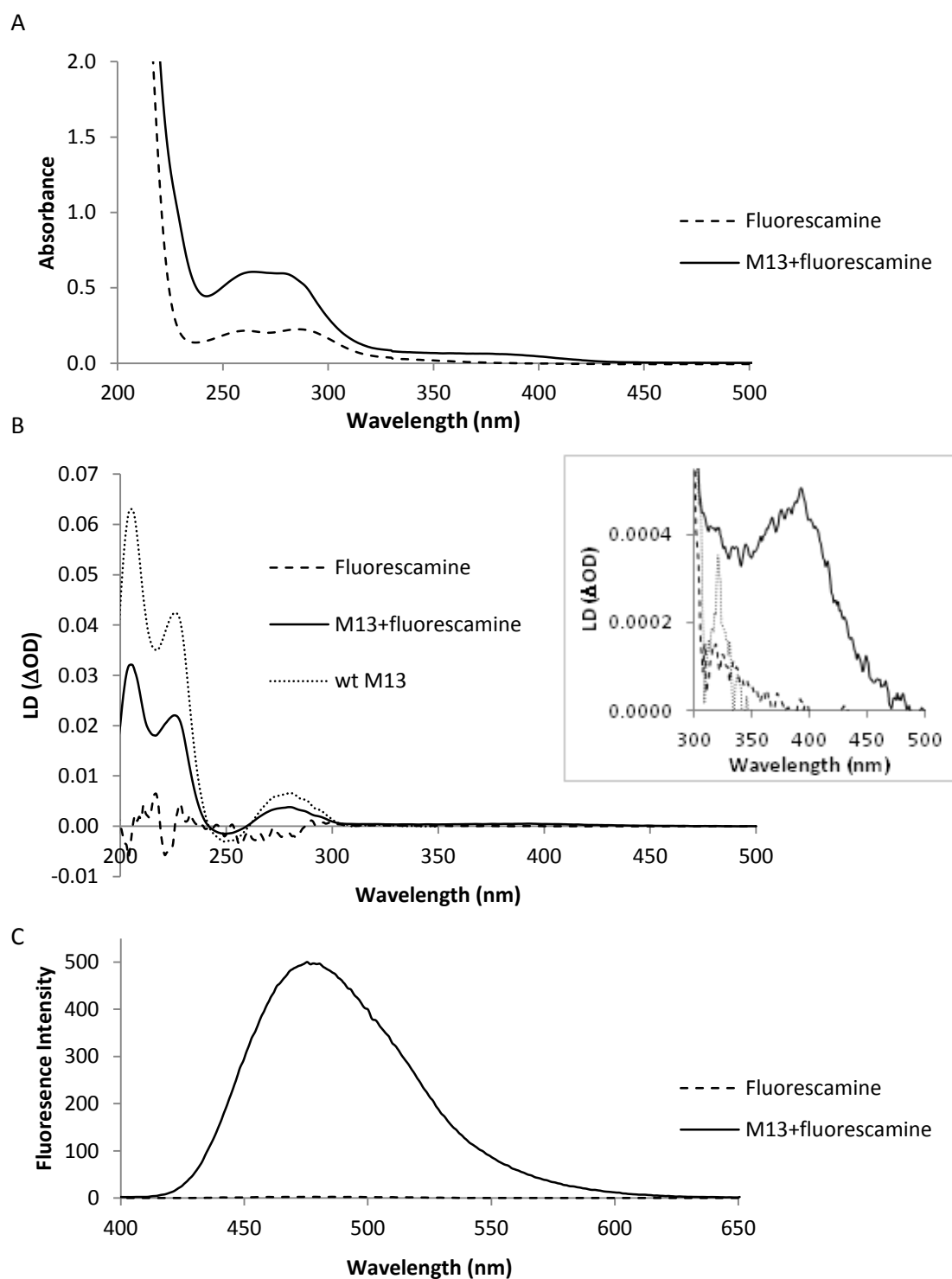


Figure 4.5 - UV/Vis absorbance spectra, LD spectra and fluorescence spectra of fluorescamine and M13 labelled with fluorescamine

(A) UV/Vis absorbance spectra of M13 labelled with fluorescamine (0.5 mg/mL) and fluorescamine alone (0.036 mM). (B) Shows the LD spectra of M13 labelled with fluorescamine (0.5 mg/mL), fluorescamine alone (0.036 mM) and wt M13 (0.35 mg/mL). Inset highlights the peak caused by fluorescamine when conjugated to M13. (C) Shows the fluorescence spectra of M13 labelled with fluorescamine (0.5 mg/mL) and fluorescamine alone (0.036 mM). Excitation wavelength - 381 nm.

Fluorescamine alone absorbs at 381 nm and the UV/Vis absorbance shows that fluorescamine has a peak at 381 nm (figure 4.5A). M13 labelled with fluorescamine also has a peak at 381 nm, therefore indicating that there is fluorescamine present. The presence of an LD signal further confirms that fluorescamine has labelled the M13 because fluorescamine alone cannot align and consequently cannot produce an LD signal. M13 labelled with fluorescamine produces a peak at approximately 381 nm (figure 4.5B), indicating that when M13 aligns, the dye aligns with it because it is bound to the M13. The positive peaks at 200-240 nm and 260-300 nm and the negative band between 240-260 nm are all characteristic of M13, indicating the presence of M13 in the sample. The positive peak at 200-240 nm arises from the peptide backbone transitions, whilst the negative band between 240-260 nm arises from DNA transitions indicating that the base pairs are perpendicular to the long axis of the bacteriophage. The positive peak between 260 nm and 300 nm is due to aromatic transitions of Tyrosine, Tryptophan (maximum at 280 nm) and Phenylalanine.

Fluorescence measurements also show that fluorescamine does not fluoresce alone, but when it forms the animine bond with the primary amine groups (on the lysine side chains and N-terminus amine groups) on the M13 it produces a large peak between 450-500 nm (figure 4.5C).

4.2. Labelling M13 bacteriophage with rhodamine B isothiocyanate

Rhodamine reacts with the primary amine group on the lysine side chains and N-terminus on the p8 coat proteins on the M13 to form a thiourea linkage (figure 4.6). Rhodamine has an absorption maximum of 556 nm (Haugland, 1996); this is in the visible region. The molecular weight of rhodamine is 536 g/mol, and so again it would not be expected that rhodamine would affect the alignment of the M13 in an LD experiment.

Rhodamine, like fluorescamine is a light sensitive molecule, so all reactions were carried out in the absence of light.

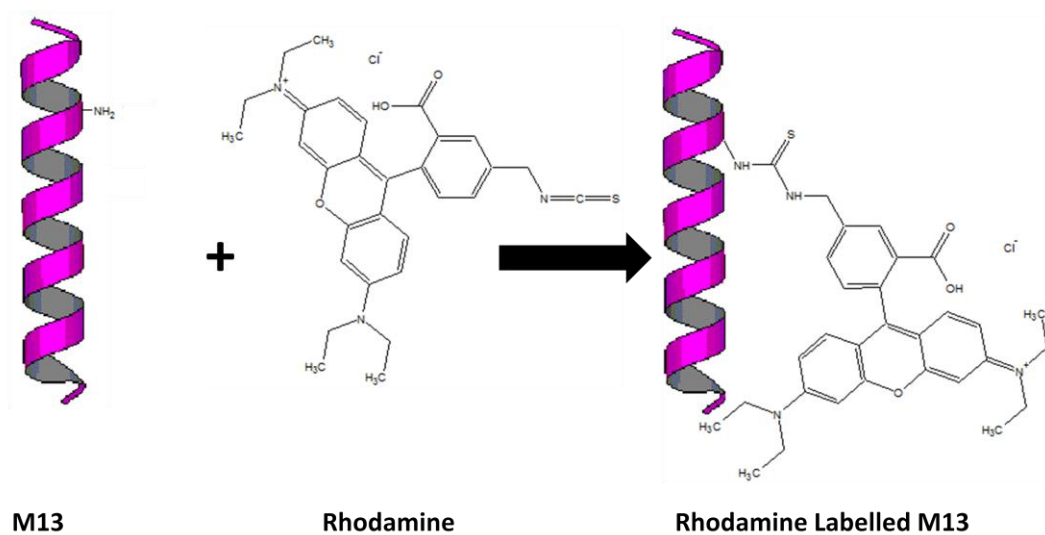


Figure 4.6 - Labelling M13 with rhodamine

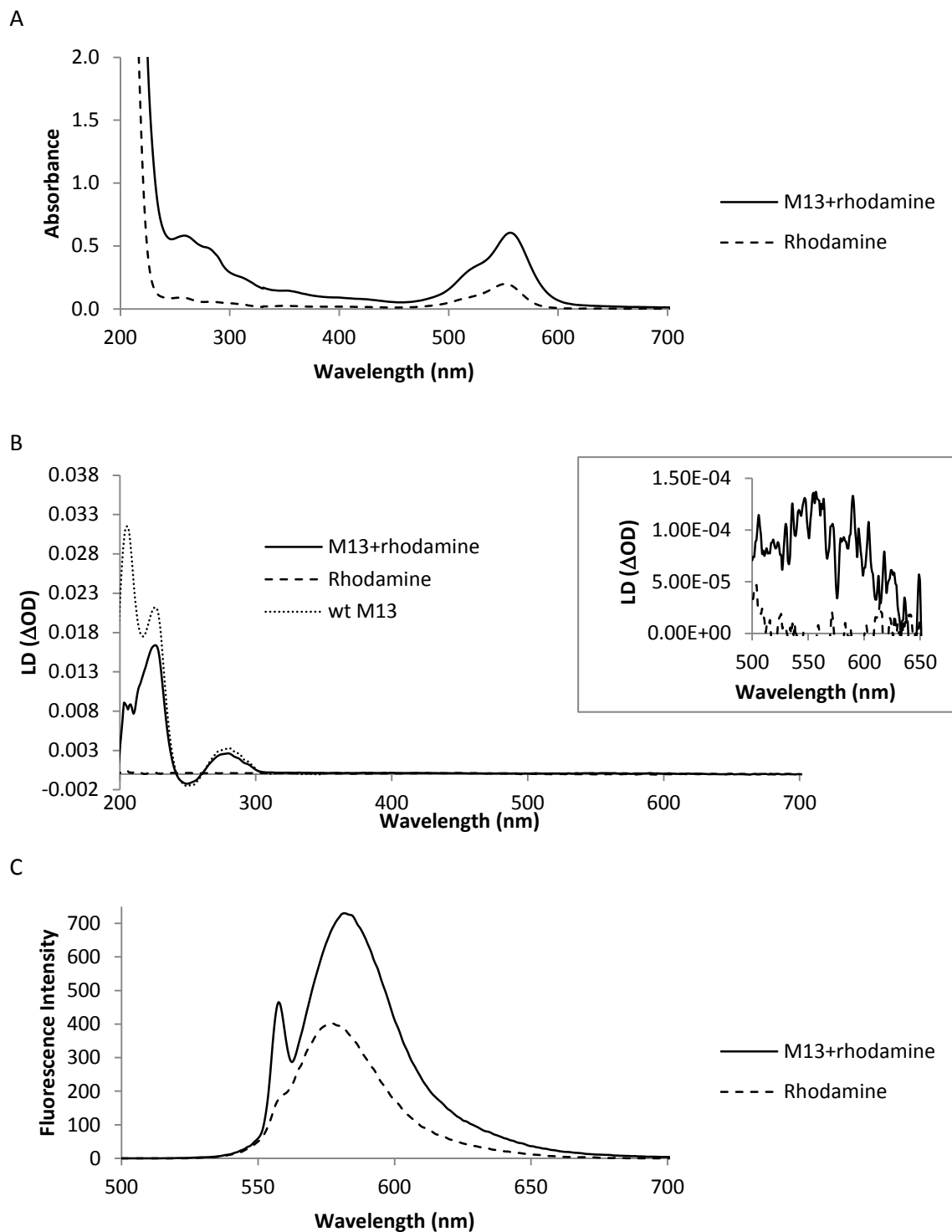


Figure 4.7 - UV/Vis absorbance spectra, LD spectra and fluorescence spectra of rhodamine and M13 labelled with rhodamine

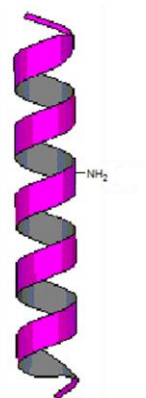
(A) UV/Vis absorbance spectra of M13 labelled with rhodamine (0.4 mg/mL) and rhodamine alone (0.012 mM). (B) LD spectra of M13 labelled with rhodamine (0.2 mg/mL), rhodamine alone (0.012 mM) and wt M13 (0.3 mg/mL). Inset highlights the peak caused by rhodamine when conjugated to M13. (C) Fluorescence spectra of M13 labelled with rhodamine (0.4 mg/mL) and rhodamine alone (0.012 mM). Excitation wavelength - 556 nm.

The UV/Vis absorbance spectra of rhodamine and M13 labelled with rhodamine shows that rhodamine alone absorbs at 556 nm and the M13 labelled with rhodamine also produces a peak at 556 nm (figure 4.7A) therefore suggesting that rhodamine has covalently linked to M13. The LD spectra verify this because rhodamine alone produces no LD signal, but the M13 labelled with rhodamine produces a modest peak at 556 nm. The positive peaks at 200-240 nm and 260-300 nm and the negative band between 240-260 nm are all characteristic of M13, indicating the presence of M13 in the sample (figure 4.7B). Figure 4.7C also shows how both rhodamine and M13 labelled with rhodamine both fluoresce between 550-600 nm, this indicates successful labelling. A small stokes shift peak can be seen in figure 4.7C at 550 nm. The fluorescence spectra also show that there is a red shift of approximately 4 nm when the rhodamine is covalently attached to the M13 bacteriophage. A possible explanation for this is that rhodamine is in a more polar environment because it is in contact with glutamates which are adjacent to the lysine and N-terminus in p8 where the dye is bound.

4.3. Labelling M13 bacteriophage with 4-chloro-7-nitrobenzofurazan

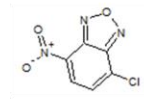
Unconjugated NBD chloride is not a fluorescent compound, but like fluorescamine produces fluorescent products on reaction with primary amine groups and also thiol groups (Fager *et al.*, 1973). Therefore, in this case a coloured solution after a reaction indicates the attachment of NBD chloride to a primary amine group. The molecular weight of NBD chloride is 200 g/mol, and so again should not affect the alignment of the M13 in an LD experiment.

NBD chloride is also a light sensitive molecule, so all reactions were carried out in the absence of light.

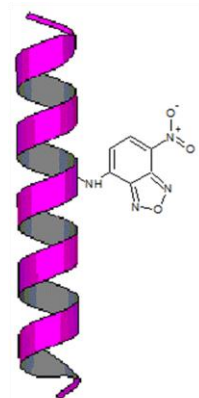


M13

+



NBD Chloride



NBD Chloride Labelled M13

Figure 4.8 - Labelling M13 with NBD chloride

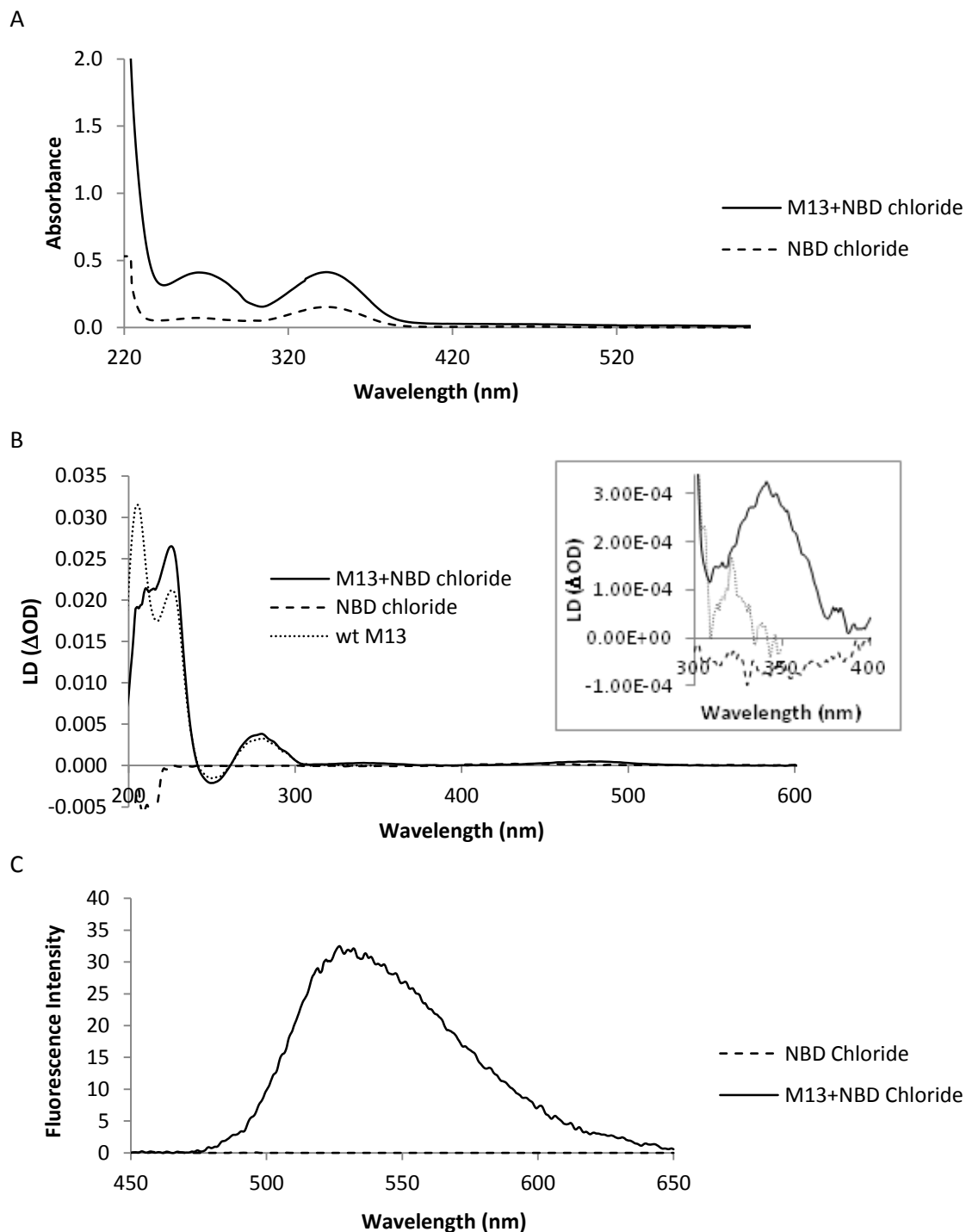


Figure 4.9 - UV/Vis absorbance spectra, LD spectra and fluorescence spectra of NBD chloride and M13 labelled with NBD chloride

(A) UV/Vis absorbance spectra of M13 labelled with NBD chloride (0.35 mg/mL) and NBD chloride alone (0.05 mM). (B) LD spectra of M13 labelled with NBD chloride (0.35 mg/mL), NBD chloride alone (0.5 mM) and wt M13 (0.3 mg/mL). Inset highlights the peak caused by NBD chloride when conjugated to M13. (C) Fluorescence spectra of M13 labelled with NBD chloride (0.35 mg/mL) and NBD chloride alone (0.5 mM). Excitation wavelength - 337 nm.

The UV/Vis absorbance spectra of NBD chloride and M13 labelled with NBD chloride both show peaks at approximately 336 nm. This is characteristic of NBD chloride, indicating the presence of the chromophore in both samples (figure 4.9A). The LD spectrum of M13 labelled with NBD chloride also shows a peak at 336 nm, confirming that the dye has covalently attached to the M13. The LD spectrum also shows peaks characteristic of M13 (positive peaks at 200-240 nm and 260-300 nm and the negative band between 240-260 nm) (figure 4.9B). This indicates the successful labelling of M13 with NBD chloride.

NBD chloride is similar to fluorescamine as it does not fluoresce alone, however on producing the amine bond with M13 it fluoresces and emits light between 500-600 nm (figure 4.9C).

4.4. Labelling M13 bacteriophage with black hole quencher-10

BHQ-10 is a non-fluorescent dye that is often used to quench the fluorescence of other dyes. The lack of fluorescence makes this sort of dye attractive for use in LD assays as it is possible the fluorescence could interfere with LD detection in simple assay instruments. BHQ-10 like the other dyes in this chapter reacts with the primary amine groups on the lysine side chains and N-terminus on the p8 coat proteins on the M13 (figure 4.10). The molecular weight of BHQ-10 is 703 g/mol, and so should not affect the alignment of the M13 in an LD experiment. For these reasons BHQ-10 was chosen as a labelling dye. BHQ-10 is not fluorescent and so the fluorescence was not measured.

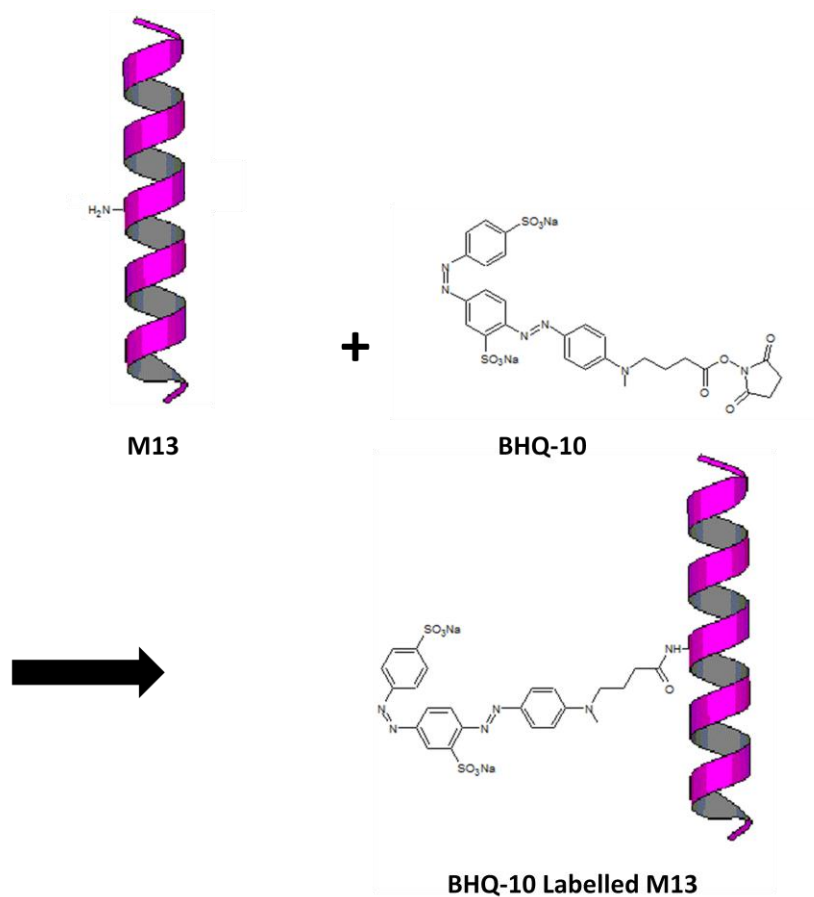
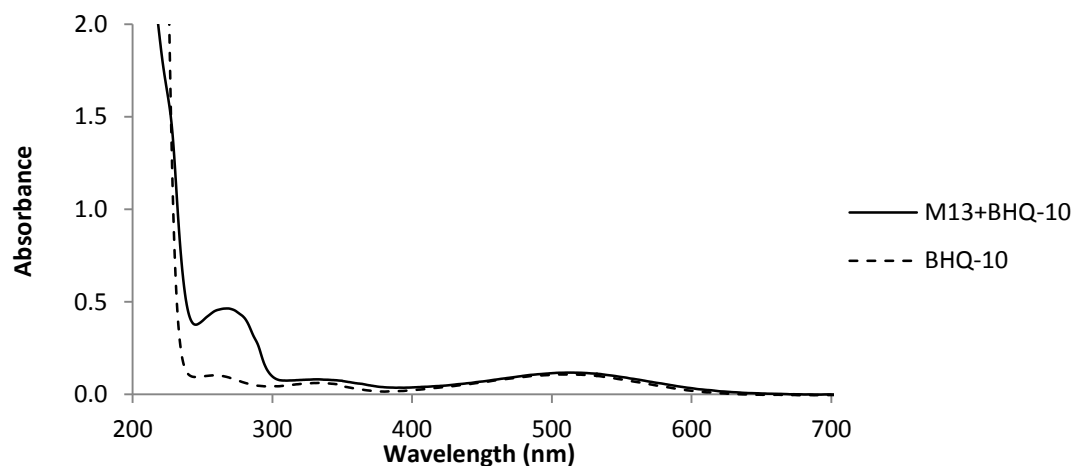


Figure 4.10 - Labelling M13 with BHQ-10

A



B

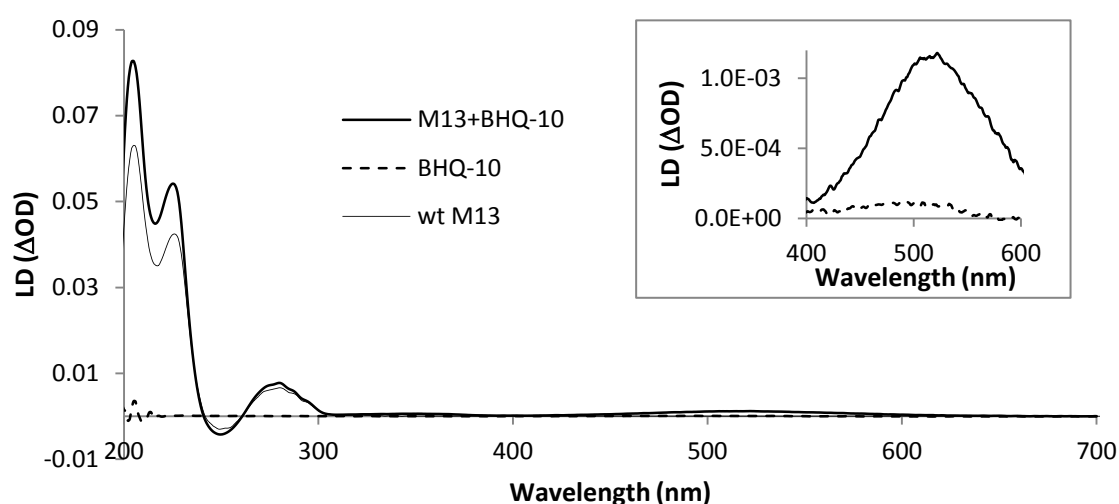


Figure 4.11 - UV/Vis absorbance spectra and LD spectra of BHQ-10 and M13 labelled with BHQ-10

(A) UV/Vis absorbance spectra of M13 labelled with BHQ-10 (0.4 mg/mL) and BHQ-10 alone (0.014 mM). (B) LD spectra of M13 labelled with BHQ-10 (0.4 mg/mL), BHQ-10 alone (0.014 mM) and wt M13 (0.35 mg/mL). The inset highlights the peak caused by the BHQ-10 labelling the M13.

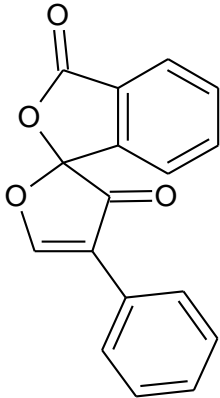
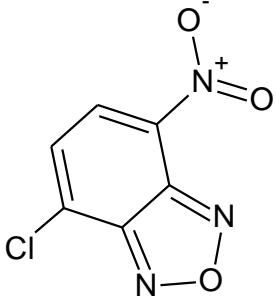
The UV/Vis absorbance spectrum of BHQ-10 reveals that it absorbs at a broad range (400-600 nm) with a maximum at 516 nm. The M13 labelled with BHQ-10 also produces a peak at 516 nm (figure 4.11A) therefore suggesting that BHQ-10 is present in the sample with M13. The LD spectra confirm that BHQ-10 dye has covalently labelled the M13 because BHQ-10 alone

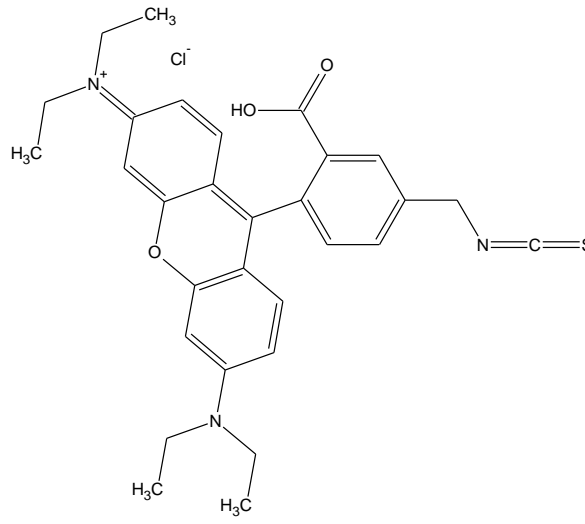
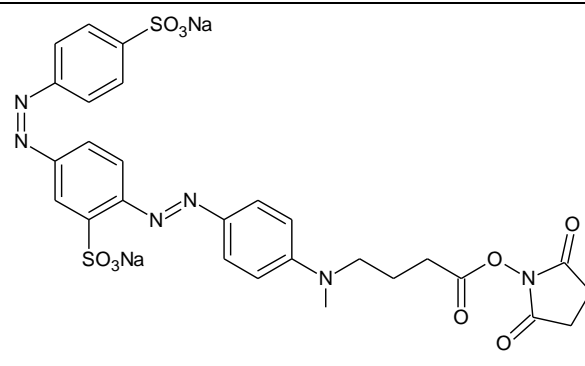
produces no LD signal, but M13 labelled with BHQ-10 produces a peak at 516 nm. The positive peaks at 200-240 nm and 260-300 nm and the negative band between 240-260 nm are all characteristic of M13, confirming the presence of M13 in the sample.

4.5. Summary

Table 4.2 - Percentage labelling and dye LD to M13 LD ratios

Table shows the percentage labelling of M13 with dye and dye LD to M13 LD ratio achieved when different dyes are used to label M13 bacteriophage.

Sample	Extinction Coefficient of dye ($M^{-1} cm^{-1}$)	Absorbance of dye (nm)	Mr	% Labelling	$\frac{LD_{dye}}{LD_{M13} (280nm)}$	Chemical structure of dye
M13 + fluorescamine	7600 (Haugland, 1996)	381	278	27.5 (SE +/- 2.2)	0.120	
M13 + NBD chloride	9800 (Haugland, 1996)	337	200	261.7 (SE +/- 9.6)	0.079	

M13 + rhodamine	87000 (Ma <i>et al.</i> , 2008)	556	536	30.5 (SE +/-0.87)	0.047	 <p>The structure shows a rhodamine core with a trimethylammonium group at the 3-position, a dimethylamino group at the 6-position, and a 4-(isothiocyanatomethyl)benzoic acid group at the 2-position. A chloride ion (Cl⁻) is shown as the counterion.</p>
M13 + BHQ-10	28700 (Biosearch Technologies, 2010)	516	703	24.3 (SE +/-7.6)	0.147	 <p>The structure shows a triphenylmethane derivative with two sulfonate groups (SO₃Na) on the leftmost ring, a 4-(dimethyl(4-oxo-2-oxo-1,2,3,4-tetrahydropyridin-5-yl)butyl)amino group on the rightmost ring, and a diazo group (-N=N-) connecting the middle ring to the leftmost ring.</p>

A comparison of each labelling reaction shows that percentage labelling for each dye is surprisingly repeatable but varies considerably between the different dyes (table 4.2). The largest dye used to label M13 was BHQ-10, and this produced the lowest percentage of labelling (24%). This could be due to its large size (703 g/mol) which sterically hinders the formation of covalent bonds with the accessible amine groups on the M13 bacteriophage. Rhodamine is smaller than BHQ-10, with a molecular weight of 536 g/mol and when combined with M13 bacteriophage resulted in 30.5% labelling. This is slightly larger than the percentage labelling seen with BHQ-10 and this may be due to rhodamine being smaller and so is more accessible to the free amine groups on M13 bacteriophage. Fluorescamine is smaller than rhodamine with a molecular weight of 278 g/mol, and produced a very slightly lower percentage of labelling to rhodamine of 27.5%. This could be due to the differing chemical structure of fluorescamine. The rigid central ring of fluorescamine could be sterically hindering the p8 amine groups from reacting with it. However rhodamine has a long, flexible linker which allows for easier incorporation into the M13 structure. The percentage labelling significantly increased when NBD chloride was used to label M13. NBD chloride has a molecular weight of 200 g/mol and resulted in 261.7% labelling of M13. This means there was roughly 2.5 NBD chloride dye molecules per p8 coat protein. There are only 2 primary amine groups which are accessible on the p8, one on a lysine side chain at position 8 and one at the N-terminus. There are 4 other lysine residues in the p8 structure but these are thought to be inaccessible (Niu *et al.*, 2008). However, because NBD chloride is extremely small it may gain access to some of them and therefore form covalent linkages and increase labelling. Mass spectrometry could be used get an accurate picture of the covalent attachment sites of these dyes and has been used in a number of papers (Lee *et al.*, 2012, Li *et al.*, 2010, Muzard *et al.*, 2012). However a number of attempts were made during this study to obtain similar results, with little success.

All of the dyes used to label M13 bacteriophage proved to produce peaks consistent with their absorbance peaks within their LD signal. This confirmed that the dyes had all been conjugated to the M13 bacteriophage. To investigate which dyes produced larger LD signals, a ratio was derived which compared the intensity of the dye LD signal to that of the M13 core particle. This was calculated by dividing the dye absorbance peak in LD by the 280 nm absorbance peak in LD for M13. This value indicates the ratio of dye peak to M13 peak; consequently a larger value indicates a larger dye peak to M13 peak. Therefore a larger value is more desirable as a large dye peak is required for the assay.

There are several factors which determine the size of an LD signal produced by a dye attached to M13. The first factor is how much dye is covalently attached to the M13, since if more dye molecules are attached then more dye molecules will align with the M13 in shear flow, leading to a larger LD signal. Secondly, the mobility of the dye is an important factor because if the dye is sterically hindered (e.g. large molecular weight) it will form a more rigid structure with the M13, and therefore align much better in shear flow and produce a larger LD signal. In addition the extinction coefficient of the dye is also a factor to be considered because if the dye has a larger extinction coefficient it will absorb more and hence produce a larger LD signal. Lastly the alignment of the transition polar moments is also a key factor because if they are aligned more parallel than perpendicular to the long axis of the M13, the LD signal will be more positive. In contrast, if the transition polar moments are aligned more perpendicular than parallel to the long axis of the M13, the LD signal will be more negative. Whilst if the transition polar moments are exactly in between (at approximately 54.7°) to the long axis of M13, then the LD signal will be zero. All of these factors affect the size of the dye peak in the LD spectra.

Table 4.3 - Factors affecting the LD signal of chromophore labelled M13

Table compares the LD ratios of dye peak to M13 peak when different dyes are used to label M13 bacteriophage, along with the factors causing these LD signals.

Sample	$\frac{LD_{\text{dye}}}{LD_{\text{M13 (280nm)}}}$	% Labelling	Dye Mobility	Extinction Coefficient of dye ($M^{-1} \text{ cm}^{-1}$)	Alignment of transition polar moments
M13 + fluorescamine	0.120	27.5 (SE +/- 2.2)	<ul style="list-style-type: none"> • Low molecular weight provides high dye mobility. • Sterically hindered by rigid central ring. 	7600 (Haugland, 1996)	More parallel than perpendicular to the long axis of the M13.
M13 + rhodamine	0.047	30.5(SE +/-0.87)	<ul style="list-style-type: none"> • Long flexible linker provides high dye mobility. 	87000 (Ma <i>et al.</i> , 2008)	More parallel than perpendicular to the long axis of the M13.
M13 + NBD chloride	0.079	261.7 (SE +/- 9.6)	<ul style="list-style-type: none"> • Low molecular weight provides high dye mobility. 	9800 (Haugland, 1996)	More parallel than perpendicular to the long axis of the M13.
M13 + BHQ-10	0.147	24.3 (SE +/-7.6)	<ul style="list-style-type: none"> • Large molecular weight provides low dye mobility. 	28700 (Biosearch Technologies, 2010)	More parallel than perpendicular to the long axis of the M13.

The results indicate that M13 labelled with BHQ-10 produced the largest dye peak in comparison to the other dyes as it produced the largest ratio value (0.147) (table 4.3). This is surprising because BHQ-10 provided the lowest percentage labelling of M13. However this might be explained by the size of BHQ-10, because it is much larger than the other dyes and therefore is providing a more rigid structure which will lead to a larger dye LD signal. Also BHQ-10 has the second largest extinction coefficient of the dyes used in this chapter. The LD signal produced from BHQ-10 is also positive, indicating that the transition polar moments are more parallel than perpendicular to the long axis of the M13.

M13 labelled with fluorescamine produced a slightly smaller dye peak with a ratio value of 0.120 in comparison to M13 labelled with BHQ-10. An explanation for this is that despite M13 labelled with fluorescamine producing a larger percentage of labelling than M13 labelled with BHQ-10, fluorescamine has a much lower extinction coefficient, the lowest of all of the dyes used. Also fluorescamine is much smaller in size in comparison to BHQ-10 and this therefore makes it more mobile in shear flow, reducing the LD signal. However fluorescamine is also sterically hindered by its rigid central ring, which restricts movement of the dye, therefore producing a larger LD in comparison to NBD chloride and rhodamine. The positive LD signal produced from fluorescamine also reveals that the transition polar moments are more parallel than perpendicular to the long axis of the M13.

M13 labelled with NBD chloride produced the largest percentage of labelling in comparison to the other dyes used, interestingly however, it produced the second smallest dye peak, with a ratio of 0.079. This can be explained by the high mobility of NBD chloride due to its small molecular weight as there is more space to move around (figure 4.12). Furthermore, the extinction coefficient for NBD chloride is small; the second smallest of the dyes used. The LD

signal of the NBD chloride also reveals that the transition polar moments are more parallel than perpendicular to the long axis of the M13 because the dye produces a positive signal.

Lastly, M13 labelled with rhodamine produced the smallest ratio value (0.047) indicating a smaller dye peak. This is in spite of the reasonable percentage of labelling and rhodamine having the largest extinction coefficient and second largest molecular weight. However, this can be explained by the chemistry used to covalently attach rhodamine to the M13. The thiourea linkage between rhodamine and M13 is a longer and more flexible link, which may be increasing the mobility of rhodamine in shear flow and therefore preventing it from aligning and forming a rigid structure with M13 bacteriophage. Thus a low LD signal was produced. Although small, the LD signal produced was positive, indicating that the transition polar moments were more parallel than perpendicular to the long axis of the M13.

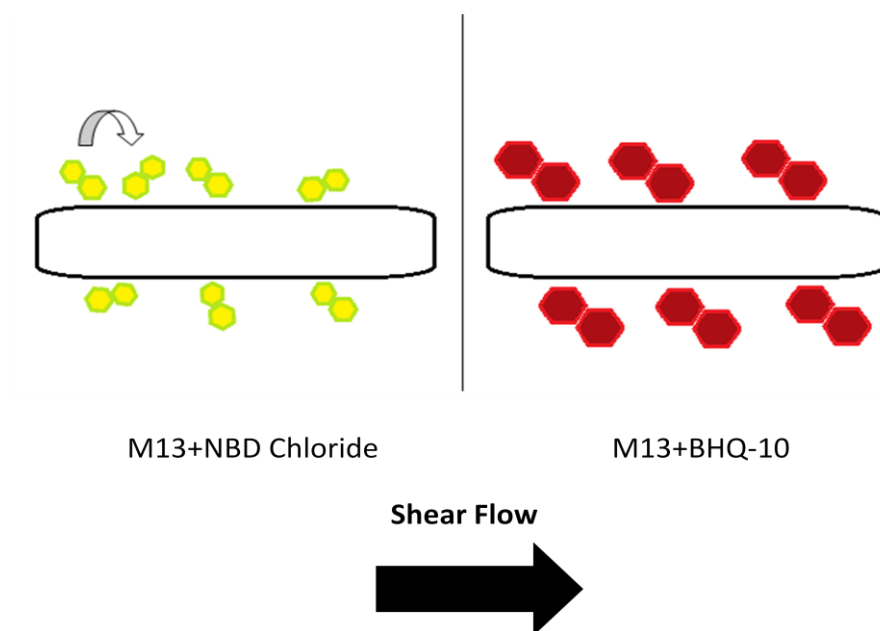


Figure 4.12 - Schematic diagram illustrating M13 labelled with NBD chloride and M13 labelled with BHQ-10

Schematic diagram illustrating M13 labelled with NBD chloride and M13 labelled with BHQ-10 in shear flow within an LD cell. NBD chloride is a small chromophore and when it is covalently attached to M13 this allows it to be flexible and mobile which results in a smaller LD signal. In contrast BHQ-10 is much larger and therefore provides a more rigid structure with M13 which is less mobile and this could explain why it provides a larger LD signal. The arrow in the top left illustrates the flexibility of the NBD chloride when conjugated to the M13 bacteriophage.

4.6. Conclusion

To develop this assay system, which currently involves M13 bacteriophage and LD, it is important that it is able to detect more than one target at once and that it has embedded control reactions within it. In addition, to make the instrumentation more compact, transportable and economical, signals in the visible region need to be attained.

One way of achieving this is to incorporate dyes into the assay which provide a signal in the visible region and provide an independent signal for each assay in a multiplexed test. Covalently linking dyes on to the p8 coat proteins of M13 bacteriophage along with specific antibodies will allow the M13 to detect its target whilst also producing specific peaks in the LD spectrum relating to the dye used. If the target is present then the peak drops and this

indicates the presence of the target. The dyes are therefore useful as they allow for the assay to be multiplexed and can allow for controls to ensure the assay is valid.

Various dyes were chosen to label M13 bacteriophage, based on cost, spectroscopic characteristics and linkage chemistry. The dyes used included fluorescamine, rhodamine, NBD chloride and BHQ-10, and all reacted with the amine groups present on the p8 coat protein. The results confirmed that they had all successfully labelled M13 bacteriophage. The UV/Vis absorbance spectra were used initially to indicate that the dye was present with the M13 bacteriophage. The LD spectra confirmed whether the dye had labelled the M13 because dye alone cannot align due to its small size. However when covalently attached to M13, the dye is able to produce an LD peak corresponding to where the dye absorbs.

The UV/Vis absorbance spectra of the dye labelled M13 allowed for the percentage labelling of M13 to be calculated. The results highlighted that molecular weight may play a role in determining how well a dye labels the M13. The results showed that BHQ-10, the largest dye used, produced the lowest percentage labelling whilst NBD chloride, the smallest dye used, produced the highest percentage labelling. An explanation for this is that larger dye molecules are sterically precluded from interacting with amine groups on the M13 and therefore fail to label the M13. Whilst smaller dye molecules are able to obtain access to the free amine groups and therefore result in a larger percentage of labelled M13.

The LD spectra of M13 conjugated with various dyes confirmed that all of the dyes used had formed covalent attachments with the M13. The results indicated that 4 specific factors determined the size of the dye peaks within the LD spectrum and these are:

- percentage of labelling
- dye mobility

- extinction coefficient of dye
- alignment of transmission polar moments

M13 labelled with BHQ-10 produced the largest ratio value which compared the dye absorbance peak to the M13 peak at 280 nm. This was explained by the large molecular weight of BHQ-10, as this would cause steric hindrance when conjugated to the M13, resulting in a very rigid structure which consequently produced a large LD signal for the dye. Contrastingly, NBD chloride which had a very small molecular weight produced a lower ratio value, indicating that it was more flexible and able to move around in shear flow. Fluorescamine and rhodamine both proved that the linkage chemistry also affects the dye mobility, which consequently can affect the size of the dye peak. Since long flexible linkers can increase the dye mobility, as was seen with rhodamine which produced the lowest LD ratio value. Whereas fluorescamine was covalently linked via its central ring which essentially stuck the dye to the M13, providing a very rigid structure which provided a reasonably large LD ratio value.

This research has demonstrated the potential to use dyes in assay systems, however only a small group of dyes were investigated and more work is required to investigate a broader range of dyes with varying absorbance maxima. Also the linkage chemistry used to attach the dyes can be further examined to optimise the labelling and LD dye peak.

Overall the results demonstrate that dyes can be incorporated into the assay and this demonstrates the potential of this detection system to become multiplexed, multimodal and miniaturised into a smaller and more affordable format.

CHAPTER 5

- DEVELOPMENT OF A HIGH SENSITIVITY ASSAY USING M13 BACTERIOPHAGE AND LINEAR DICHROISM

Pacheco-Gomez *et al.* (2012) established that LD and M13 bacteriophage can be coupled together to form a detection assay which can successfully detect *E. coli* O157. The assay was developed by producing M13 bacteriophage with an FB domain fused to the p3 protein (FB-M13) (figure 5.1). The FB domain was able to specifically bind to the secondary antibody, via its constant region, forming a complex which was found to be aligned in a flow cell producing a characteristic M13 LD signal. The primary antibody that was used in this study was raised to specifically bind to an antigen on the surface of *E. coli* O157 and was therefore used to detect *E. coli* O157. When the anti-*E. coli* O157 and *E. coli* O157 were added to the conjugated FB-M13, the LD signal dropped significantly (figure 1.22 and figure 5.2). This detection assay proved to be a promising method for the detection of bacteria. However, this assay was only capable of detecting 10^7 cells/mL which is well below that required for a clinical assay where a limit of 10^5 cells/mL is more usual. It is therefore clear that the sensitivity of this assay needed to be improved. In addition, the reliance of the assay on a non-covalent interaction between the secondary antibody and primary antibody also meant that the assay was not suitable for

assay multiplexing. This is because the antibodies would be able to dissociate from one set of M13 particles and re-associate with a second set thus scrambling the assay.

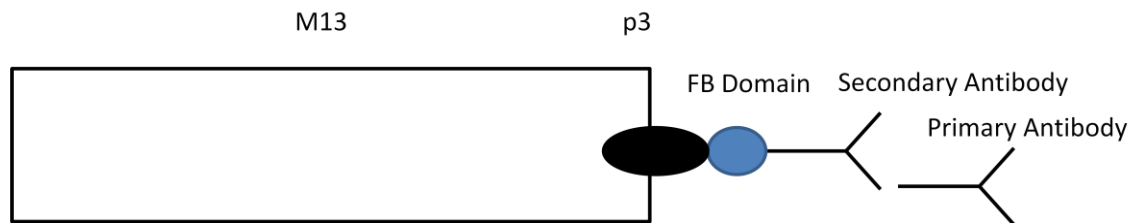


Figure 5.1 - A schematic diagram of the M13 reagent used by Pacheco-Gomez *et al.* (2012)

A schematic diagram of the M13 reagent used by Pacheco-Gomez *et al.* (2012) in their detection assay. They produced M13 bacteriophage with an FB domain fused to the p3 coat protein. The FB domain specifically attached to a secondary antibody via the constant region. The primary antibody was raised to specifically bind to an antigen.

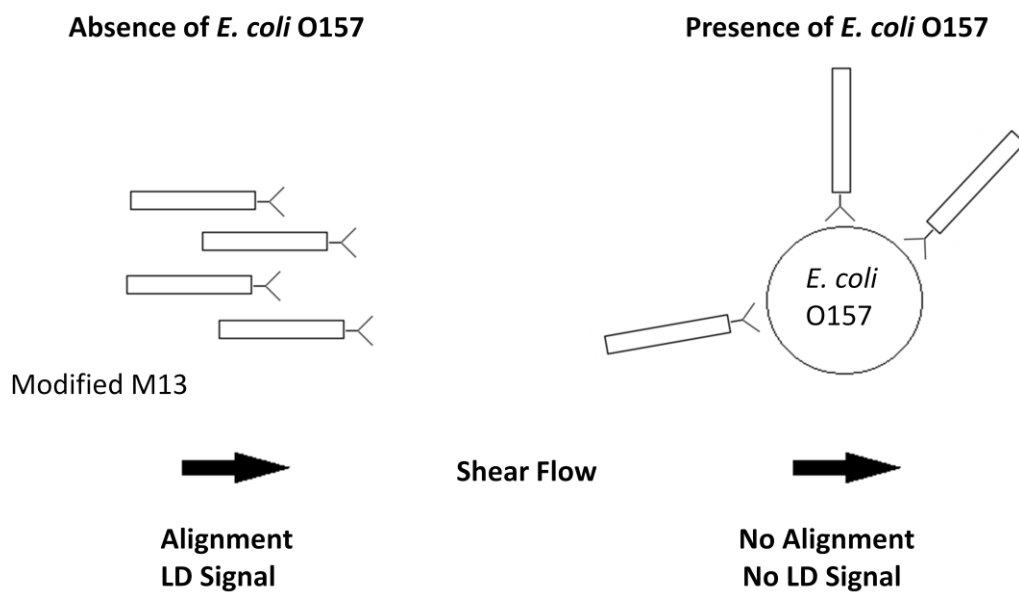


Figure 5.2 - A schematic diagram illustrating the principle behind the pathogen detection assay used by Pacheco-Gomez *et al.* (2012).

A schematic diagram illustrating the principle behind the pathogen detection assay used by Pacheco Gomez *et al.* (2012) which utilised LD and M13 bacteriophage. M13 bacteriophage labelled with anti-*E. coli* O157 antibody (via the p3 coat protein) aligns under shear flow, thus a LD signal is seen. If a sample containing *E. coli* O157 is added to the M13 reagent, alignment is disrupted due to the formation of bonds between the antibody labelled M13 and the *E. coli* O157. Therefore a reduction in the LD signal is observed.

It was clear from the work done by Pacheco-Gomez *et al.* (2012) that the assay could be further developed by utilising a covalent linkage to conjugate the primary antibody directly (e.g. anti-*E. coli* O157) on to the M13. This removes the need for a secondary antibody and therefore reduces costs and time and also makes the structure more stable for detection. Also rather than utilising the p3 coat protein of which there is only 5 copies in each M13 particle, the p8 coat protein could be used to chemically conjugate the primary antibody (figure 5.3). The primary reason for this is because there are 2700 copies of the p8 coat protein within the M13 coat. This increases the number of antibodies on each particle potentially leading to an increase in assay avidity. The conjugation of antibodies onto the p8 coat protein which runs the whole length of the M13 also ensures that the M13 adheres to the target along its length ensuring a full disruption of M13 alignment and hence maximum signal change (figure 5.4). In addition to this, utilising the p8 coat protein and directly conjugating a primary antibody to it will help establish a multiplexed assay; the previous method used by Pacheco-Gomez *et al.* (2012) involving a primary and secondary antibody would not support a multiplexed assay.

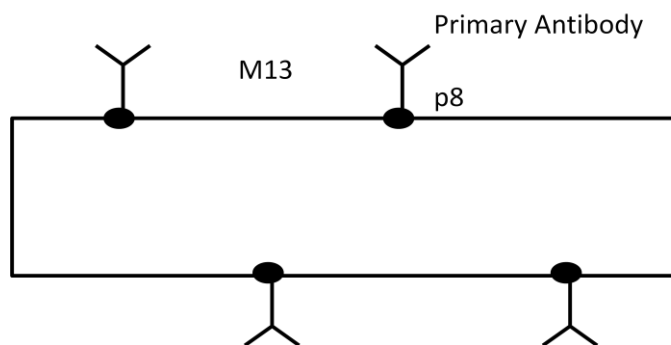


Figure 5.3 - A schematic diagram of the M13 reagent proposed for a detection assay

A schematic diagram of the M13 reagent proposed for a detection assay based on the work done by Pacheco-Gomez *et al.* (2012). The M13 bacteriophage is covalently conjugated with primary antibodies via the p8 coat protein which runs along the length of M13.

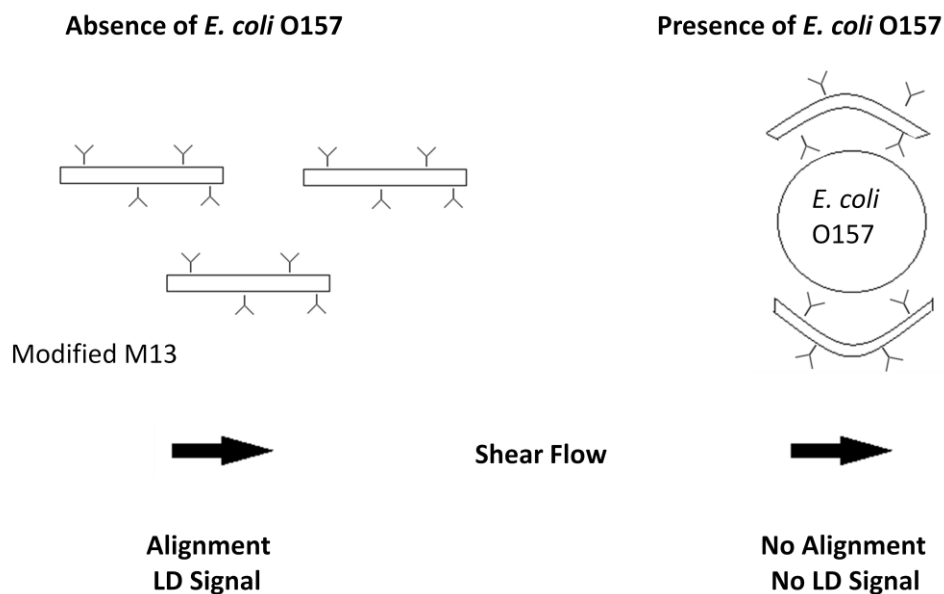


Figure 5.4 - A schematic diagram illustrating the development of the M13/LD based assay

A schematic diagram illustrating assay development based on the work done by Pacheco-Gomez *et al.* (2012) where LD and M13 bacteriophage are utilised for pathogen detection. M13 bacteriophage labelled with anti-*E. coli* O157 antibody (via the p8 coat protein) aligns under shear flow, thus a LD signal is seen. If a sample containing *E. coli* O157 is added to the M13 reagent, alignment is disrupted due to the formation of bonds between the antibody labelled M13 and the *E. coli* O157. Therefore a reduction in the LD signal is observed.

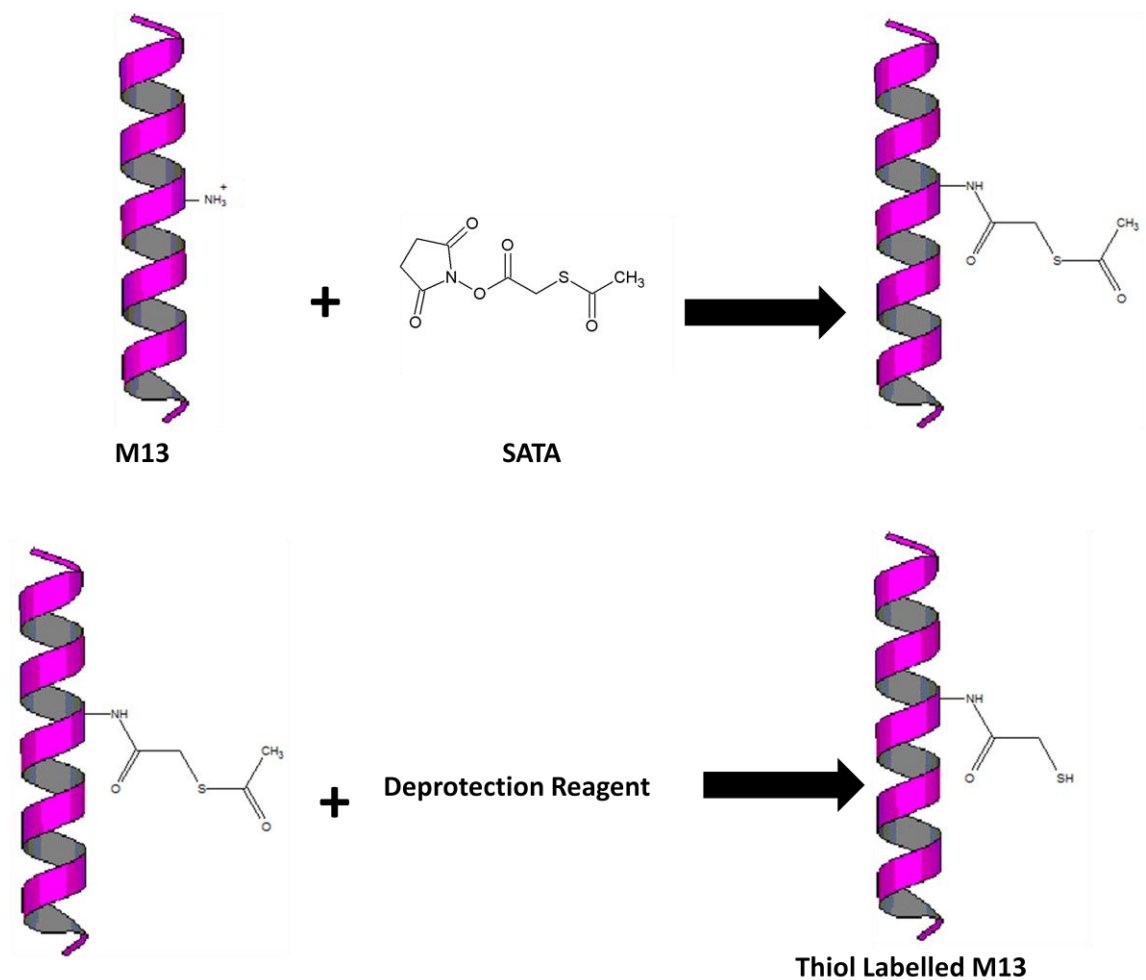
5.1. Conjugation methods

M13 bacteriophage has to be conjugated to an antibody in this assay; the heterobifunctional coupling of amines to thiols method was used to achieve this (Aslam and Dent, 1998).

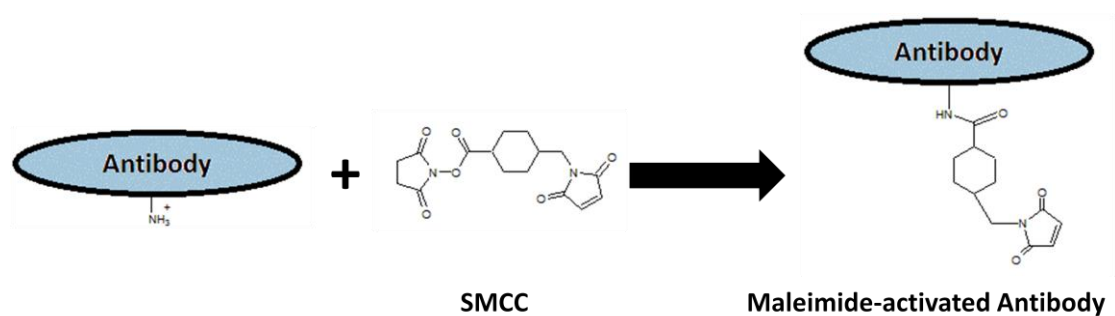
For bioconjugation to occur the p8 coat protein on M13 and the antibody need to be chemically activated. The p8 coat protein on M13 is activated using succinimidyl acetylthioacetate (SATA); this introduces protected sulfhydryl groups onto the primary amine groups on the lysine residue and N-terminus of the p8 coat protein. Deprotection reagent (hydroxylamine/EDTA) is then added to free the sulfhydryl group by deacylating (removing the RCO- group) the sulfhydryl group. In parallel the antibody is activated using succinimidyl-4-(*N*-maleimidomethyl) cyclohexane-1-carboxylate (SMCC), which modifies the amine groups to create derivatives that terminate in sulfhydryl reactive maleimide groups. The maleimide

activated antibody is then added to the thiol labelled M13 and as a result undergoes a nucleophilic reaction and a thioether bond forms (figure 5.5).

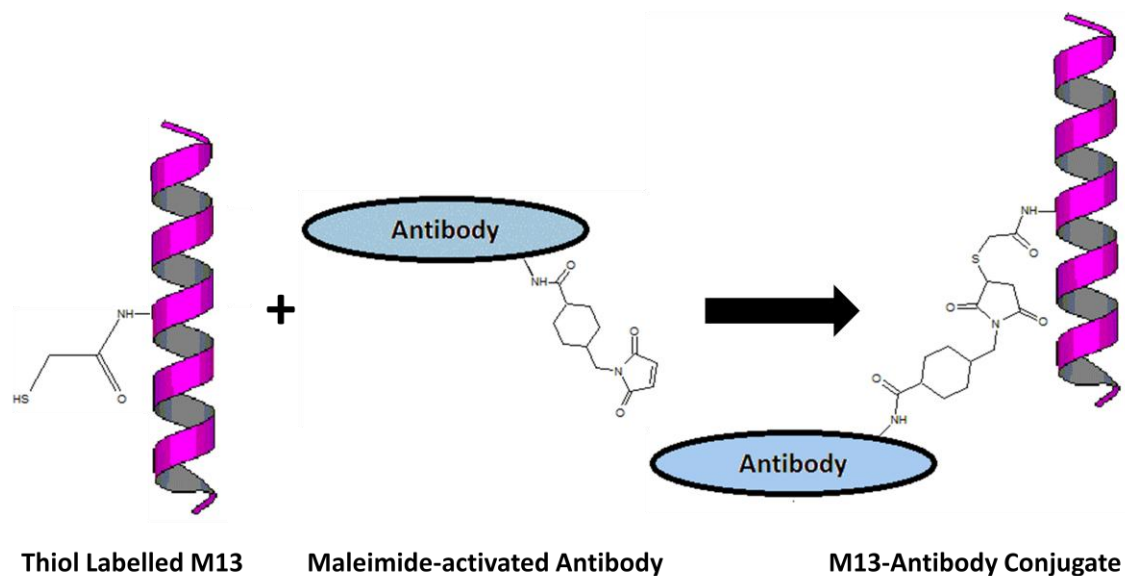
The conjugated M13 does not affect the ability of M13 to align or its LD signal, and this therefore helps to provide a stable assay (Pacheco-Gomez *et al.*, 2012).



A) SATA is incubated with M13 and introduces sulfhydryl groups to the amine groups on the p8 coat protein. Deprotection reagent (hydroxylamine/EDTA) is then added to deacylate the sulfhydryl groups to produce thiol labelled M13.



B) SMCC is added to the antibody and it modifies its amine groups to form amide linkages, which upon modification then creates derivatives that terminate in reactive maleimide groups.



c) The maleimide-activated antibody is added to the thiol labelled M13 and a thioether bond forms.

Figure 5.5 - Chemistry used to conjugate M13 to an antibody.

SMCC and SATA allow for the formation of a thioether bond between M13 bacteriophage and the antibody.

A three step strategy was used to develop this conjugation method, each stage beginning with M13 modified to contain thiol groups:

1. The number of available thiol groups on the derivatised M13 was assessed by derivatisation with a thiol specific reagent, eosin-5-maleimide.
2. The availability of thiol groups for conjugation to maleimide derivatised antibodies was assessed using a readily available antibody with the resultant complexes visualised using transmission electron microscopy.
3. The final conjugate between M13 and an *E. coli* O157 specific antibody was produced and its ability to detect *E. coli* O157 assessed.

5.2. Labelling M13 bacteriophage with eosin-5-maleimide

To conjugate an antibody to the p8 coat protein of M13 bacteriophage, both the p8 and antibody need to be activated using SATA and SMCC respectively. This will result in a thioether linkage between the two. To examine and visualise this conjugation method, a dye was initially used to mimic the maleimide-antibody reagent. Eosin-5-maleimide is an inexpensive dye and already contains a maleimide group (which therefore removes the need to use SMCC) and is able to react with thiol groups to form thioether bonds (figure 5.6). For M13 to react with eosin-5-maleimide it would therefore require the introduction of sulfhydryl groups on to the primary amine groups on the lysine residues and the N-terminus on the p8 coat proteins using SATA. Deprotection reagent was used to free the sulfhydryl groups by deacylating them (removing the RCO- group), thus resulting in thiol labelled M13.

Eosin-5-maleimide has an absorption maximum of 524 nm (Haugland, 1996); this is in the visible region. To determine if eosin-5-maleimide was present in the final sample of M13 after labelling, the UV/Vis absorbance and fluorescence was measured. The LD signal of the conjugate was also measured to assess the formation of the covalent complex (a peak should appear at 524 nm where the dye absorbs) as well as the structural integrity of the M13 particle. The molecular weight of eosin-5-maleimide is 743 g/mol, and so should not affect the alignment of M13 in an LD experiment. Eosin-5-maleimide was therefore selected as the labelling agent.

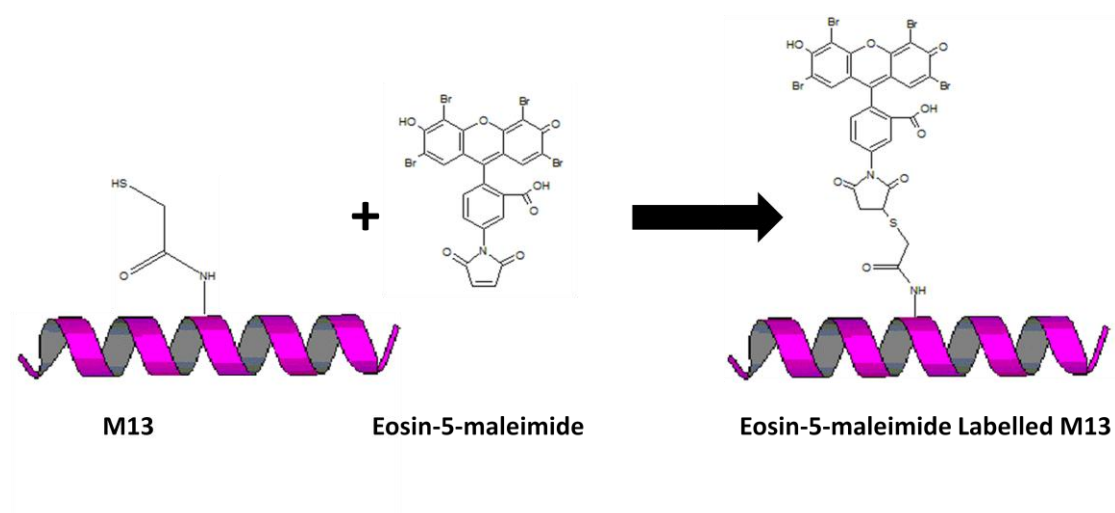


Figure 5.6 - Labelling M13 with eosin-5-maleimide

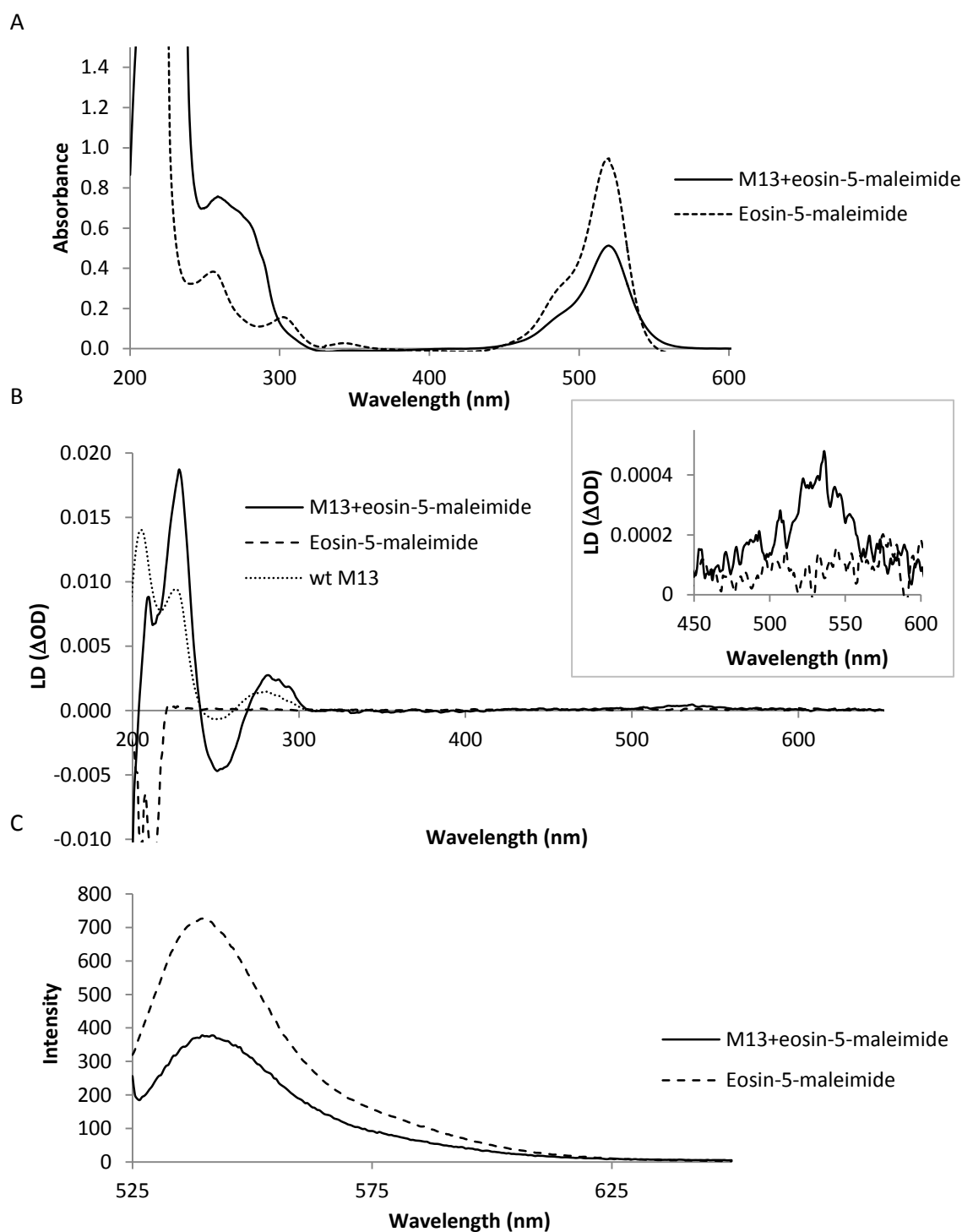


Figure 5.7 - UV/Vis absorbance spectra, LD spectra and fluorescence spectra of eosin-5-maleimide and M13 labelled with eosin-5-maleimide

(A) UV/Vis absorbance spectra of M13 labelled with eosin-5-maleimide dye (0.6 mg/mL) and of eosin-5-maleimide dye (0.04 mM). (B) LD spectra of M13 labelled with eosin-5-maleimide dye (0.6 mg/mL), eosin-5-maleimide dye (0.1 mM) and wt M13 (0.2 mg/mL). Inset highlights the peak caused by eosin-5-maleimide when conjugated to M13. (C) Fluorescence spectra of M13 labelled with eosin-5-maleimide dye (0.26 mg/mL) and of eosin-5-maleimide dye (concentration of 0.01 mM). Excitation wavelength - 520 nm.

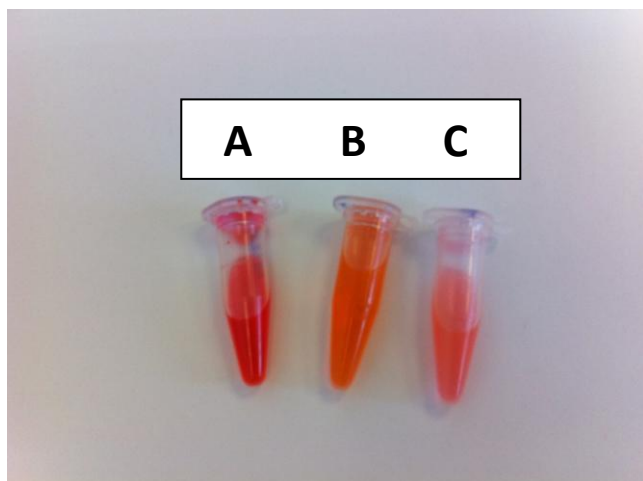


Figure 5.8 - Image showing the change in colour during the labelling process

Comparison of the colour of three solutions, where (A) is eosin-5-maleimide dye alone. After leaving eosin-5-maleimide dye to react with M13, the solution was precipitated and centrifuged to spin down the M13 labelled with eosin-5-maleimide. The resulting supernatant (B) thus contained the free unreacted eosin-5-maleimide dye. The pellet of M13 labelled with eosin-5-maleimide was resuspended in phosphate buffer (C).

Eosin-5-maleimide alone produces an absorbance peak at 524 nm in the UV/Vis spectrum. M13 labelled with eosin-5-maleimide also absorbs at this wavelength, indicating the presence of the dye with M13 (figure 5.7A). The fluorescence spectrum (figure 5.7C) also highlights how M13 labelled with eosin-5-maleimide dye emits light between 530-560 nm which is also where the eosin-5-maleimide dye emits light.

The LD spectrum of M13 labelled with eosin-5-maleimide dye confirms that the dye was bound to the M13 because a peak is seen at 524 nm (5.7B). Eosin-5-maleimide alone does not produce any LD signal. The LD spectrum of M13 labelled with eosin-5-maleimide dye also displayed the characteristic peaks of M13. The percentage of labelled p8 coat proteins calculated from the UV/Vis absorbance spectra was 16.5%. To put this into context, if this level of labelling was replicated with antibodies then each M13 particle would have more than 400 antibodies on its surface. These results show that the modification of amine groups on the surface of M13 to produce thiol groups has been achieved successfully with a sufficient labelling yield to proceed with antibody conjugation. It is of course possible to attempt to

optimise the yield of conjugate further. However in the previous chapter it was shown that conjugation levels for eosin-like moieties seldom increase above 30%.

5.3. M13 bacteriophage conjugated with GAM

The formation of a thioether bond as a means of conjugating another molecule to M13 has previously been proved successful with eosin-5-maleimide dye. The next stage of this process is to conjugate an antibody on to M13 via the p8 coat proteins. Development of the assay requires the covalent attachment of antibodies on to M13 so that it is able to detect particular targets. The model antibody being used to confirm conjugation on to M13 is a goat anti-mouse (GAM) antibody which offers two benefits over using the *E. coli* O157 specific antibody:

1. The antibody is considerably cheaper than the *E. coli* O157 specific antibody
2. The M13-GAM conjugate that results from these experiments could be a useful reagent in assays where a covalent coupling between the M13 and a target mouse antibody is not required.

To couple the GAM to M13, the GAM must be treated with SMCC in order for it to acquire a maleimide group. Similarly M13 has to be treated with SATA and deprotection reagent to acquire thiol groups, after which the GAM and M13 will be combined to form thioether bonds with each other.

UV/Vis spectroscopy was used to measure the absorbance of the GAM solution, the GAM solution following treatment with SMCC for one hour and the M13 solution following treatment with SATA for one hour. The UV/Vis and LD absorbance of the final solution of M13 conjugated with GAM was also measured to determine if its spectrum would retain its characteristic features. This would in turn allow us to determine if the structure of the M13 would be maintained after conjugation. To also determine if the GAM had conjugated the

M13, transmission electron microscopy (TEM) was utilised to visualise the covalent linkages between the two structures.

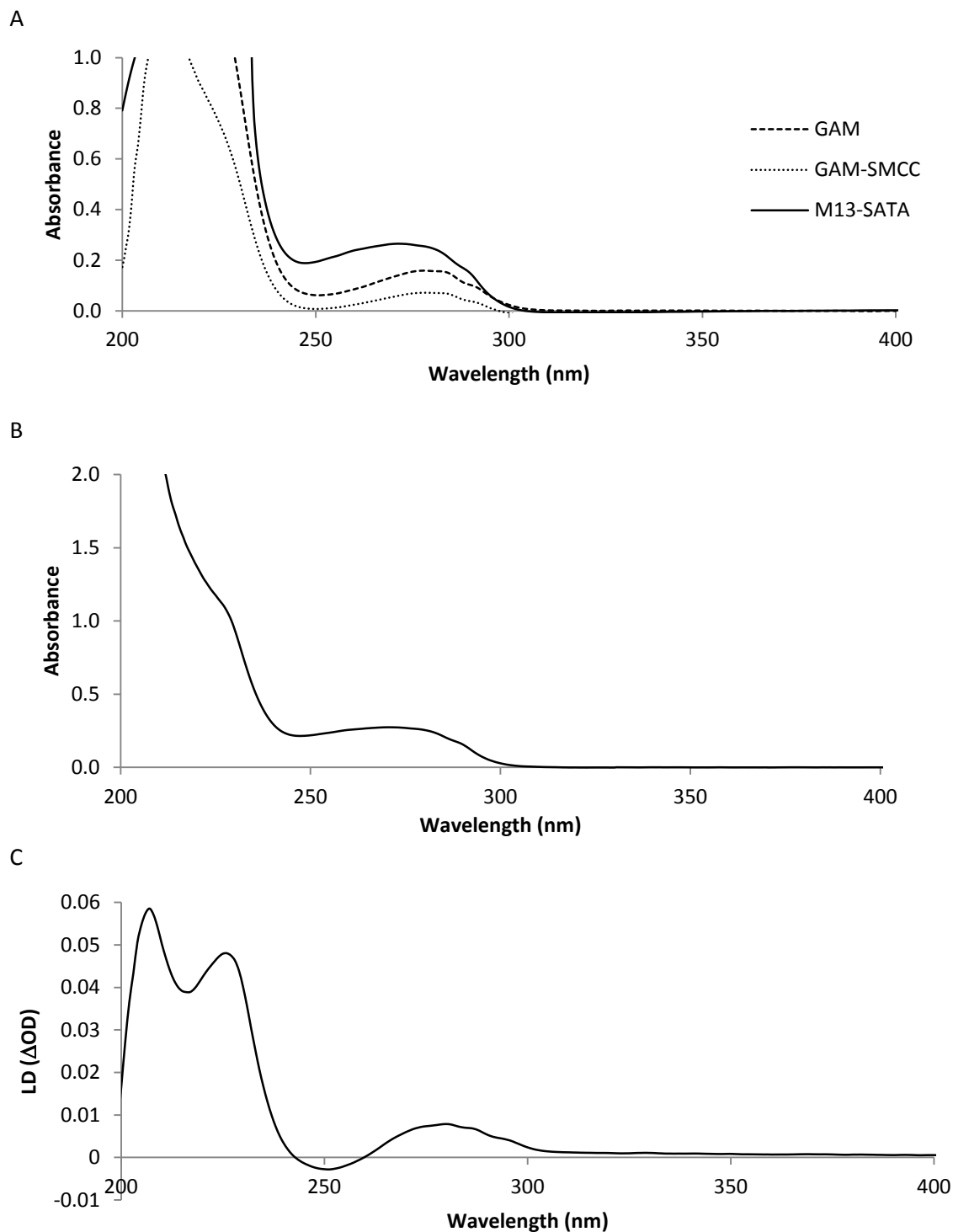
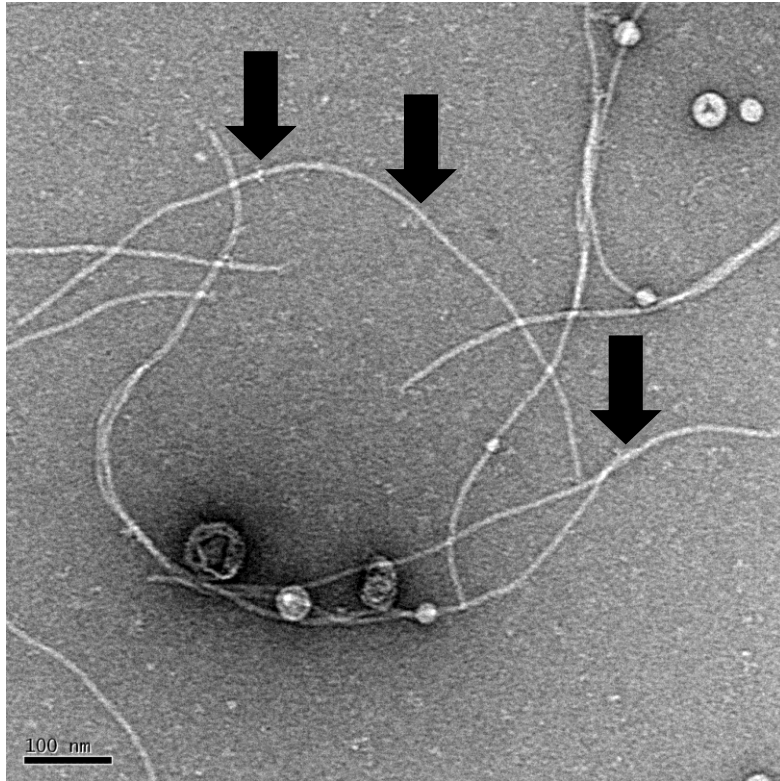


Figure 5.9 - The UV/Vis and LD spectra of the process of bioconjugating M13 with GAM

Graph A shows the UV/Vis absorbance spectra of GAM (0.38 mg/mL) in distilled water, GAM following treatment with SMCC for one hour and undergoing a PEG precipitation step to remove the SMCC (GAM-SMCC) (0.17 mg/mL) and M13 following treatment with SATA for one hour and deprotection reagent and a PEG precipitation step to remove the SATA once reacted (M13-SATA) (0.22 mg/mL). Graphs B and C show the UV/Vis absorbance and LD spectrum of M13 conjugated with GAM (0.2 mg/mL) respectively.

A



B

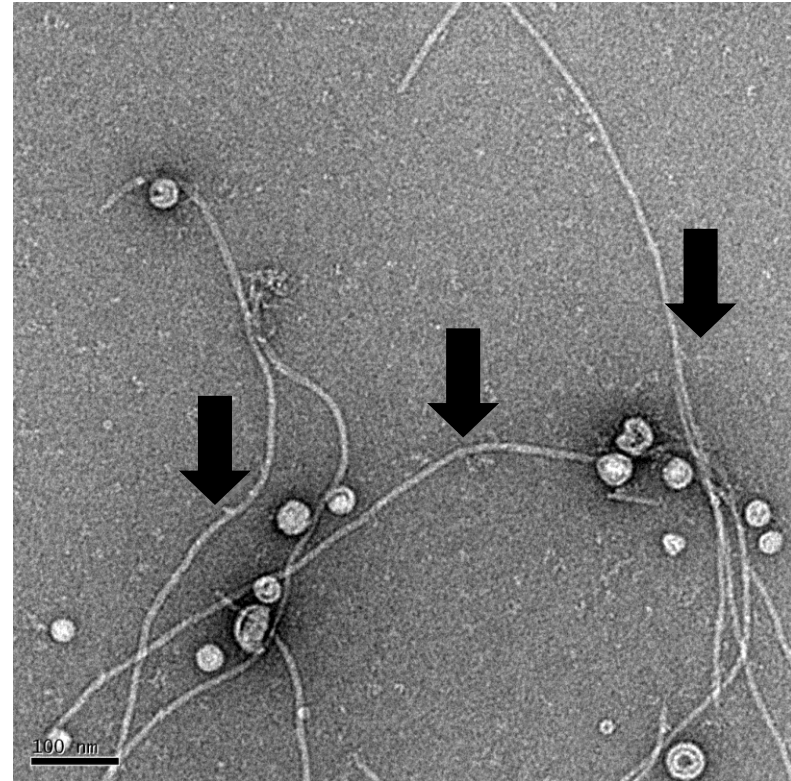


Figure 5.10 - Transmission electron microscopy images of M13 conjugated with GAM

Transmission electron microscopy images, the bar represents 100 nm; A and B both display 0.3 mg/mL M13 conjugated with GAM. The arrows point to where the GAM has covalently attached to M13.

Conjugating M13 with GAM proved to be successful. Figure 5.9 demonstrates that following M13 conjugation with GAM, the M13 still maintains its characteristic spectrum. The TEM images display where the antibodies conjugated onto the M13 bacteriophages, confirming that the chemistry used achieved covalent attachments (figure 5.10).

5.4. Production of double labelled M13 reagent

Given the success with conjugating M13 to chromophores and antibodies, the next stage was to couple the M13 to the *E. coli* O157 specific antibody. The chosen target pathogen was *E. coli* O157 as detection of this pathogen is appropriate for food samples and medical samples, since *E. coli* O157 can be found in both food and human samples (Pennington, 2010). In addition to coupling this antibody to the M13 we also aim to couple a dye to the surface of the same M13 to produce a double labelled M13. As discussed in an earlier chapter the addition of a dye to the M13 with an LD signal in the visible part of the spectrum enables the simplification of the instrument used to detect the LD signal. The addition of different dyes to different M13:antibody conjugates also provides the basis for a multiplexed test.

Double labelled M13 was produced using goat anti-*E. coli* O157 antibody (GAE) as the chosen antibody and BHQ-10 as the chosen dye. GAE antibody was chosen because it is able to detect the O and H antigens present on *E. coli* O157 (information provided by Thermo Fisher Scientific). BHQ-10 was chosen because it proved to produce an LD signal with a large peak where it absorbed at 516 nm. The dye was inexpensive and the chemistry used to covalently link it to M13 via the amine groups on the p8 coat proteins was straightforward.

M13 had to be modified with SATA in order to covalently attach GAE and BHQ-10 to its p8 coat proteins. SATA works by attaching sulfhydryl groups on to the free amine groups (one on the N-terminus and one on a lysine residue). The GAE was modified by the addition of SMCC which attaches a maleimide group on to the GAE (figure 5.5). The maleimide groups on the GAE react

with the thiol groups on the M13 and form thioether bonds. The BHQ-10 was similarly modified by the addition of N-(2-Aminoethyl) maleimide (AEM). The amine group of the AEM reacts with the carbonyl group of the N-hydroxysuccinimide ester (NHS ester) on BHQ-10, substituting the NHS for a maleimide group. This then allows BHQ-10 to form a thioether bond with M13 (figure 5.11).

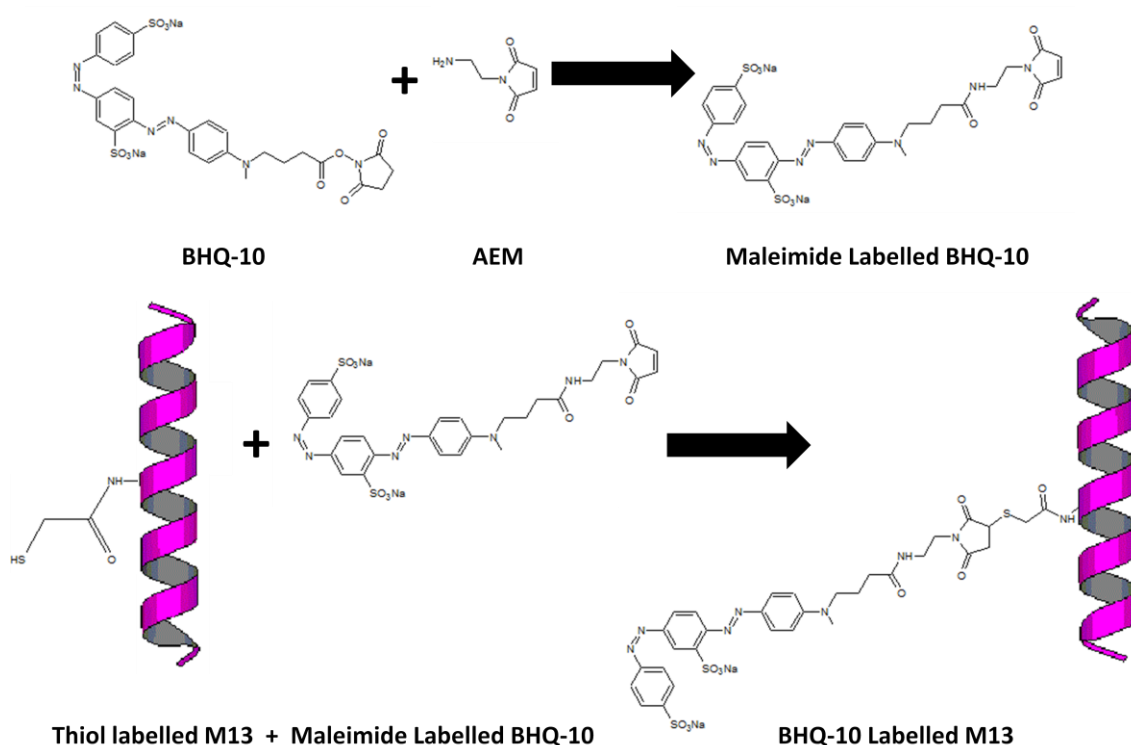


Figure 5.11 - Covalently linking thiol labelled M13 with maleimide labelled BHQ-10

Chemistry used to attach maleimide groups on to BHQ-10 using AEM and chemistry used to react this with thiol labelled M13 to form a thioether bond.

To produce the double labelled M13, the thiol labelled M13 was initially incubated with maleimide labelled GAE overnight. Following this the maleimide labelled BHQ-10 was added to the M13 and GAE solution and left to incubate for a further hour. This solution was then allowed to precipitate with PEG and centrifuged to spin down the double labelled M13 and these pellets were resuspended in phosphate buffer (see section 2.2.5.). The UV/Vis absorbance spectrum was then measured to determine the concentration.

BHQ-10 dye absorbs at 516 nm, and figure 5.12A shows that double labelled M13 produces a fairly large broad peak at 516 nm, confirming the presence of the dye in solution. The LD signal confirmed that the BHQ-10 had covalently attached to the M13 as there was a peak at 516 nm in the LD spectrum (figure 5.12B).

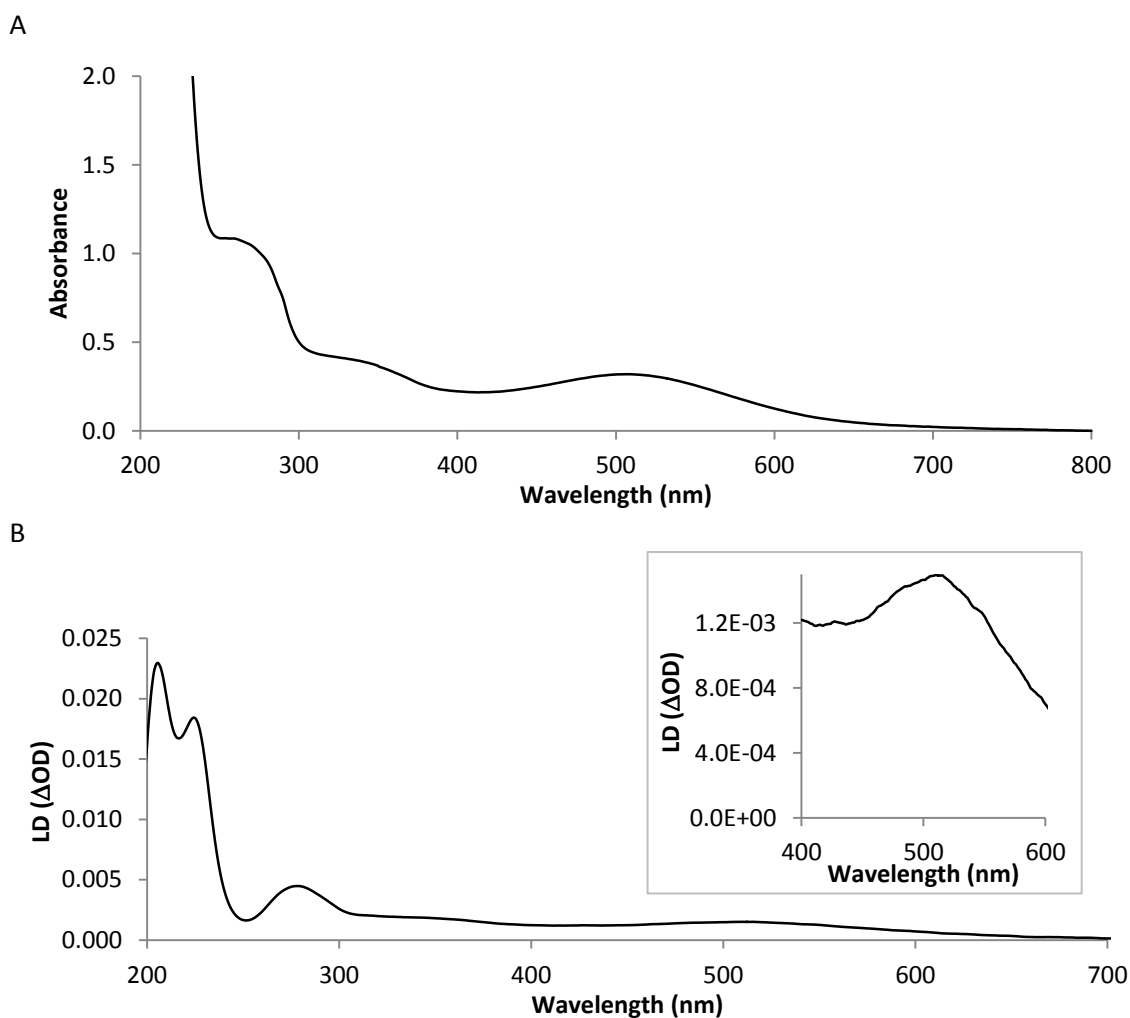


Figure 5.12 - UV/Vis spectrum and LD spectrum of double labelled M13

The UV/Vis spectrum (A) and LD spectrum (B) of double labelled M13 made by covalently linking GAE and BHQ-10 to the M13 (0.9 mg/mL).

5.5. Detection of *E. coli* O157 using double labelled M13 and LD

LD was examined as a diagnostic method by adding *E. coli* O157 into a solution of double labelled M13 (M13 conjugated with a dye and anti-*E. coli* O157 antibody). Solutions containing 10^5 , 10^6 and 10^7 cells/mL of *E. coli* O157 were added to the double labelled M13 to determine the sensitivity of the assay. A control of double labelled M13 alone was used to determine the baseline LD signal. To determine the specificity of the assay, *E. coli* XL10 was added to the double labelled M13.

Three different dilutions of *E. coli* O157 (10^5 , 10^6 and 10^7 cells/mL) were introduced to double labelled M13 and then placed into the LD instrument to examine the sensitivity of the assay. The LD spectra verifies that the addition of *E. coli* O157 causes a significant drop in LD signal as the double labelled M13 is no longer able to align. This confirms that LD and double labelled M13 are able to detect *E. coli* O157. All of the samples produced LD spectra with the characteristic M13 signals (positive peaks at 200-240 nm and 260-300 nm and the negative band between 240-260 nm), and all samples likewise produced a peak at 516 nm which corresponded to the BHQ-10 dye used to label the M13. The peaks however decreased as the concentration of *E. coli* O157 cells present in the solution increased. A further comparison was made between the peaks at 280 nm and 516 nm to indicate if both peaks decreased with increasing concentrations of *E. coli* O157 cells. A t-test was used to determine the significance of the results in comparison to the control.

The control sample which consisted of double labelled M13 with 0.1 M phosphate buffer pH 7.5 and tween (0.05%) (tween was used to prevent any non-specific binding) produced a large LD signal (0.004 Δ OD at 280 nm and 0.0014 Δ OD at 516 nm) (figure 5.13). A similar signal was produced when 10^7 cells/mL of *E. coli* XL10 was added to the double labelled M13 and 0.1 M phosphate buffer pH 7.5 and tween (0.05%) (0.0039 Δ OD at 280 nm and 0.0011 Δ OD at 516

nm). The *E. coli* XL10 cells were used to test the specificity of the assay. An unpaired two tailed t-test between the control and the addition of *E. coli* XL10 cells at 280 nm and 516 nm showed no significance as both p values at 280 nm (0.31) and 516 nm (0.097) exceeded the 0.05 significance level. The results therefore show that the assay is specific.

A considerable drop in LD signal was seen when 10^7 cells/mL of *E. coli* O157 was added to the double labelled M13 and 0.1 M phosphate buffer pH 7.5 and tween (0.05%). The LD signal at both 280 nm and 516 nm was approximately 3 times smaller than that of the control. A t-test comparing the LD signals at 280 nm between the control and the presence of 10^7 cells/mL of *E. coli* O157 show a significant difference as the p value (0.003) was lower than the 0.01 significance level. Similarly the peak at 516 nm was significantly lower in comparison to the control as the p value (0.0036) was lower than the 0.01 significance level. These results clarified that the LD signals at 280 nm and 516 nm were significantly smaller in comparison to those in the control. This significant change in LD signal provides evidence that this assay is able to detect *E. coli* O157.

A comparable LD signal was generated when 10^6 cells/mL of *E. coli* O157 was added to the double labelled M13. The peaks produced at 280 nm and 516 nm were again significantly smaller in comparison to the peaks seen in the control, with both p values being lower than the 0.01 significance level (p value of 0.0018 and 0.0025 respectively).

The addition of 10^5 cells/mL of *E. coli* O157 into the assay resulted in an LD signal which was much lower than that of the control (approximately 1.3 times smaller than the LD signal at 280 nm and 1.75 times smaller than the signal at 516 nm) but also larger than the LD signals produced in the presence of 10^7 and 10^6 cells/mL of *E. coli* O157. Both peaks at 280 nm and 516 nm were significantly smaller than those seen in the control (p values of 0.044 and 0.015 respectively). However these results were not as significant as when 10^7 and 10^6 cells/mL of *E.*

coli O157 cells were added into the assay as the p values are not lower than the 0.01 significance level, but lower than the 0.05 significance level. The results however still show that when 10^5 cells/mL of *E. coli* O157 are present in the assay, a significantly lower LD signal is produced in comparison to the control.

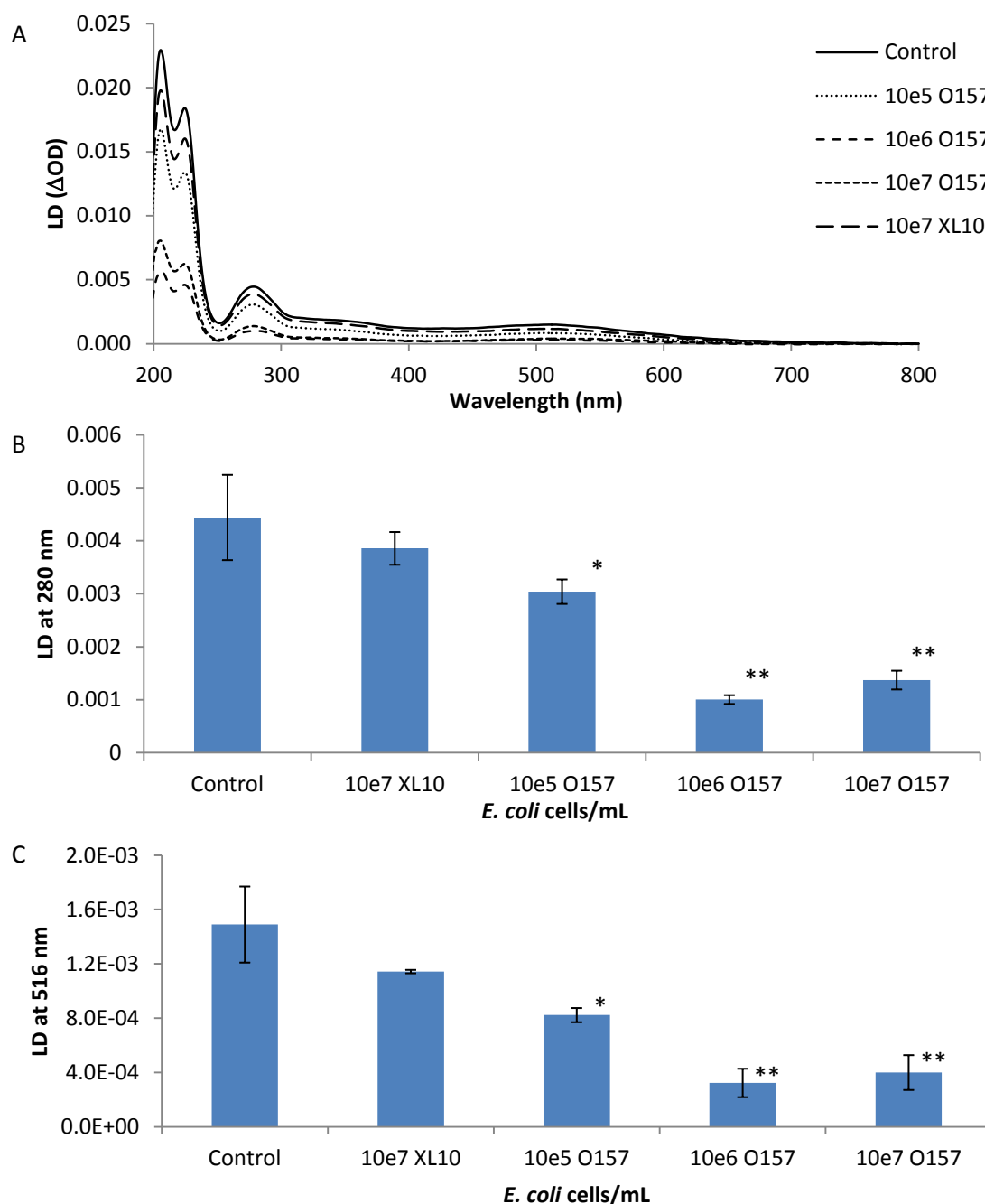


Figure 5.13 - Detection of *E. coli* O157 using double labelled M13 and LD

The LD spectra displayed in A demonstrates the drop in LD signal when *E. coli* O157 is added to double labelled M13 (M13 conjugated with GAE and BHQ-10). The control consisted of double labelled M13 (3.6 mg/mL) and 0.1 M phosphate buffer pH 7.5 and tween (0.05%). Differing dilutions of *E. coli* O157 (10^5 , 10^6 and 10^7 cells/mL) were added to the double labelled M13 and 0.1 M phosphate buffer pH 7.5 and tween (0.05%). An additional control of 10^7 cells/mL of *E. coli* XL10 was added to the assay to determine specificity. Graph B compares the LD signals at 280 nm of the control and the addition of 10^5 , 10^6 and 10^7 cells/mL of *E. coli* O157 to the double labelled M13, as well as the 10^7 cells/mL of *E. coli* XL10. Graph C compares the LD signals at 516 nm of the control and the addition of 10^5 , 10^6 and 10^7 cells/mL *E. coli* O157 to the double labelled M13, as well as the 10^7 cells/mL of *E. coli* XL10. Unpaired two tailed t-test, * significant at $p < 0.05$ and ** significant at $p < 0.01$. The error bars show the standard deviation.

These results indicate that this assay is sensitive enough to detect 10^5 cells/mL of *E. coli* O157. This suggests that when 10^5 cells/mL of *E. coli* O157 are added to the double labelled M13, the GAE antibodies attached on to the M13 are able to detect the O and H antigens present on the surfaces of the heat-killed *E. coli* O157. As they detect these cells, they cluster around the cells and are no longer able to align; this causes the notable drop in LD signal. If the M13 is not able to align this then affects the BHQ-10 dye molecules which are covalently linked to the p8 coat proteins on the M13. Since they are no longer able to align with the M13 and therefore a decline in signal is also seen at 516 nm. When the number of cells increase from 10^5 cells/mL to 10^6 and 10^7 cells/mL, the LD signal drops further as the double labelled M13 cluster around more of the cells. When 10^6 cells/mL of *E. coli* O157 was added to the double labelled M13 it appears from figure 5.13B that on average it produced a lower signal at 280 nm than when 10^7 cells/mL of *E. coli* O157 was added to the double labelled M13. However the standard deviations of both samples appear to overlap and this therefore may just be a matter of variation. This is supported by the results in figure 5.13C where the LD signal is examined at 516 nm, because the standard deviation of both the 10^6 and 10^7 cells/mL of *E. coli* O157 samples noticeably overlap.

As well as being a sensitive assay, this assay has also proved to be a specific assay. The LD signal produced when 10^7 cells/mL of *E. coli* XL10 was added into the assay proved to be insignificant when compared to the control. This highlights that the GAE antibodies attached to M13 are only specific to the O and H antigens present on *E. coli* O157. The presence of *E. coli* XL10 cells in the assay therefore did not prevent the double labelled M13 from aligning and producing a large LD signal.

5.6. Conclusion

Raul Pacheco-Gomez *et al.* (2012) demonstrated that it was possible to detect *E. coli* O157 using LD and M13 bacteriophage. His assay however had limitations, including the lack of sensitivity as it was only able to detect 10^7 cells/mL and its inability to multiplex due to the non-covalent bonds between the primary and secondary antibodies. The experiments described in this chapter looked at how this assay could be improved to produce an assay that is 2 orders of magnitude more sensitive than that developed by Pacheco-Gomez *et al.* (2012). The work also takes the first step to develop an assay which is able to detect more than one pathogen at one time.

The assay used by Pacheco-Gomez *et al.* (2012) was improved by using p8 coat protein as the point of contact for an antibody. This was chosen because there are 2700 copies of this protein along the full length of the bacteriophage, in comparison to just 5 at one end of the bacteriophage, which is the case for p3 coat protein. This would therefore lead to a more abundant conjugation of antibodies to the M13 particle. This in turn would increase the number of contact points between the M13 bacteriophages and the pathogens encouraging the de-alignment of the M13 and therefore increasing the sensitivity of the assay. The direct conjugation of the primary antibody to the p8 coat protein also removed the need for a secondary antibody reducing the cost of the assay. To enable a multiplexed system, the use of dyes conjugated to the M13 coat was introduced to produce an LD signal that could be used to distinguish between different targets.

Before the assay was trialled, the chemistry used to conjugate the primary antibody on to the p8 was confirmed using eosin-5-maleimide dye and TEM of M13 conjugated with GAM.

The improved assay consisting of double labelled M13 and LD proved to successfully detect *E. coli* O157 at a 100 fold greater sensitivity than the original assay and with the capability of

multiplexing the assay. The results show that this assay can detect 10^5 cells/mL of *E. coli* O157 (in an 80 μ L Couette this corresponds to a detection of 10^4 cells), with a reasonable degree of statistical certainty. Following these results further investigation would be required to determine if an even lower concentration of cells could be detected. Also a key experiment would be to investigate the detection of more than one pathogen e.g. *E. coli* O157 and MRSA to determine if the assay can be multiplexed. This would involve producing two lots of double labelled M13 reagents with two different dyes and two different antibodies determined by the target pathogens. This double labelled M13 combined with the target pathogens and LD would provide experimental evidence that this assay can be multiplexed.

CHAPTER 6

- DETECTION OF SMALL MOLECULES USING M13 BACTERIOPHAGE AND LINEAR DICHROISM

The detection system described in the previous chapter proved to be successful in detecting *E. coli* O157. However this detection system is only able to detect large target ligands which are therefore able to de-align the double labelled M13. Consequently this detection system is well suited for pathogens, but not for small molecules like toxins, drugs and explosives, since these much smaller molecules are unable to de-align the M13 bacteriophages. Producing a multimodal detection system, capable of detecting pathogens, small molecules and also DNA would significantly expand the use of the M13/LD assay (figure 6.1). In order to develop a multimodal detection system using LD and M13 bacteriophage, the different techniques to detect the different targets must be examined. Research into the detection of DNA is already being developed in the Dafforn laboratory. The next stage is to look at the detection of small molecules which will focus on the detection of toxins, drugs and explosives.

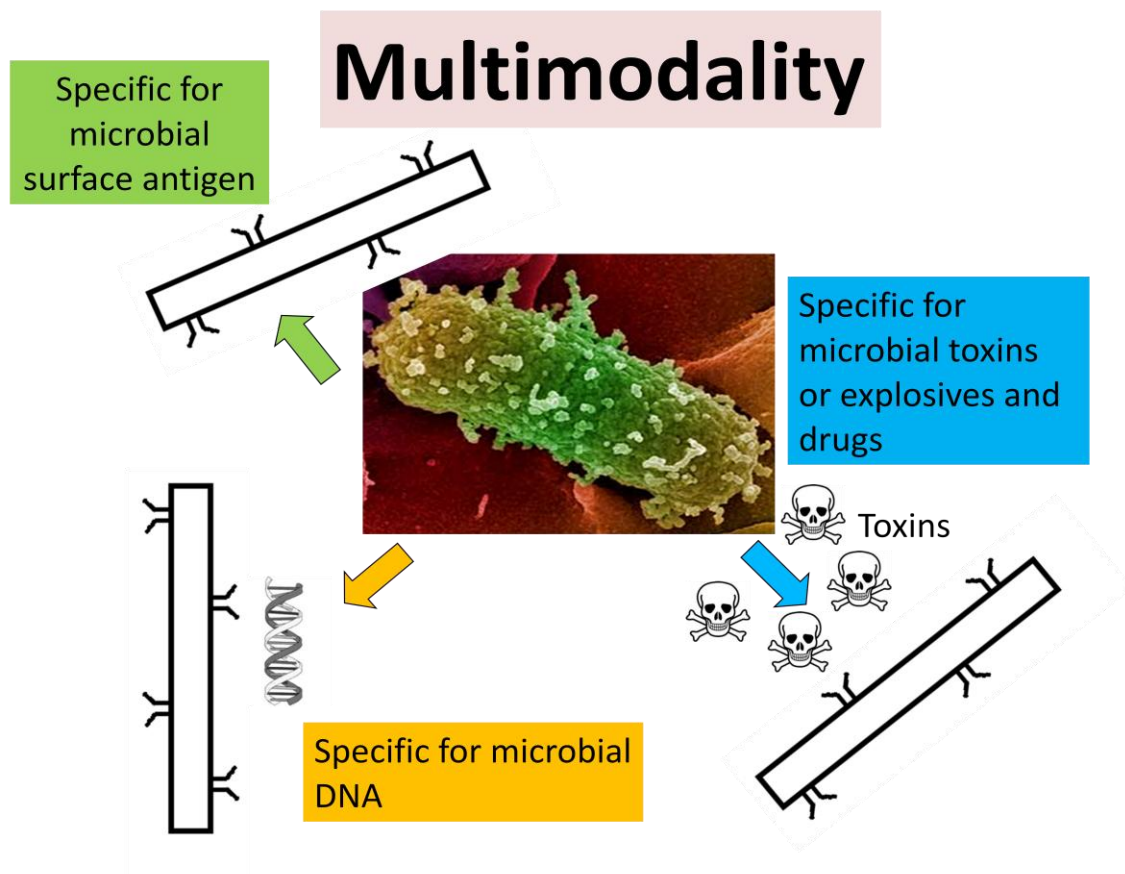


Figure 6.1 - Diagram illustrating the idea of creating a multimodal detection system

Diagram illustrates the idea of creating a multimodal detection system capable of detecting small molecules (e.g. toxins, explosives and drugs), DNA from pathogens and the surface antigens of pathogens. This multimodal system uses LD and M13 bacteriophage and can detect any of these target ligands in one test.

6.1. Why small molecule detection?

The detection of toxins is very important in the diagnosis of disease as various pathogens are known to produce toxins. Examples of such pathogens include Shiga-toxin-producing *E. coli* (STEC), *Staphylococcus aureus* (*S. aureus*) which produces toxic shock syndrome toxin-1 (TSST-1), several enterotoxins (A, B, C 1, C 2, C 3, D and E), exfoliative toxins (ETA and ETB) and leukocidin, *Bacillus cereus* which produces a highly stable toxin less than 10 kDa in size and *Clostridium botulinum* which produces a potent neurotoxin (Pimbley and Patel, 1998). These toxins have the potential to cause severe harm, for example 10-15% of individuals infected with *E. coli* O157 go on to develop haemolytic uraemic syndrome which is associated with

renal failure, anaemia and bleeding (Tarr *et al.*, 2005). Similarly TSST-1 producing *S. aureus* is known to cause toxic shock syndrome (TSS) and caused an epidemic in the early 1980s in the USA, which was associated with the use of tampons during menstruation (Dinges *et al.*, 2000).

The detection of drugs is also important; in 2012-2013 it was reported that 1 in 12 adults had taken an illicit drug in England (Health and Social Care Information Centre, 2013). In addition, the United States recorded 27,000 deaths due to unintentional drug overdoses in 2007 (Centers for Disease Control and Prevention, 2012). The illicit drug trade is reportedly growing with global opium production increasing from 4,700 tons in 2010 to 7,000 tons in 2011 and in the United States, annual prevalence of cannabis use increased by 0.4% between 2009 and 2010 (United Nations Office on Drugs and Crimes, 2012). These facts demonstrate the importance and complexity of tackling the worldwide drug trade.

Similarly, chemical explosives also pose a threat on a national and global scale. In recent years a growth in explosive based terrorism has been observed, this is predominantly due to the simple production and distribution methods as well as the shear harm they are capable of causing (Senesac and Thundat, 2008). For example in 1993 a urea nitrate based car bomb was detonated below the North Tower of the World Trade Centre (Aubrey, 2004). In 1994 a terrorist used a nitroglycerin compound concealed in a contact lens fluid bottle to bring down a Philippine plane on its way to Tokyo (Steven and Gunaratna, 2004). More recently in 2005 a group of terrorists set off several home-made peroxide-based explosives on the London transport system which resulted in 56 deaths and hundreds injured (Segell, 2006).

To reduce and prevent the harmful effects of bacterial toxins, drugs and explosives they need to be detected rapidly on a molecular scale.

6.2. Detection methods for toxins, illicit drugs and explosives

Currently small molecules such as bacterial toxins are detected primarily using immunological assays (Pimbley and Patel, 1998). These include ELISAs, radioimmunoassays (RIA) (figure 6.2) and agglutination assays (Pimbley and Patel, 1998). Immunological assays are similarly used to detect drugs and explosives; these assays include enzyme multiplied immunoassay technique (EMIT), ELISA, RIA, fluoroimmunoassay (figure 6.3) and fluorescence polarization immunoassay (FPIA) (Smith *et al.*, 2008b, Moeller *et al.*, 2008).

Antibodies used in immunological assays are highly selective and this makes them good at discriminating between different closely related molecules (Smith *et al.*, 2008b). However immunological assays do have many limitations (please see Chapter 1 for details). Although new research is being done to improve small molecule detection, for example Ruta *et al.* (2009) combined aptamers with fluorescence polarisation to produce a sensitive, easy to use and simple detection assay (Ruta *et al.*, 2009).

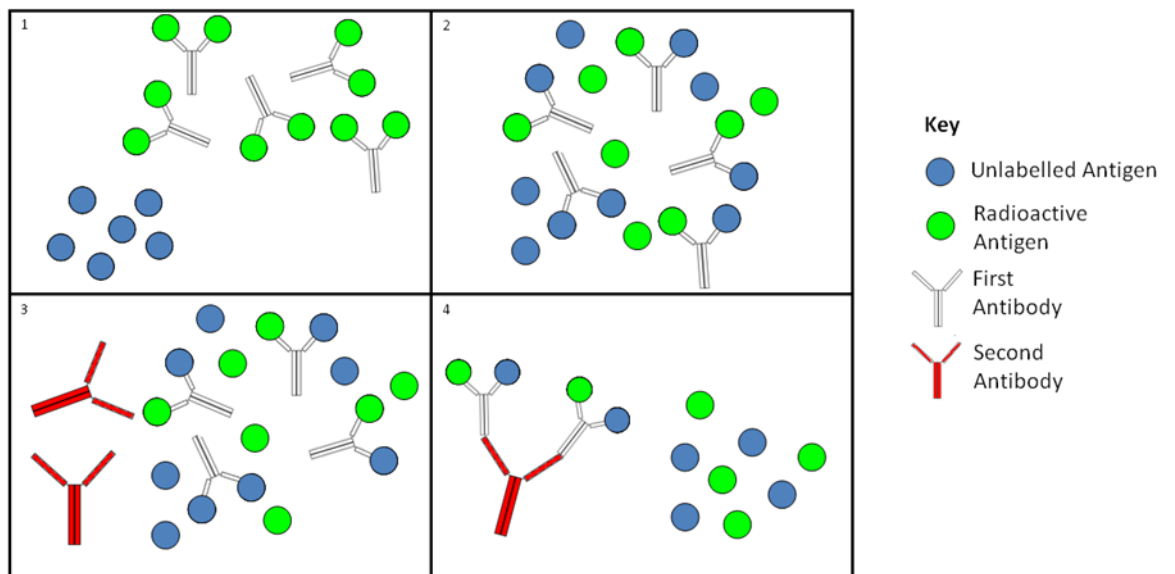


Figure 6.2 - Schematic diagram of how a radioimmunoassay works

RIAs are competition assays where radioactive labelled target molecules and unlabelled target molecules both compete for the anti-target antibody. The assay mixture is incubated and any unbound antigens are separated and the radioactivity of both or either fractions is determined and the concentration of unlabelled target molecules is calculated. This heterogeneous assay is less frequently used due to washing steps which prolong the assay time, health and safety concerns associated with radioactivity (Bonwick and Smith, 2004) and degradation issues with radioactive labels (Drost *et al.*, 1977).

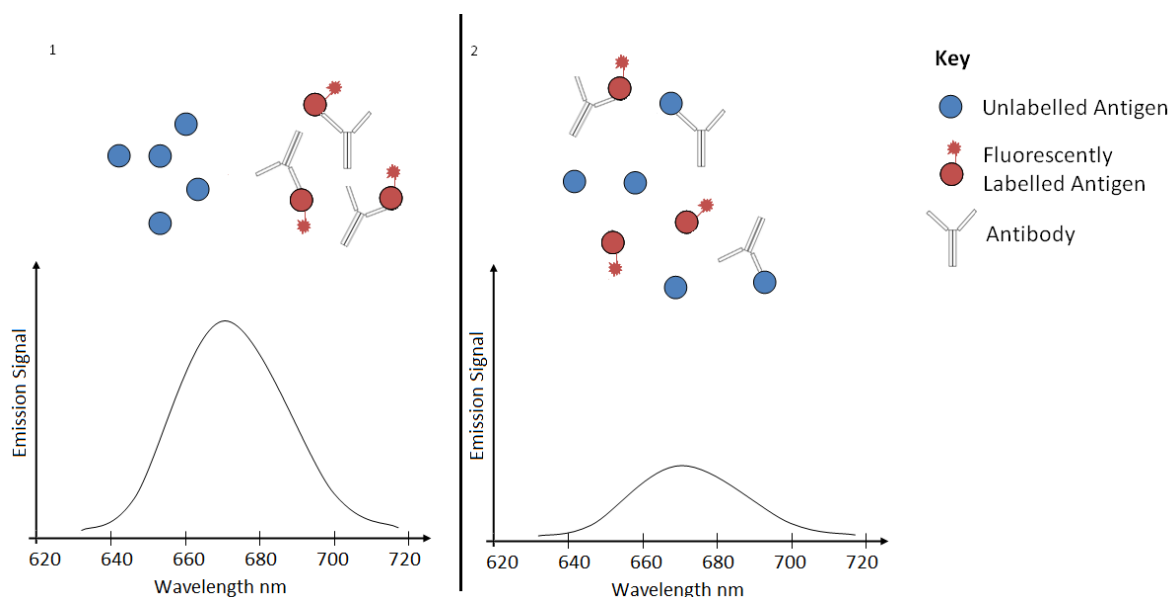


Figure 6.3 - Schematic diagram illustrating how fluoroimmunoassays work

Fluoroimmunoassays are competition assays as fluorescently labelled analogues of the target molecule compete with unlabelled target molecules from a sample to bind to anti-target antibodies. The difference in fluorescence emission intensity is measured and the concentration of the target molecule in the sample can be determined by examining the decline in fluorescence. Fluoroimmunoassays are commonly used for the detection of explosives (Smith *et al.*, 2008b, Goldman *et al.*, 2003) and are well suited for field use as they provide more rapid throughput than ELISA and high performance liquid chromatography. However, some biological molecules are able to naturally emit light and they can affect fluorescence measurements (Smith *et al.*, 2008b).

A major limitation of using immunological assays are that they are capable of producing false positive results (Moeller *et al.*, 2008). Consequently when detecting drugs, a confirmation test is routinely carried out if a positive result is produced. This secondary analysis is usually carried out using gas chromatography-mass spectrometry (GC-MS) (Moeller *et al.*, 2008). This method is able to identify and quantify a complex mixture of volatile compounds with analytical sensitivities ranging from 1-100 pg (Hites, 1997). Conversely this method can be extremely time-consuming, requiring rigorous sample preparation and up to 20 hours to perform the assay. In addition GC-MS is not able to distinguish between isomeric molecules and is limited to samples with a vapour pressure greater than 10^{-10} torr (Hites, 1997). Furthermore this assay requires a high level of expertise to perform and is very costly (Moeller *et al.*, 2008).

Ion mobility spectrometry (IMS) is an analytical technique used to identify ionised molecules and is currently used in flight security to screen for explosives (Ewing and Miller, 2001). This technique has a similar sensitivity to mass spectrometry, however IMS is less specific and is not able to screen low vapour pressures, which many explosives have, especially if deliberately concealed within containers (Steinfeld and Wormhoudt, 1998).

This is not an exhaustive list of all of the current methods used to detect toxins, illicit drugs and explosives, but indicates a few of the key assays carried out currently. It is apparent that presently small molecule detection does have many limitations and to solve the problems surrounding bacterial toxins, illicit drugs and explosive based terrorism, it is essential that an assay capable of detecting these small molecules is developed. This chapter investigates how LD combined with M13 bacteriophage can be utilised to form an assay capable of detecting small molecules and in the future it is hopeful that this can form part of a multimodal assay.

6.3. Small molecule detection

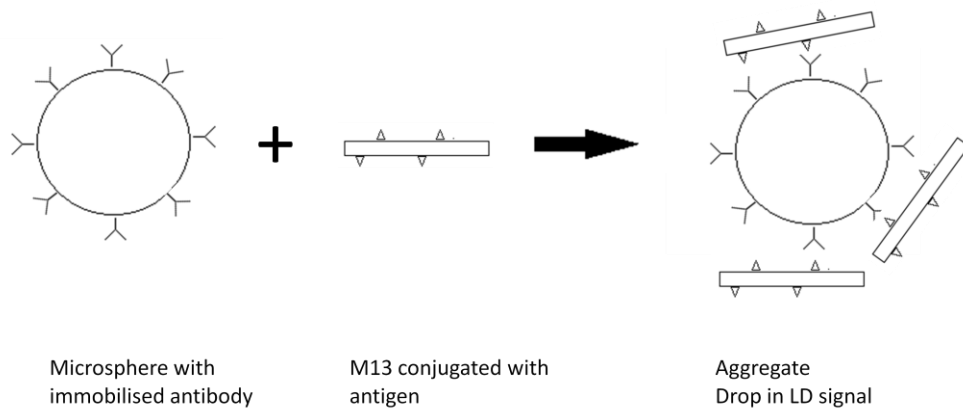
At the inception of this part of the project two detection assays were originally envisaged to detect small molecules using M13 and LD, these were the:

- microsphere aggregation assay
- M13 aggregation assay

The microsphere aggregation assay consists of M13 conjugated with target antigens which forms a complex with anti-target antibody conjugated microspheres. These complexes are large and therefore prevent the M13 bacteriophages from aligning when subject to shear flow and result in no LD signal. The addition of an unknown quantity of target molecules from a sample will compete with the target antigens conjugated on to the M13 for the binding sites on the microspheres. The target molecules will displace the conjugated M13, resulting in the

breakdown of the M13/microsphere complexes. The unbound M13 will align in shear flow, re-establishing the M13 LD signal and indicating that the target molecule is present in the sample (figure 6.4).

Absence of free antigen



Presence of free antigen

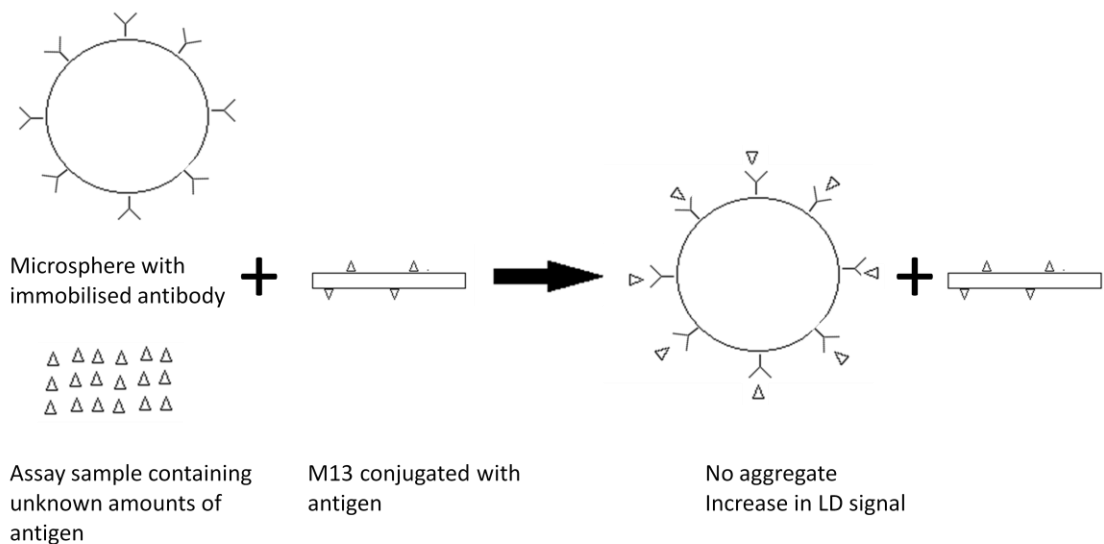


Figure 6.4 - Schematic diagram illustrating how microspheres, M13 and LD may be used to detect small molecules

Schematic diagram illustrates how in principle microspheres and M13 bacteriophage may be able to detect small molecules using LD. In the absence of free antigen a complex forms between microspheres conjugated with antibody and M13 conjugated with the target antigen. The formation of an aggregate prevents the M13 from aligning and hence the LD signal drops. In the presence of free antigen a competition assay forms as the free antigen competes with the antigen conjugated on the M13 to bind to the antibody conjugated on to the microspheres. The free antigen breaks down the aggregate and the M13 is able to align and this causes an increase in LD signal.

This assay was trialled in the laboratory (in collaboration with Toby Proctor and Florence Gower, University of Birmingham) with M13 bacteriophage which was conjugated with an antigen, fluorescein isothiocyanate isomer 1 (FITC-M13), in the hope of detecting fluorescein as the target molecule. The microspheres used consisted of microspheres conjugated with anti-fluorescein antibodies (α -microspheres) and non bioconjugated microspheres (microspheres). After incubating the FITC-M13 with the α -microspheres and the microspheres, a drop in LD signal was expected for the FITC-M13 incubated with α -microspheres and no signal change was expected for the FITC-M13 incubated with microspheres. However this was not seen as an increase in LD signal was seen for both samples (figure 6.5). A possible explanation for this was that the microspheres increased the viscosity of the sample and therefore increased the M13 bacteriophage alignment and consequently increased the LD signal. The assay in this form was felt to be unsuccessful although it is possible that with extra optimisation the method could be made to work. However success in the second small molecule assay method meant that research into the microsphere based method was stopped so that we could concentrate on the second method.

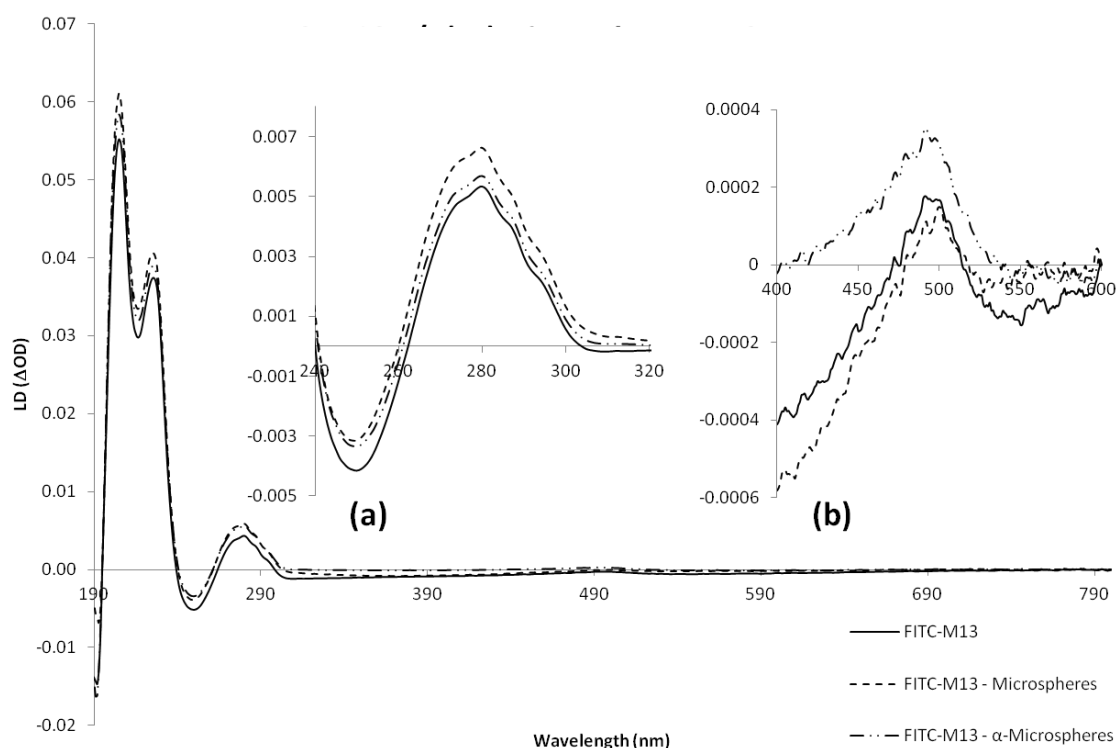


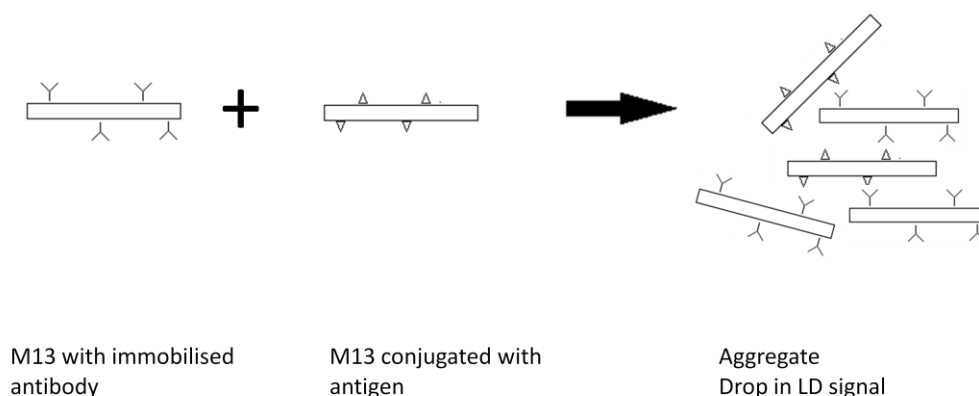
Figure 6.5 - LD spectra produced from the microsphere aggregation assay

M13 bacteriophage was conjugated with fluorescein isothiocyanate isomer 1 (FITC-M13) and incubated with microspheres conjugated with anti-FITC antibodies (FITC-M13- α -Microspheres) and non-bioconjugated microspheres (FITC-M13-Microspheres). According to the microsphere aggregation assay it had been hypothesised that the LD signal from FITC-M13 would decline in the presence of the α -microspheres as they would aggregate. It was also thought that FITC-M13 in the presence of microspheres would result in no signal change as no aggregation would result. However the FITC-M13- α -Microspheres sample demonstrated an increase in LD signal at 280 nm (a) and 494 nm where FITC absorbs (b). This indicated that the presence of the microspheres supported the alignment of FITC-M13 and hence increased the LD signal. Similarly the FITC-M13-Microsphere sample also resulted in a slight increase at 280 nm, this indicated that both the microspheres and the α -microspheres had the same effect on the FITC-M13. This assay proved to be unsuccessful due to this non-specific binding.

The M13 bacteriophage aggregation assay behaves like a competition assay. It consists of M13 conjugated with target antigens which form a complex with anti-target antibody conjugated M13. This complex reduces the LD signal. The addition of a sample containing an unknown amount of target molecules will compete with the target antigens conjugated on to the M13 for the binding sites on the M13 bacteriophages. The target molecules will displace the M13 conjugated with target antigens, resulting in the breakdown of the M13 complexes. The M13

will align in shear flow, re-establishing the M13 LD signal and indicating that the target molecule is present in the sample (figure 6.6).

Absence of free antigen



Presence of free antigen

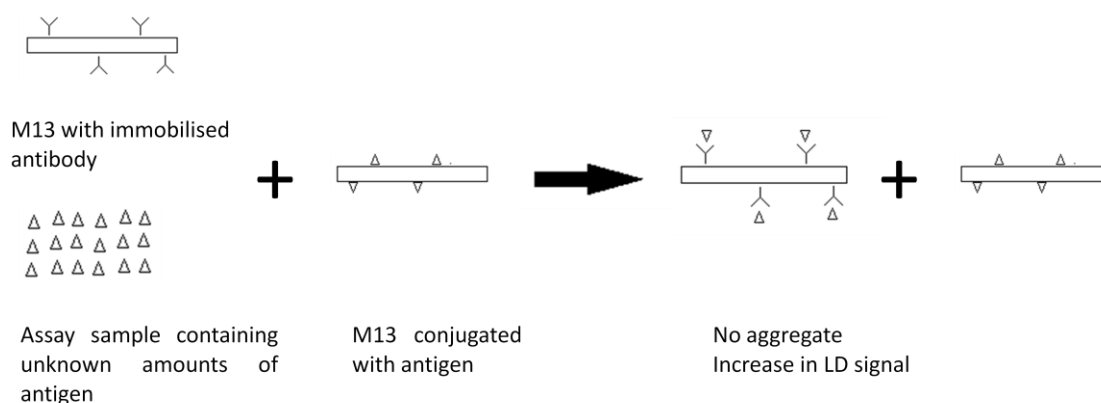


Figure 6.6 - Schematic diagram illustrating how LD and M13 bacteriophage are able to detect small molecules

In the absence of free antigen a complex forms between M13 conjugated with antibody and M13 conjugated with the target antigen. The formation of an aggregate prevents the M13 from aligning and hence the LD signal drops. In the presence of free antigen a competition assay forms as the free antigen competes with the antigen conjugated to the M13 to bind to the antibody conjugated on to the M13. The free antigen breaks down the aggregate and the M13 is able to align and this causes an increase in LD signal.

This chapter investigates and examines this assay as a technique for small molecule detection.

6.4. M13 bacteriophage aggregation assay

The target molecule chosen for detection using the M13 bacteriophage aggregation assay was fluorescein. Fluorescein was an ideal molecule to show proof of concept of this assay because it is a small molecule with a molecular weight of 376 g/mol, which is similar in size to some of the eventual targets (e.g. molecular weight of cocaine is 303 g/mol). It is also an inexpensive, harmless molecule, and so could be used with minimal regulatory or safety considerations.

6.4.1. Production of M13 labelled with FITC and M13 labelled with anti- FITC

Fluorescein isothiocyanate isomer 1 (FITC) was used as the antigen to covalently label M13 bacteriophage. FITC is a derivative of fluorescein; it differs because it is functionalised with an isothiocyanate reactive group, which is reactive towards nucleophiles including amine groups, which are present on the p8 coat proteins on M13. FITC was covalently linked to the free amine groups (one on the N-terminus and one on the lysine residue) on the p8 coat protein by forming a thiourea linkage. FITC absorbs in the visible region (494 nm) so the drop or increase in LD signal could be observed here.

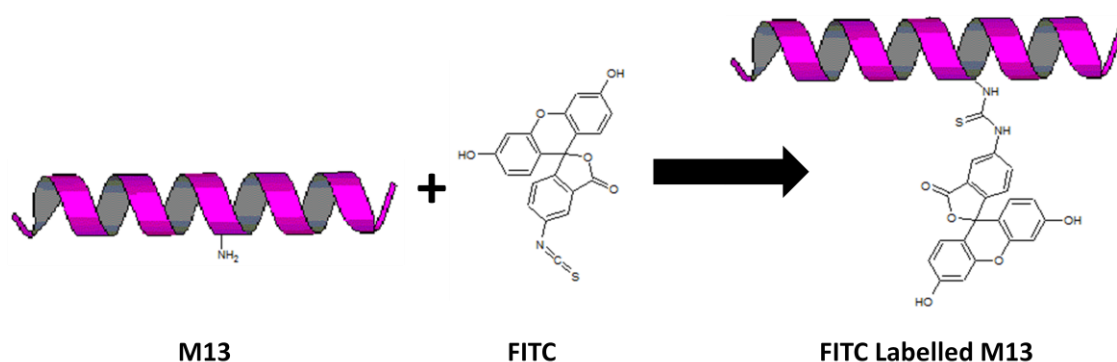


Figure 6.7 - Labelling M13 with FITC

In order to conjugate M13 with anti-FITC antibodies, M13 had to be modified with SATA and anti-FITC antibodies had to be modified with SMCC. The SATA attached sulfhydryl groups on to free amine groups on the p8 coat protein. SMCC attached maleimide groups on to the

antibody and the maleimide groups were able to react with the thiol groups on the M13 to form thioether bonds (figure 5.5). To remove the unwanted SMCC and SATA from the final anti-FITC conjugated M13 solution, size exclusion chromatography (SEC) was utilised, this eliminated any contaminants, thus producing a pure sample (figure 6.8). The results show that M13 conjugated with anti-FITC antibodies eluted first, closely followed by anti-FITC antibodies alone. The contaminants, including SATA and SMCC eluted last with a volume between 100-120 mL.

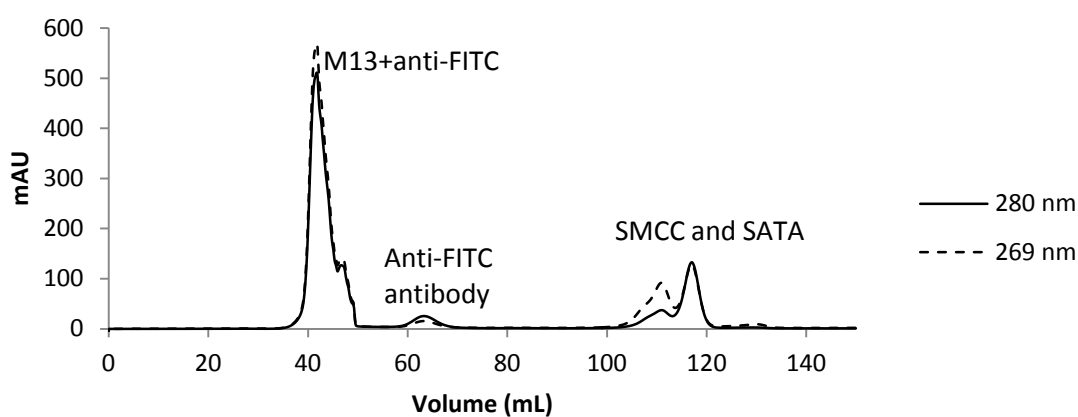


Figure 6.8 - Absorbance spectra of M13 conjugated with anti-FITC when it is subjected to size exclusion chromatography

Absorbance spectra of M13 conjugated with anti-FITC when it is subjected to size exclusion chromatography. This process allowed for the removal of unwanted contaminants including SATA and SMCC to provide a pure sample. The absorbance was measured at both 280 nm and 269 nm. M13 conjugated with anti-FITC antibodies eluted first, followed by anti-FITC antibodies alone. The peaks between 100 and 120 mL are caused from excess SATA and SMCC.

Once M13 conjugated with anti-FITC and M13 conjugated with FITC were produced, the UV/Vis absorbance spectrum was measured to determine their concentration and an LD spectrum was measured to check the structural integrity of the M13 had not been disrupted.

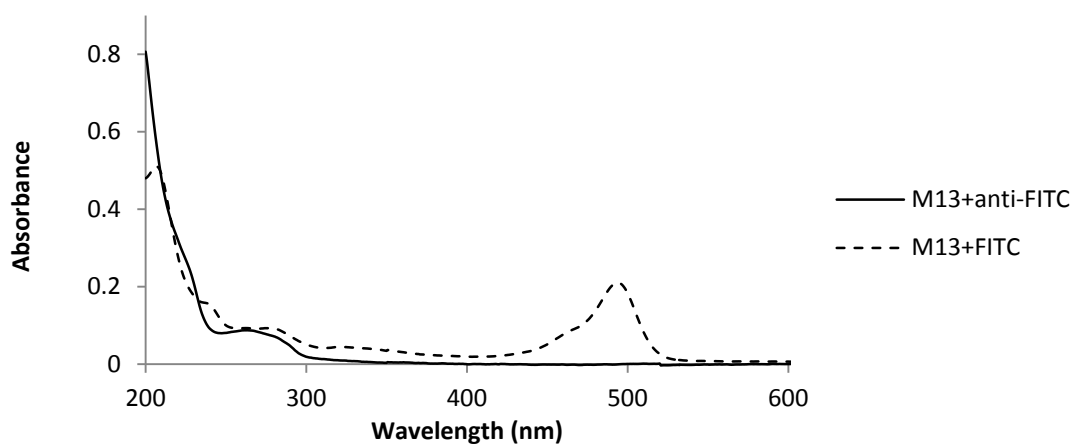


Figure 6.9 - UV/Vis spectra of M13 conjugated with anti-FITC and M13 conjugated with FITC

UV/Vis spectra of 0.07mg/mL M13 conjugated with anti-FITC (M13+anti-FITC) and 0.08 mg/mL M13 conjugated with FITC (M13+FITC).

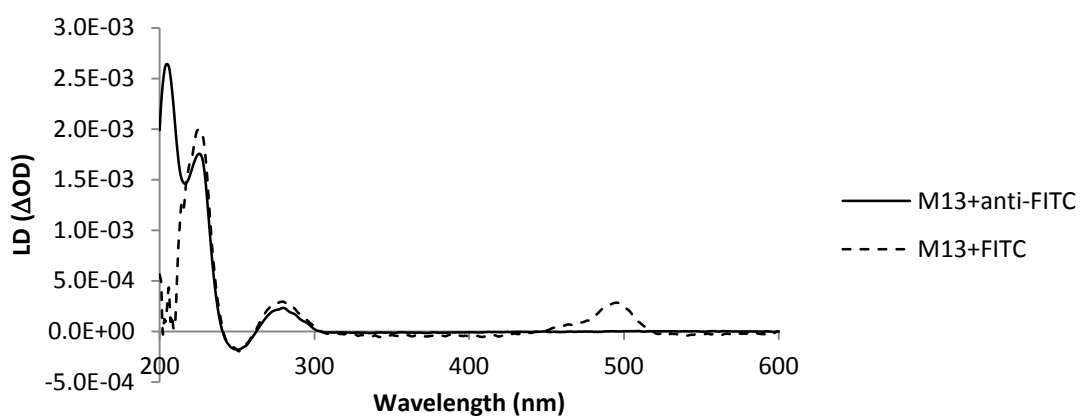
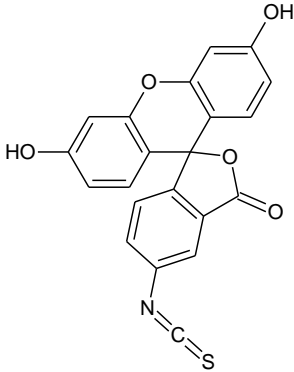


Figure 6.10 - LD spectra of M13 conjugated with anti-FITC and M13 conjugated with FITC

LD spectra of 30 μ L of 0.08 mg/mL M13 conjugated with FITC and 50 μ L of 50 mM phosphate buffer pH 8.0 (M13+FITC) and 30 μ L of 0.07mg/mL M13 conjugated with anti-FITC and 50 μ L of 50 mM phosphate buffer pH 8.0 (M13+anti-FITC).

Table 6.1 - Table displaying the percentage labelling of M13 conjugated with FITC and the FITC to M13 LD ratio

Extinction Coefficient of FITC ($M^{-1} cm^{-1}$)	Absorbance of FITC (nm)	Mr of FITC	% Labelling	$LD_{FITC}/LD_{M13(280nm)}$	Chemical structure of dye
73000 (Haugland, 1996)	494	389	76	0.963	

FITC dye absorbs at 494 nm, and figure 6.9 shows that M13 conjugated with FITC produces a fairly large peak at 494 nm, confirming the presence of the dye in solution. The LD signal confirmed that the FITC had covalently attached to the M13 as there was a peak at 494 nm in the LD spectrum (figure 6.10). The percentage of labelling of M13 conjugated with FITC was calculated from the UV/Vis absorbance spectrum, and was found to produce a very high labelling percentage of 76%. This could be due to FITC having a low molecular weight, allowing it to access the amine groups present on the p8 coat proteins of M13. The LD spectrum for M13 conjugated with FITC also displayed a very large peak at 494 nm, and the ratio value of the FITC peak to the M13 peak at 280 nm is much larger than those seen in chapter 4. This indicates that the FITC is much better at producing a large LD signal and this could be due to a number of factors including its large extinction coefficient, its high percentage labelling of M13 and the alignment of its transmission polar moments being more parallel than perpendicular to the long axis of the M13. Also despite FITC being a small dye, it may be that when it has

covalently linked to M13, it becomes inflexible and rigid, and this may be supported by the high labelling which results in a compact and firm structure.

Similar concentrations of M13 conjugated with FITC and anti-FITC were used in the assay.

6.4.2. Detection of fluorescein using LD and anti-FITC and FITC labelled M13

The initial stage of this assay involved showing that the addition of M13 conjugated with FITC to M13 conjugated with anti-FITC leads to an expected decrease in LD signal reflecting the formation of a non-alignable complex.

M13 conjugated with anti-FITC produced an LD signal of 2.32×10^{-4} Δ OD at 280 nm and M13 conjugated with FITC produced an LD signal of 2.94×10^{-4} Δ OD at 280 nm (figure 6.11). When these two solutions were added together to form a mixture, a significant drop in LD signal (5.15×10^{-5} Δ OD at 280 nm) of approximately 80% was seen. A two tailed unpaired t-test was used to statistically compare the LD signals at 280 nm of the M13 conjugated with anti-FITC (p value of 0.04) and M13 conjugated with FITC (p value of 0.00006) to the mixture and found that the mixture was significantly smaller in both cases. Theoretically if no complex was formed then the signal from the mixture should have been twice as large (approximately 5.26×10^{-4} Δ OD at 280 nm) because twice the amount of M13 was present in this sample. However it is thought that the mixture produces a much lower LD signal because there is cross linking between the M13 bacteriophages, as the FITC antigens cross link with the anti-FITC antibodies. This will prevent the M13 bacteriophages from aligning and thus causes a drop in LD signal.

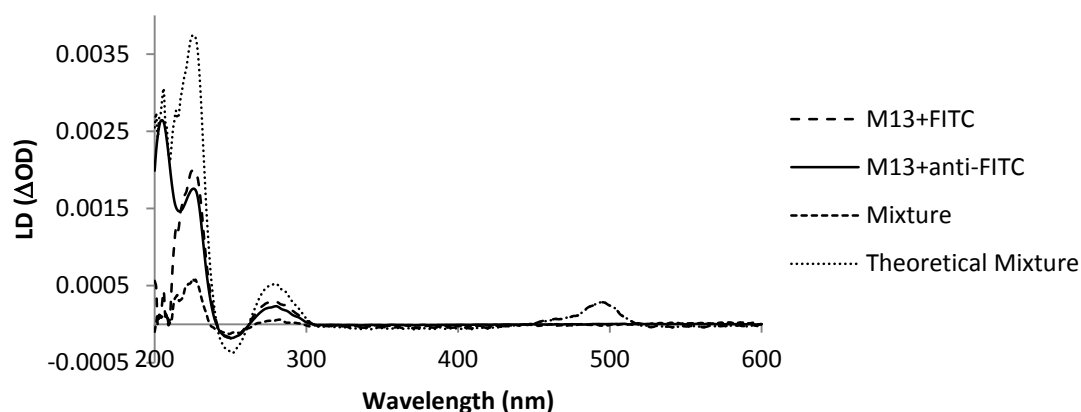


Figure 6.11 - LD spectra illustrating how M13 conjugated with FITC and M13 conjugated with anti-FITC can disrupt the LD signal

LD spectra of 30 μ L of 0.08 mg/mL M13 conjugated with FITC and 50 μ L of 50 mM phosphate buffer pH 8.0 (M13+FITC), 30 μ L of 0.07mg/mL M13 conjugated with anti-FITC and 50 μ L of 50 mM phosphate buffer pH 8.0 (M13+anti-FITC) and 30 μ L of 0.08mg/mL M13 conjugated with FITC and 30 μ L of 0.07mg/mL M13 conjugated with anti-FITC and 20 μ L of 50 mM phosphate buffer pH 8.0 (Mixture). The theoretical mixture is the theoretical LD signal if the LD spectra produced from M13+FITC and M13+anti-FITC was simply added together.

The next step was to see whether the presence of free antigen (fluorescein) would disrupt the formation of the complex between the M13 conjugated with FITC and M13 conjugated with anti-FITC. To test this, the LD absorbance was measured of the M13 mixture with and without 1 mM fluorescein. This data shows that in the presence of free fluorescein the LD signal increases, as predicted, to a value close to that expected if the two M13 bacteriophages did not interact (figure 6.12).

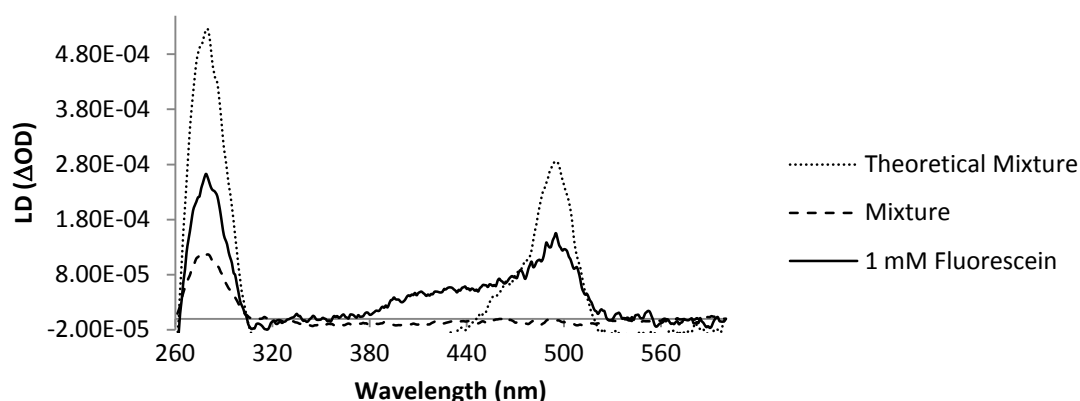


Figure 6.12 - LD spectra illustrating how the presence of fluorescein can re-establish the LD signal

LD spectra of 30 μ L of 0.08mg/mL M13 conjugated with FITC and 30 μ L of 0.07mg/mL M13 conjugated with anti-FITC and 20 μ L of 50 mM phosphate buffer pH 8.0 (Mixture), and the “1 mM Fluorescein” solid line is the result of incubating 1 mM fluorescein with 30 μ L of 0.07mg/mL M13 conjugated with anti-FITC overnight and then competing it off with 30 μ L of 0.08mg/mL M13 conjugated with FITC. The theoretical mixture is the theoretical LD signal if the LD spectra produced from M13 conjugated with FITC and M13 conjugated with anti-FITC was simply added together.

Once it had been established that the complex was disrupted by free antigen an experiment was carried out to examine how much free antigen was required to initiate disruption and hence a measure of sensitivity of the assay. This was done by the addition of varying concentrations of fluorescein to the assay. Increasing concentrations of fluorescein (0.01 mM, 0.02 mM, 0.04 mM, 0.1 mM, 0.2 mM, 0.5 mM and 1 mM) was added to M13 conjugated with anti-FITC and left to incubate overnight. M13 conjugated with FITC was added to the solution, after which the LD signal was measured to indicate if increasing concentrations of fluorescein were able to compete with the FITC conjugated on the M13 to bind with the anti-FITC antibodies. These signals were compared to the mixture which consisted of M13 conjugated with anti-FITC and M13 conjugated with FITC and contained no fluorescein.

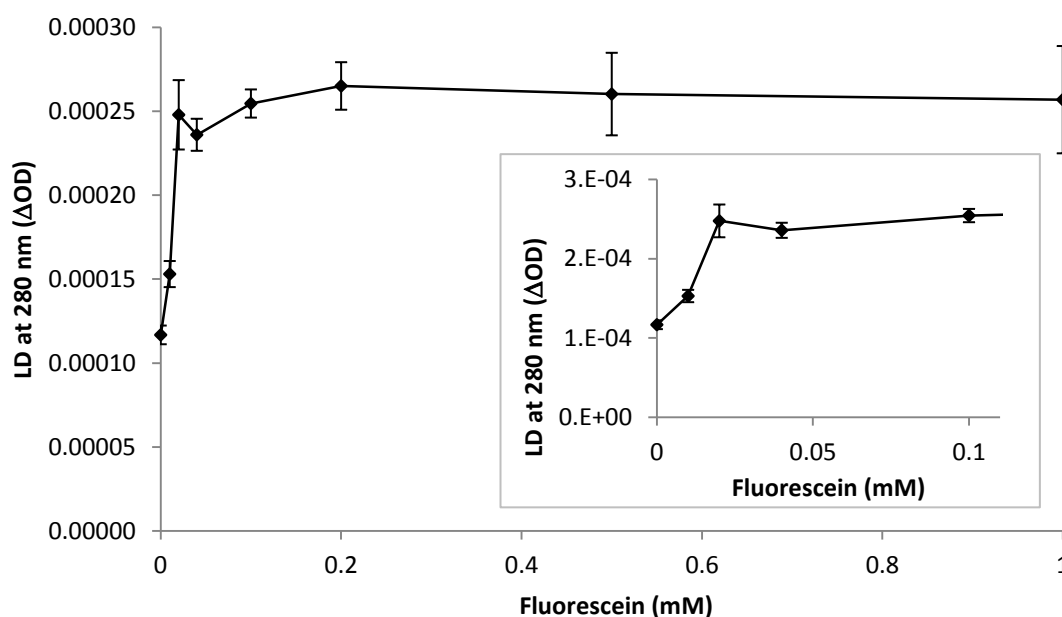


Figure 6.13 - Sensitivity of the small molecule detection assay

Graph demonstrates the LD signal at 280 nm when 0.01 mM, 0.02 mM, 0.04 mM, 0.1 mM, 0.2 mM, 0.5 mM and 1 mM fluorescein is added to M13 conjugated with anti-FITC and competed off with M13 conjugated with FITC. The mixture containing M13 conjugated with anti-FITC and M13 conjugated with FITC and containing no fluorescein is also plotted. Inset highlights concentrations between 0 and 0.1 mM fluorescein. The error bars show the standard deviation.

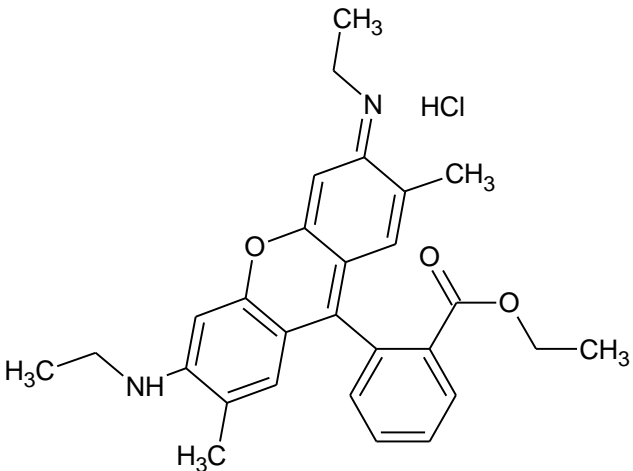
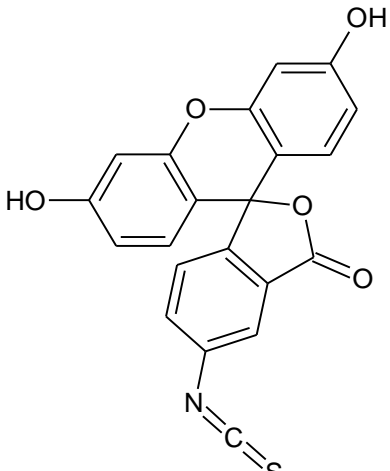
The mixture, which contained no fluorescein, revealed a low LD signal of $1.17\text{E-}04$ ΔOD at 280 nm. The addition of fluorescein was then used to investigate whether fluorescein could be detected by an increase in LD signal. When 0.01 mM of fluorescein was added to M13 conjugated with anti-FITC and competed with M13 conjugated with FITC, the signal notably increased by 31%. The LD signal increased by 112% when 0.02 mM of fluorescein was added to the assay. After this point, increasing the fluorescein concentration appeared to saturate the assay as the LD signal plateaus (figure 6.13).

The low LD signal produced by the mixture which contains no fluorescein is thought to be as a result of cross linking. Since M13 conjugated with FITC and M13 conjugated with anti-FITC will form attachments as the antibodies detect their target antigens on the M13. This is likely to cause the formation of mesh-like structures. This will therefore prevent the M13 from aligning

and result in a low LD signal, which was also seen earlier in this chapter in figure 6.11. The initial increase in LD signal seen when 0.01 mM fluorescein was added to the assay is due to the free fluorescein competing with the FITC conjugated on the M13 to attach to the anti-FITC antibodies conjugated on the M13. The free fluorescein acts to reduce any cross linking and mesh-like structures from forming and thus allows the M13 to align in shear flow. The addition of 0.02 mM fluorescein further increased the LD signal and this LD signal was maintained despite additional increases in fluorescein concentration. An explanation for this is that 0.02 mM fluorescein saturated all of the available anti-FITC antibodies in the assay, thus allowing the M13 bacteriophage to align to their full capacity and thus reaching their LD signal potential. Essentially, these results indicate that M13 and LD are capable of detecting small molecules whilst maintaining a high sensitivity of 0.01 mM.

To verify that the assay was specific to the target ligand a closely related chemical, rhodamine 6G, was introduced to the assay.

Table 6.2 - Comparing the structures of rhodamine 6G and FITC.

Rhodamine 6G	FITC
	

Rhodamine 6G was added to M13 conjugated with anti-FITC and then competed off with M13 conjugated with FITC. It was expected that the anti-FITC antibodies would be specific and

would consequently not detect the presence of rhodamine 6G in the sample. The complex between the M13 conjugated with anti-FITC and M13 conjugated with FITC would therefore continue to form resulting in a low LD signal (figure 6.14).

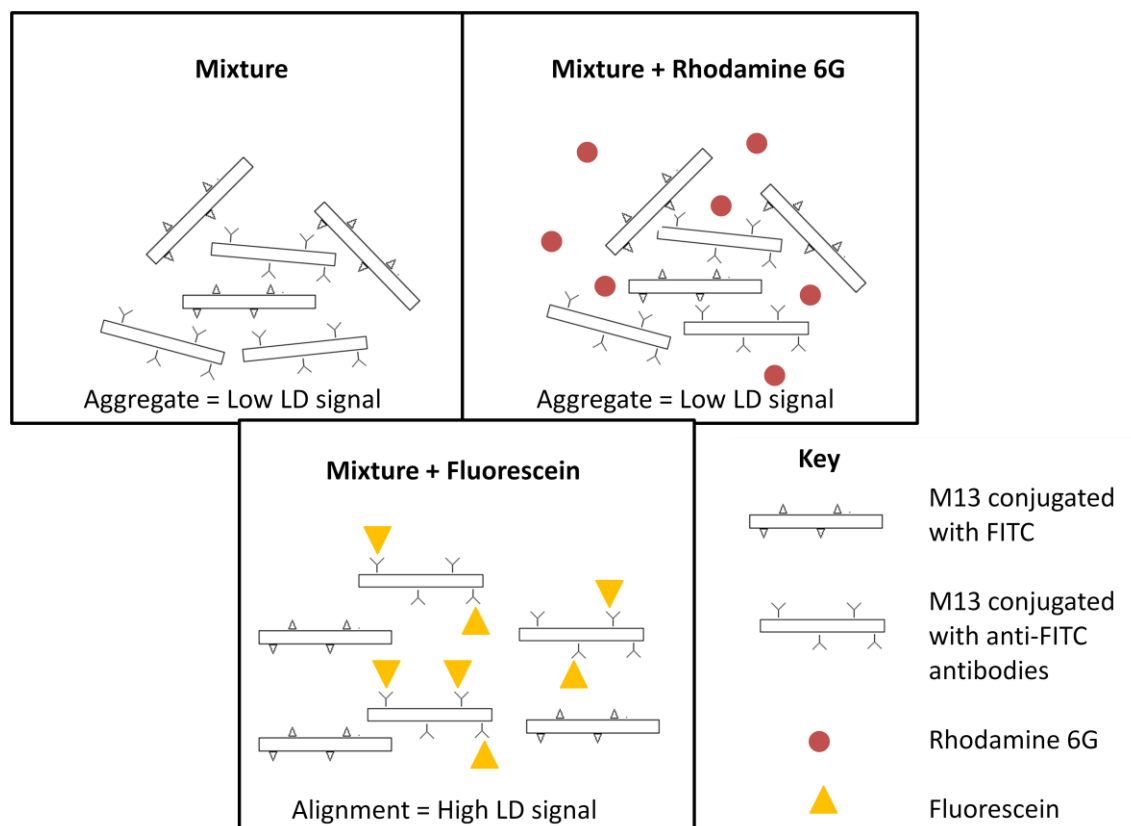


Figure 6.14 - Schematic diagram illustrating the principle of this small molecule detection assay

Schematic diagram displaying the mixture of M13 conjugated with FITC and anti-FITC resulting in a low LD signal followed by the addition of rhodamine 6G which has no proposed effect on the aggregated M13. However the addition of fluorescein to the mixture results in the breakdown of the aggregate resulting in a large LD signal.

The results show that the LD spectra of both the mixture and the rhodamine 6G sample are very similar (figure 6.15), as both produce very similar LD signals at 280 nm ($1.17\text{E-}04 \Delta\text{OD}$ and $1.18\text{E-}04 \Delta\text{OD}$ respectively). A two tailed unpaired t-test further supported this as it revealed no significant difference between the mixture and rhodamine 6G sample at 280 nm (p value was 0.7). This indicates that the rhodamine (although chemically similar to the fluorescein) does not interfere with the assay.

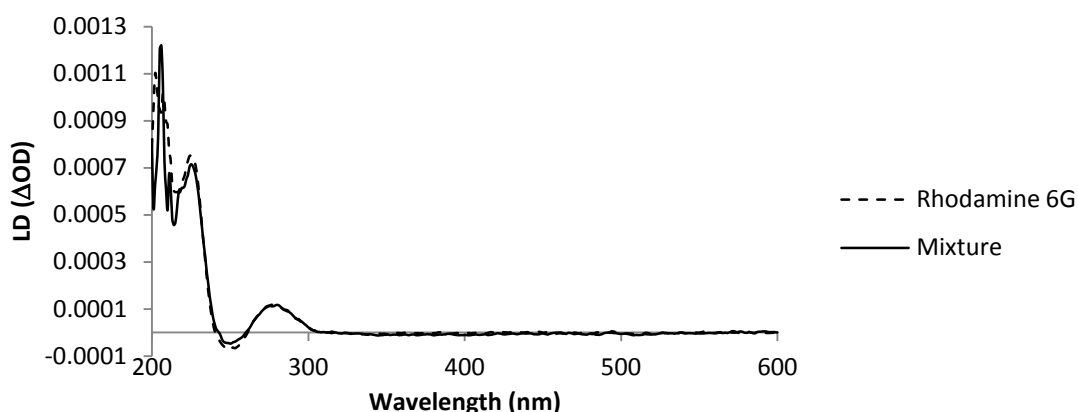


Figure 6.15 - LD spectra illustrating the specificity of this small molecule detection assay

LD spectra of rhodamine 6G which consisted of 8 μ L of rhodamine 6G (0.02 mM) in solution with 30 μ L of M13 conjugated with anti-FITC (0.07 mg/mL) and 30 μ L of M13 conjugated with FITC (0.08 mg/mL) and 12 μ L of 50 mM phosphate buffer pH 8.0. The mixture consisted of 30 μ L of M13 conjugated with anti-FITC (0.07 mg/mL), 30 μ L of M13 conjugated with FITC (0.08 mg/mL) and 20 μ L of 50 mM phosphate buffer pH 8.0.

These results demonstrate that M13 and LD combined are able to detect small molecules with a sensitivity of 0.01 mM and maintaining specificity.

6.5. Conclusion

The previous chapter demonstrated that LD combined with M13 bacteriophage could successfully form a detection assay capable of detecting pathogens with a high sensitivity and specificity. However that detection system was limited to large target ligands. The eventual goal of this research is to develop a multiplexed and multimodal system, capable of detecting pathogens, small molecules and DNA. The next step in this process was to look at small molecule detection which is vital when looking at toxins, drugs and explosives. The current assay used for pathogen detection had to be redesigned to detect small molecules as small molecules are not able to disrupt M13 alignment and therefore cause an LD signal change. Consequently a competition assay was developed which used two M13 bacteriophage reagents, one with a target ligand and one with a cognate antibody. These reagents produce LD signals that are lower than would be expected if the reagents did not interact indicating the formation of a complex with a low propensity to align. Addition of free ligand disrupted this

complex inducing a reappearance of the LD signal. This assay was found to detect 0.01 mM of the target ligand while not being disrupted by a chemically related ligand indicating good specificity.

CHAPTER 7

- CONCLUSIONS AND FURTHER WORK

The initial objective of this project was to produce a detection system using LD and M13 bacteriophage to detect assay targets. The reasoning behind developing a detection technique was that despite almost 100 years of research, detection techniques still lack either in speed, sensitivity, specificity, cost or stability. Additionally, many of the current techniques involve large machinery which acts as a barrier to bedside diagnosis.

This project utilised a simple hypothesis based on LD as the optical technique which is sensitive to the molecular alignment of M13 bacteriophage and is therefore utilised as the reagent in this homogeneous assay. M13 bacteriophage can be chemically modified to allow for antibody conjugation to its coat proteins and therefore enables it to detect target molecules. In the presence of its target, the alignment of the bacteriophage is disrupted and consequently causes a change in LD signal. This concept had been investigated by Pacheco-Gomez *et al.* (2012); their research provided the first stepping stone in developing M13 and LD as a detection assay. This research has moved on from their preliminary work to establish M13 and LD as a platform technology.

LD is a spectroscopic technique utilising linearly polarised light and is typically used to analyse long biological molecules. LD only requires approximately 3 minutes to take a measurement; this is extremely rapid in comparison to most of the current detection techniques used.

Previous research has proved that M13 bacteriophage is a very stable scaffold (Holliger *et al.*, 1999, Olofsson *et al.*, 2001, Petrenko and Vodyanoy, 2003) and can easily be chemically modified and conjugated with foreign molecules including dyes and antibodies (Lee *et al.*, 2012, Li *et al.*, 2010). This made M13 bacteriophage a suitable reagent for this assay.

The first limitation faced during the development of this assay was the production of M13 bacteriophage. M13 bacteriophage had previously been produced in small quantities, however for this assay, large amounts were required. Current M13 production methods by Sambrook and Russell (2001) and New England Biolabs (2011) were investigated, more specifically their methodology, product yield and specific activity. UV absorbance and LD were utilised to measure their yield and specific activity. It was found that both methods had limitations concerning their methodologies, yields and specific activity. The two methods were combined to form an optimised M13 production method. It was later found that the precipitation steps involved in M13 production could produce further improvements (Branston *et al.*, 2011a) and this led to varying the precipitation times to optimise the M13 yield and M13 specific activity. The steps taken to optimise and improve the M13 production process proved to be rewarding because enough M13 bacteriophage was produced to progress with the development of the assay. If time had permitted, further work could have been done to look at producing M13 on an industrial scale using fermenters (a larger number of *E. coli* cells will enable a larger number of bacteriophage), since if this assay is to be successful, its demand of M13 bacteriophage will have to be catered for. Research already suggests that M13 bacteriophage is a viable process material for industrial applications (Branston *et al.*, 2011b). If M13 is produced on an industrial scale then long term storage will be another area of research that may be required.

The assay developed by Pacheco-Gomez *et al.* (2012) is not able to multiplex and is reliant on detecting the wt M13 signal which is located in the near UV region of the electromagnetic

spectrum. Subsequently, expensive, large and complex machinery is required to probe the near UV wavelengths and to detect different targets several experiments would be required. To ensure this assay reaches an accessible and multiplexed format, chromophores were chemically introduced to the protein coat of M13, moving the optical signals to the visible region of the electromagnetic spectrum. This will facilitate the development of an affordable, small and portable detection system, capable of multiplexing and multimodality.

Various chromophores were covalently attached to M13 bacteriophage and tested using UV/VIS absorbance and LD. The results showed that different dyes behave differently when conjugated to M13. The dyes produced varying LD signals and it was concluded that several factors determined the size of the LD signal, including the percentage labelling of the M13 (calculated from the UV/Vis absorbance spectrum), dye mobility, dye extinction coefficient and lastly the alignment of transition polar moments. M13 conjugated with BHQ-10 was found to produce the largest ratio of dye LD signal to M13 LD signal. This was predominantly explained by the large molecular weight of BHQ-10 which would have caused steric hindrance and therefore increased the rigidity of the structure. This along with the large extinction coefficient, reasonable labelling and the alignment of transition polar moments all contributed to the large LD signal. Whereas M13 conjugated with rhodamine produced the lowest ratio of dye LD signal to M13 LD signal, and this was largely explained by the long chemical linker used to conjugate the rhodamine to the coat proteins of M13. Since the flexible chemical linker increased the dye mobility and reduced the rigidity of the structure, consequently producing a smaller LD signal.

These results demonstrate that dyes can be used to label M13 bacteriophage and that they behave differently depending on several characteristics, which should be considered when selecting dyes for the assay. This work only looked at a limited number of dyes and further

work should be done to investigate a broader range of dyes and at optimising the labelling of M13 bacteriophage.

After successfully labelling M13 bacteriophage with numerous dyes, the subsequent step was to incorporate these structures into the assay. In addition to this, the assay design had been refined to improve its sensitivity by covalently conjugating the primary antibodies (anti-target antibodies) directly to the p8 coat proteins on the M13 bacteriophage. It was thought this would improve the assay sensitivity because there are 2700 copies of the p8 coat protein along the whole length of the bacteriophage, whereas previously p3 was utilised which only has 5 copies at one end of the bacteriophage. Utilising p8 would therefore increase labelling and also ensure good adherence of the M13 to the target. This new design also reduced costs and time because no secondary antibody was required and improved reagent stability.

To demonstrate that this detection assay was capable of detecting a pathogen, an attenuated form of *E. coli* O157 was used as the target molecule. M13 covalently conjugated with both GAE and BHQ-10 was utilised as the reagent. BHQ-10 was the chromophore of choice as it had previously demonstrated that it was capable of producing a large LD signal in the visible region. Following the addition of *E. coli* O157 to the assay, the results confirmed that this assay could successfully detect *E. coli* O157, and at a much higher sensitivity of 10^5 cells/mL compared to 10^7 cells/mL achieved by the existing assay. This detection assay proved to be extremely quick (less than 3 minutes), specific and sensitive with the LD signal dropping significantly in both the near UV region and the visible region of the spectrum. This research has exposed LD coupled with M13 bacteriophage as being a sensitive novel system of detection. Given further time, additional work on optimising the labelling of M13 with both chromophores and antibodies could have been done. This could primarily enhance the sensitivity of the assay, and ensure the chromophores and antibodies are efficiently used thus

reducing costs. The effect of mixing positive and negative *E. coli* on the efficiency of the assay was not investigated and could form an interesting area of future study. Moreover, it would also be interesting to examine this assay in a multiplexed format with differing M13 bacteriophages conjugated with differing antibodies and chromophores. If this is achieved it would make this detection system highly appealing, especially for the medical industry because this assay in a multiplexed format could be used to detect pathogens from patients with infections which are known to be caused by more than one pathogen. For example urinary tract infections can be caused by numerous pathogens including *E. coli* and *Klebsiella pneumoniae* (Behzadi *et al.*, 2010).

This assay demonstrated that it was effective in detecting pathogens; however the design of this assay meant it was limited to large molecules which were able to de-align M13 bacteriophage. With global issues relating to the drugs and explosives industry and health concerns associated with toxin secretion from many pathogens, it was apparent that small molecule detection should be investigated. A new assay design was hypothesized, still maintaining LD and M13 bacteriophage as the key components. This was done because there is the future prospect of incorporating the existing detection assay with small molecule detection and DNA detection to form a multimodal and multiplexed detection system. With this being the long term goal, M13 and LD was to maintain a common feature.

LD and M13 bacteriophage were combined to form the M13 bacteriophage aggregation assay, which is a competition assay capable of detecting small molecules. It was hypothesised that if M13 was conjugated with target molecules and mixed with M13 conjugated with anti-target molecule antibodies they would form a mesh-like structure and de-align and consequently produce a low LD signal. However adding free target molecules to the assay mixture was thought to compete with the target molecules conjugated on the M13 to attach to the

antibodies. This would lead to M13 bacteriophage aligning and therefore an increase in LD signal. This was trialled with fluorescein as the target molecule, and the results verified that this small molecule detection system could detect fluorescein. This assay was specific and sensitive, with it detecting as low as 0.01 mM fluorescein.

However this work was only preliminary and only showed proof of concept, thus more work is required on this assay. Firstly the arrangement of this assay was set up so that it initially incubated M13 conjugated with anti-FITC with the fluorescein, thus allowing the fluorescein additional time to attach to the antibodies. The M13 conjugated with FITC was then added to the assay mixture to compete with the fluorescein, which had already formed attachments to the antibodies. The results from this arrangement proved this assay could detect the presence of the fluorescein. However it would now be interesting to find out if this assay would work if M13 conjugated with anti-FITC and M13 conjugated with FITC are left to incubate first, with the addition of fluorescein to the assay after. This method would be a more realistic method for testing samples and so should be the next area of investigation. Further work also needs to be carried out on multiplexing this assay so that more than one target can be detected at once. This again could involve the use of chromophores to act as markers in detecting particular molecules.

The original aims of this project were to increase M13 bacteriophage production, covalently label M13 bacteriophage with chromophores, increase the sensitivity of the existing pathogen detection assay and finally to develop a small molecule detection assay. This thesis demonstrates that M13 bacteriophage can be produced on a larger scale and demonstrates that M13 is a very chemically flexible bio-nano structure that can be conjugated with various other molecules. This thesis confirms that M13 bacteriophage in conjunction with LD as the optical technique can be used to form a pathogen detection assay with a greater sensitivity

than what has previously been achieved. The incorporation of chromophores provides the prospect of multiplexing the assay and producing a much smaller, portable, fast and inexpensive instrument which can aid in bedside diagnosis. This project then established that the LD/M13 assay could be re-designed to form a small molecule detection assay. This provides the huge possibility of eventually producing a multimodal detection system. Preliminary studies are currently being done in the Dafforn laboratory to investigate the detection of DNA, employing both LD and M13 bacteriophage. This presents an exciting future prospect of eventually producing a multimodal, multiplexed, sensitive, specific, fast, portable and economical diagnostic tool, capable of detecting pathogens, small molecules and DNA.

List of References

- ABUBAKAR, I., IRVINE, L., ALDUS, C., WYATT, G., FORDHAM, R., SCHELENZ, S., SHEPSTONE, L., HOWE, A., PECK, M. & HUNTER, P. (2007) A systematic review of the clinical, public health and cost-effectiveness of rapid diagnostic tests for the detection and identification of bacterial intestinal pathogens in faeces and food. *Health Technology Assessment*, 11, 1–216.
- ADACHI, R., YAMAGUCHI, K., YAGI, H., SAKURAI, K., NAIKI, H. & GOTO, Y. (2007) Flow-induced Alignment of Amyloid Protofilaments Revealed by Linear Dichroism. *The journal of biological chemistry* 282, 8978-8983.
- ARORA, K., CHAND, S. & MALHOTRA, B. D. (2006) Recent developments in bio-molecular electronics techniques for food pathogens. *Analytica Chimica Acta*, 568, 259-274.
- ARSIE, M. P., MARCHIORO, L., LAPOLLA, A., GIACCHETTO, G. F., BORDIN, M. R., RIZZOTTI, P. & FEDELE, D. (2000) Evaluation of diagnostic reliability of DCA 2000 for rapid and simple monitoring of HbA1c. *Acta Diabetol*, 37, 1-7.
- ASLAM, M. & DENT, A. (1998) *Bioconjugation: protein coupling techniques for the biomedical sciences*, Macmillan Reference London.
- AUBREY, S. M. (2004) *The new dimension of international terrorism* Zurich, vdf Hochschulverlag AG.
- BACARESE HAMILTON, T., MEZZASOMA, L., ARDIZZONI, A., BISTONI, F. & CRISANTI, A. (2004) Serodiagnosis of infectious diseases with antigen microarrays. *Journal of applied microbiology*, 96, 10-17.
- BARBAS, C. F., KANG, A. S., LERNER, R. A. & BENKOVICT, S. J. (1991) Assembly of combinatorial antibody libraries on phage surfaces: The gene III site. *Proceedings of the National Academy of Sciences*, 88, 7978-7982.
- BECHINGER, B., RUYSSCHAERT, J. M. & GOORMAGHTIGH, E. (1999) Membrane helix orientation from linear dichroism of infrared attenuated total reflection spectra. *Biophysical journal*, 76, 552-563.
- BEHZADI, P., BEHZADI, E., YAZDANBOD, H., AGHAPOUR, R., CHESHMEH, M. A. & OMRAN, D. S. (2010) A survey on urinary tract infections associated with the three most common uropathogenic bacteria. *A Journal of Clinical Medicine*, 5, 111-115.
- BENDET, I. J. & MAYFIELD, J. E. (1967) Ultraviolet dichroism of fd bacteriophage. *Biophysical journal*, 7, 111-119.
- BENNER, S. A. (2003) Synthetic biology: Act natural. *Nature*, 421, 118.
- BENNER, S. A. & SISMOUR, M. A. (2005) Synthetic biology. *Nature Reviews Genetics*, 6, 533-543.
- BIOSEARCH TECHNOLOGIES (2010) BHQ-10 carboxylic acid, succinimidyl ester. Biosearch Technologies Inc.
- BOER, E. & BEUMER, R. (1999) Methodology for detection and typing of foodborne microorganisms. *International Journal of Food Microbiology*, 50, 119-130.
- BONWICK, G. A. & SMITH, C. J. (2004) Immunoassays: their history, development and current place in food science and technology. *International Journal of Food Science and Technology*, 39, 817-827.
- BRAHMS, J., PILET, J., DAMANY, H. & CHANDRASEKHARAN, V. (1968) Application of a new modulation method for linear dichroism studies of oriented biopolymers in the vacuum ultraviolet. *Proceedings of the National Academy of Sciences of the United States of America*, 60, 1130.
- BRANSTON, D. S., STANLEY, E. C., WARD, J. M. & KESHAVARZ-MOORE, E. (2013) Determination of the Survival of Bacteriophage M13 from Chemical and Physical Challenges to Assist

- in Its Sustainable Bioprocessing. *Biotechnology and Bioprocess Engineering* 18, 560-566
- BRANSTON, S., STANLEY, E., KESHAVARZ-MOORE, E. & WARD, J. (2011a) Precipitation of filamentous bacteriophages for their selective recovery in primary purification. *Biotechnology Progress*, 28, 129-136.
- BRANSTON, S., STANLEY, E., WARD, J. & KESHAVARZ-MOORE, E. (2011b) Study of Robustness of Filamentous Bacteriophages for Industrial Applications. *Biotechnology and Bioengineering*, 108, 1468-1472.
- BROWN, T. (2010) *Gene cloning & DNA analysis an introduction*, Hong Kong, Wiley-Blackwell.
- BUHRER-SEKULA, S., SMITS, H., GUSSENHOVEN, G., VAN LEEUWEN, J., AMADOR, S., FUJIWARA, T., KLATSER, P. & OSKAM, L. (2003) Simple and fast lateral flow test for classification of leprosy patients and identification of contacts with high risk of developing leprosy. *Journal of clinical microbiology*, 41, 1991.
- BULHELLER, B. M., RODGER, A., HICKS, M. R., DAFFORN, T. R., SERPELL, L. C., MARSHALL, K. E., BROMLEY, E. H. C., KING, P. J. S., CHANNON, K. J., WOOLFSON, D. N. & HIRST, J. D. (2009) Flow Linear Dichroism of Some Prototypical Proteins. *Journal of the American chemical society*, 131, 13305–13314.
- CENTERS FOR DISEASE CONTROL AND PREVENTION (2012) CDC grand rounds: prescription drug overdoses-a U.S. epidemic. *Morbidity and mortality weekly report*.
- CHAN, C. P. Y., SUM, K. W., CHEUNG, K. Y., GLATZ, J. F. C., SANDERSON, J. E., HEMPEL, A., LEHMANN, M., RENNEBERG, I. & RENNEBERG, R. (2003) Development of a quantitative lateral-flow assay for rapid detection of fatty acid-binding protein. *Journal of Immunological Methods* 279, 91- 100.
- CHIU, M., LAI, D. & MONBOUQUETTE, H. (2011) AN INFLUENZA HEMAGGLUTININ A PEPTIDE ASSAY BASED ON THE ENZYME-MULTIPLIED IMMUNOASSAY TECHNIQUE. *Journal of Immunoassay and Immunochemistry*, 32, 1-17.
- CHO, J. H. & PAEK, S. H. (2001) Semiquantitative, bar code version of immunochromatographic assay system for human serum albumin as model analyte. *Biotechnology and Bioengineering* 75, 725-732.
- CLACK, B. A. & GRAY, D. M. (1992) Flow linear dichroism spectra of four filamentous bacteriophages: DNA and coat protein contributions. *Biopolymers*, 32, 795-810.
- COLBERT, D. L. & CHLLDERSTONE, N. (1987) Multiple drugs of abuse in urine detected with a single reagent and fluorescence polarization. *Clinical Chemistry*, 33, 1921-1923.
- DAFFORN, T. R., RAJENDRA, J., HALSALL, D. J., SERPELL, L. C. & RODGER, A. (2004) Protein fiber linear dichroism for structure determination and kinetics in a low-volume, low-wavelength couette flow cell. *Biophysical journal*, 86, 404-410.
- DAFFORN, T. R. & RODGER, A. (2004) Linear dichroism of biomolecules: which way is up? *Current Opinion in Structural Biology*, 14, 541-546.
- DALLA VIA, L., GIA, O., MARCIANI MAGNO, S., DA SETTIMO, A., PRIMOFIORE, G., DA SETTIMO, F., SIMORINI, F. & MARINI, A. M. (2002) Dialkylaminoalkylindolnaphthyridines as potential antitumour agents: synthesis, cytotoxicity and DNA binding properties. *European Journal of Medicinal Chemistry*, 37, 475-486.
- DANDIKER, W. B., KELLY, R. J., DANDIKER, J., FARQUAR, J. & LEVIN, J. (1973) Fluorescence polarization fluoroimmunoassay: theory and experimental method. *Immunochemistry*, 10.
- DE BERNARDO, S., WEIGELE, M., TOOME, V., MANHART, K. & LEIMGRUBER, W. (1974) Studies on the reaction of fluorescamine with primary amines *Archives of biochemistry and biophysics*, 163, 390-399.
- DIAMANDIS, E. P. & CHRISTOPOULOS, T. K. (1996) *Immunoassay*, San Diego, Academic Press Inc.

- DINGES, M. M., ORWIN, P. M. & SCHLIEVERT, P. M. (2000) Exotoxins of *Staphylococcus aureus*. *Clinical Microbiology Reviews*, 13, 16-34.
- DRENNON, K., MORIYAMA, S., KAWAUCHI, H., SMALL, B., SILVERSTEIN, J., PARHAR, I. & SHEPHERD, B. (2003) Development of an enzyme-linked immunosorbent assay for the measurement of plasma growth hormone (GH) levels in channel catfish (*Ictalurus punctatus*): assessment of environmental salinity and GH secretagogues on plasma GH levels. *General and Comparative Endocrinology*, 133 314-322.
- DROST, R. H., PLOMP, T. A., TEUNISSEN, A. J., MAAS, A. H. J. & MAES, R. A. A. (1977) A comparative study of the homogeneous enzyme immunoassay (EMIT) and two radioimmunoassays (RIA's) for digoxin. *Clinica chimica acta*, 79, 557-567.
- EKINS, R. P. (1998) Ligand assays: from electrophoresis to miniaturized microarrays. *Clinical chemistry*, 44, 2015.
- EWING, R. G. & MILLER, C. J. (2001) Detection of Volatile Vapors Emitted from Explosives with a Handheld Ion Mobility Spectrometer. *Field Analytical Chemistry and Technology*, 5, 215-221.
- FAGER, R. S., KUTNA, C. B. & ABRAHAMSON, E. W. (1973) The use of NBD chloride (7-chloro-4-nitrobenzo-2-oxa-1,3-diazole) in detecting amino acids and as an N-terminal reagent. *Analytical biochemistry*, 53, 290-294.
- FISHER, M., ATIYA-NASAGI, Y., SIMON, I., GORDIN, M., MECHALY, A. & YITZHAKI, S. (2008) A combined immunomagnetic separation and lateral flow method for a sensitive on-site detection of *Bacillus anthracis* spores – assessment in water and dairy products. *Letters in Applied Microbiology*, 48, 413-418.
- FUJIKAWA, H. & IGARASHI, H. (1988) Rapid latex agglutination test for detection of staphylococcal enterotoxins A to E that uses high-density latex particles. *Applied and Environmental Microbiology*, 54, 2345-2348.
- GELLA, F. J., SERRA, J. & GENERX, J. (1991) Latex agglutination procedures in immunodiagnosis. *Pure and Applied Chemistry*, 63, 1131-1134.
- GHOSH, D., LEE, Y., THOMAS, S., KOHLI, A. G., YUN, D. S., BELCHER, A. M. & KELLY, K. A. (2012) M13-templated magnetic nanoparticles for targeted in vivo imaging of prostate cancer. *Nature nanotechnology*, 7, 677-682.
- GOLDMAN, E. R., COHILL, T. J., PATTERSON JR, C. H., ANDERSON, G. P., KUSTERBECK, A. W. & MAURO, J. M. (2003) Detection of 2,4,6-Trinitrotoluene in Environmental Samples Using a Homogeneous Fluoroimmunoassay. *Environmental science and technology*, 37, 4733-4736.
- GUO, X., CASTELLANO, F. N., LI, L. & LAKOWICZ, J. R. (1998) Use of a long-lifetime re(i) complex in fluorescence polarization immunoassays of high-molecular-weight analytes. *Analytical Chemistry*, 70, 632-637.
- GURTNER, L. (1996) Difficulties and strategies of HIV diagnosis. *The Lancet*, 348, 176-179.
- HAJRA, T. K., BAG, P. K., DAS, S. C., MUKHERJEE, S., KHAN, A. & RAMAMURTHY, T. (2007) Development of a Simple Latex Agglutination Assay for Detection of Shiga Toxin-Producing *Escherichia coli* (STEC) by Using Polyclonal Antibody against STEC. *Clinical and Vaccine Immunology*, 14, 600-604.
- HALSALL, D. J., RODGER, A. & DAFFORN, T. R. (2001) Linear dichroism for the detection of single base pair mutations. *Chemical Communications*, 2410-2411.
- HAUGLAND (1996) *Handbook of fluorescent probes*, USA, Molecular Probes.
- HEALTH AND SOCIAL CARE INFORMATION CENTRE (2013) Statistics on drug misuse: England 2013.
- HECHT, E. (2002) *Optics*, San Francisco, Addison Wesley.
- HIGASHI, S., KASAI, M., OOSAWA, F. & WADA, A. (1963) Ultraviolet dichroism of F-actin oriented by flow. *Journal of Molecular Biology*, 7, 421-430.

- HITES, R. A. (1997) Chapter 31: Gas chromatography mass spectrometry. IN SETTLE, F. A. (Ed.) *Handbook of instrumental techniques for analytical chemistry*. Prentice-Hall PTR, Upper Saddle River.
- HOBOM, B. (1980) Gene surgery: on the threshold of synthetic biology. *Medizinische Klinik* 75, 834-841.
- HOLLIGER, P., RIECHMANN, L. & WILLIAMS, R. L. (1999) Crystal structure of the two N-terminal domains of g3p from filamentous phage fd at 1.9 Å: Evidence for conformational lability. *Journal of Molecular Biology*, 288, 649-657.
- HONG, J. Y. & CHOI, M. J. (2002) Development of one-step fluorescence polarization immunoassay for progesterone. *Biological & Pharmaceutical Bulletin*, 25, 1258-1262.
- HORTON, J., SWINBURNE, S. & O'SULLIVAN, M. (1991) A novel, rapid, single-step immunochromatographic procedure for the detection of mouse immunoglobulin. *Journal of Immunological Methods*, 140, 131.
- JOHNSON, D. K. (2003) Fluorescence polarization immunoassays for metal ions *Combinatorial Chemistry and High Throughput Screening*, 6, 245-255.
- KERR, P., CHART, H., FINLAY, D., POLLOCK, D. A., MACKIE, D. P. & BALL, J. P. (2001) Development of a monoclonal sandwich ELISA for the detection of animal and human *Escherichia coli* O157 strains. *Journal of Applied Microbiology*, 90, 543-549.
- KHALIL, A. S. & COLLINS, J. J. (2010) Synthetic Biology: Applications come of age *Nature Reviews Genetics*, 11, 367-379.
- KONGMUANG, U., HONDA, T. & MIWATANI, T. (1987) Enzyme-Linked Immunosorbent Assay to Detect Shiga Toxin of *Shigella dysenteriae* and Related Toxins. *JOURNAL OF CLINICAL MICROBIOLOGY*, 25, 115-118.
- KUEHN, B. M. (2013) IDSA: better, faster diagnostics for infectious diseases needed to curb overtreatment, antibiotic resistance. *Journal of the American Medical Association* 310, 2385-2386.
- KUNKEL, G. R., MASERT, R. L., CALVETT, J. P. & PEDERSON, T. (1986) U6 small nuclear RNA is transcribed by RNA polymerase III. *Proceedings of the National Academy of Sciences* 83, 8575-8579.
- LEE, J. H., DOMAILLE, D. W. & CHA, J. N. (2012) Amplified protein detection and identification through DNA-conjugated M13 bacteriophage. *ACS Nano*, 6, 5621-5626.
- LEE, S., LEE, Y., LEE, H. M., LEE, J. Y., KIM, D. H. & KIM, S. K. (2002) Rotation of Periphery Methylpyridine of meso-Tetrakis (nN-methylpyridiniumyl) porphyrin (n= 2, 3, 4) and Its Selective Binding to Native and Synthetic DNAs. *Biophysical journal*, 83, 371-381.
- LI, K., CHEN, Y., LI, S., NGUYEN, H. G., NIU, Z., YOU, S., MELLO, C. M., LU, X. & WANG, Q. (2010) Chemical Modification of M13 Bacteriophage and Its Application in Cancer Cell Imaging. *Bioconjugate Chemistry*, 21, 1369-1377.
- LIPSKY, B. A., IRETON, R. C., FIHO, S. D., HACKETT, R. & BERGER, R. E. (1987) Diagnosis of bacteriuria in men: specimen collection and culture interpretation. *The Journal of Infectious Diseases*, 155, 847-854.
- LIU, L., KOMORI, K., ISHINO, S., BOCQUIER, A. A., CANN, I. K. O., KOHDA, D. & ISHINO, Y. (2001) The Archaeal DNA Primase. *Journal of Biological Chemistry* 276, 45484-45490.
- LOGAN, R. P. H. & WALKER, M. M. (2001) Epidemiology and diagnosis of *Helicobacter pylori* infection. *Bmj*, 323, 920.
- MA, O., LAVERTU, M., SUN, J., NGUYEN, S., BUSCHMANN, M. D., WINNIK, F. M. & HOEMANN, C. D. (2008) Precise derivatization of structurally distinct chitosans with rhodamine B isothiocyanate. *Carbohydrate Polymers*, 72, 616-624.
- MARAGOS, C. (2009) Fluorescence polarization immunoassay of mycotoxins: a review. *Toxins*, 1, 196-207.

- MARRINGTON, R., DAFFORN, T. R., HALSALL, D. J. & RODGER, A. (2004) Micro-volume Couette flow sample orientation for absorbance and fluorescence linear dichroism. *Biophysical journal*, 87, 2002-2012.
- MARRINGTON, R., SEYMOUR, M. & RODGER, A. (2006) A new method for fibrous protein analysis illustrated by application to tubulin microtubule polymerisation and depolymerisation. *Chirality*, 18, 680-690.
- MAZUMDER, P., CHUANG, H. Y., WENTZ, M. W. & WIEDBRAUK, D. L. (1988) Latex agglutination test for detection of antibodies to *Toxoplasma gondii*. *Journal of Clinical Microbiology*, 26, 2444-2446.
- MIKI, M. & MIHASHI, K. (1976) Fluorescence and flow dichroism of F-actin-ADP; the orientation of the adenine plane relative to the long axis of F-actin. *Biophysical Chemistry*, 6, 101-106.
- MOELLER, K. E., LEE, K. C. & KISSACK, J. C. (2008) Urine Drug Screening: Practical Guide for Clinicians. *Mayo Clinic Proceedings*, 83, 66-76.
- MULLEN, L. M., NAIR, S. P., WARD, J. M., RYCROFT, A. N. & HENDERSON, B. (2006) Phage display in the study of infectious diseases. *Trends in Microbiology* 14, 141-147.
- MURUGESAN, M., ABBINENI, G., NIMMO, S. L., CAO, B. & MAO, C. (2013) Virus-based Photo-Responsive Nanowires Formed By Linking Site-Directed Mutagenesis and Chemical Reaction. *Scientific Reports*, 3, 1-7.
- MUZARD, J., PLATT, M. & LEE, G. U. (2012) M13 Bacteriophage-Activated Superparamagnetic Beads for Affinity Separation. *Small*, 8, 2403-2411.
- MYRICK, B. A. & ELLNER, P. D. (1982) Evaluation of the latex slide agglutination test for identification of *Staphylococcus aureus*. *Journal of clinical microbiology*, 15, 275.
- NAKATOMI, Y. & SUGIYAMA, J. (1998) A rapid latex agglutination assay for the detection of penicillin-binding protein 2. *Microbiology and Immunology*, 42, 739-743.
- NASIR, M. S. & JOLLEY, M. E. (1999) Fluorescence Polarization: An analytical tool for immunoassay and drug discovery. *Combinatorial Chemistry and High Throughput Screening*, 2, 177-190.
- NEW ENGLAND BIOLABS (2011) *Ph.D.-12 Phage Display Peptide Library Kit (E8110)*, Phage Display, NEB.
- NGUYEN, B. HAMELBURG, D. BAILLY, C. COLSON, P. STANEK, J. BRUN, R. NEIDLE & S. WILSON, W. D. (2004) Characterisation of a novel DNA minor-groove complex. *Biophysical Journal*, 86, 1028-1041.
- NIU, Z., BRUCKMAN, M. A., HARP, B., MELLO, C. M. & WANG, Q. (2008) Bacteriophage M13 as a scaffold for preparing conductive polymeric composite fibers. *Nano Research*, 1, 235-241.
- NORDEN, B., RODGER, A. & DAFFORN, T. R. (2010) *Linear Dichroism and Circular Dichroism: A Textbook on Polarized-Light Spectroscopy*, Cambridge, Royal Society of Chemistry.
- OELLERICH, M. (1980) Enzyme immunoassays in clinical chemistry: present status and trends. *Clinical Chemistry and Laboratory Medicine*, 18, 197-208.
- OLOFSSON, L., ANKARLOO, L., ANDERSSON, P. O. & NICHOLLS, I. A. (2001) Filamentous bacteriophage stability in non-aqueous media. *Chemistry & Biology*, 8, 661-671.
- PACHECO-GOMEZ, R., KRAEMER, J., STOKOE, S., ENGLAND, H., PENN, C. W., RODGER, A., STANLEY, E., WARD, J., HICKS, M. R. & DAFFORN, T. R. (2012) Detection of Pathogenic Bacteria Using a Homogeneous Immunoassay Based on Shear Alignment of Virus Particles and Linear Dichroism. *Analytical Chemistry*, 84, 91-97.
- PAULIE, S., PERLMANN, H. & PERLMANN, P. (2005) Enzyme-linked Immunosorbent Assay. *Encyclopedia of Life Sciences*.
- PENNINGTON, H. (2009) The Public Inquiry into the September 2005 Outbreak of *E.coli* O157 in South Wales.

- PENNINGTON, H. (2010) *Escherichia coli* O157. *Lancet* 376, 1428–35.
- PENZER, G. R. (1968) Applications of Absorption Spectroscopy in Biochemistry *Journal of Chemical Education* 45, 692-701.
- PERUSKI, A. H. & PERUSKI JR, L. F. (2003) Immunological methods for detection and identification of infectious disease and biological warfare agents. *Clinical and Vaccine Immunology*, 10, 506.
- PETRENKO, V. A. & VODYANOY, V. J. (2003) Phage display for detection of biological threat agents. *Journal of Microbiological Methods*, 53, 253-262.
- PIMBLEY, D. W. & PATEL, P. D. (1998) A review of analytical methods for the detection of bacterial toxins. *Journal of Applied Microbiology Symposium Supplement*, 84, 98-109.
- PORSTMANN, T. & KIESSIG, S. (1992) Enzyme immunoassay techniques an overview. *Journal of Immunological Methods*, 150, 5-21.
- POSTHUMA-TRUMPIE, G. A., KORF, J. & AMERONGEN, A. (2008) Lateral flow (immuno)assay: its strengths, weaknesses, opportunities and threats. A literature survey. *Analytical and Bioanalytical Chemistry*, 569 - 582.
- PRESCOTT, L. M., HARLEY, J. P. & KLEIN, D. A. (2005) *Microbiology*, New York, McGraw-Hill Companies.
- REIDY, L., WALLS, H. C. & STEELE, B. W. (2011) Crossreactivity of bupropion metabolite with enzyme-linked immunosorbent assays designed to detect amphetamine in urine. *Therapeutic Drug Monitoring*, 33, 366-368.
- REIMER, L. G., WILSON, M. L. & WEINSTEIN, M. P. (1997) Update on detection of bacteremia and fungemia. *Clinical Microbiology Reviews*, 10, 444-465.
- RICE, L. B. (2011) Rapid diagnostics and appropriate antibiotic use. *Clinical Infectious Diseases*, 52, 357-360.
- RODGER, A. (1993) Linear Dichroism. *Methods in Enzymology*, 226, 232-258.
- RODGER, A., MARRINGTON, R., GEEVES, M. A., HICKS, M., DE ALWIS, L., HALSALL, D. J. & DAFFORN, T. R. (2006) Looking at long molecules in solution: what happens when they are subjected to Couette flow? *Phys. Chem. Chem. Phys.*, 8, 3161-3171.
- RODGER, A., RAJENDRA, J., MARRINGTON, R., ARDHAMMAR, M., NORDE N, B., HIRST, J. D., GILBERT, A. T. B., DAFFORN, T. R., HALSALL, D. J. & C.A., W. (2002) Flow oriented linear dichroism to probe protein orientation in membrane environments. *Physical Chemistry Chemical Physics*, 4, 4051-4057.
- ROSENTHAL, A. F., VARGAS, M. G. & KLASS, C. S. (1976) Evaluation of enzyme-multiplied immunoassay technique (EMIT) for determination of serum digoxin. *Clinical chemistry*, 22, 1899.
- RUCH, F. (1957) Ultraviolet dichroism of nucleic acids and proteins in cell structures. *Acta Histochemica*, 4, 193-6.
- RUTA, J., PERRIER, S., RAVELET, C., FIZE, J. & PEYRIN, E. (2009) Noncompetitive Fluorescence Polarization Aptamer-based Assay for Small Molecule Detection. *Analytical Chemistry*, 81, 7468-7473.
- SAEIDI, N., WONG, C. K., LO, T., NGUYEN, H. X., LING, H., LEONG, S. S. J., POH, C. L. & CHANG, M. W. (2011) Engineering microbes to sense and eradicate *Pseudomonas aeruginosa*, a human pathogen. *Molecular Systems Biology*, 7, 521.
- SAMBROOK, J. & RUSSELL, D. W. (2001) *Molecular cloning: a laboratory manual*, CSHL press.
- SCHACHTER, E. M., BENDET, I. J. & LAUFFER, M. A. (1966) Orientation of the RNA in tobacco mosaic virus* 1. *Journal of Molecular Biology*, 22, 165-172.
- SCHARPE, S., COOREMAN, W. M., BLOMME, W. J. & LAEKEMAN, G. (1976) Quantitative enzyme immunoassay: current status. *Clinical chemistry*, 22, 733.
- SCHNEIDER, R. S., LINDQUIST, P., WONG, E. T., RUBENSTEIN, K. E. & ULLMAN, E. F. (1973) Homogeneous enzyme immunoassay for opiates in urine. *Clinical chemistry*, 19, 821.

- SEGELL, G. M. (2006) Terrorism on London Public Transport. *Defense & Security Analysis*, 22, 45-59.
- SENEAC, L. & THUNDAT, T. G. (2008) Nanosensors for trace explosive detection. *Materials Today*, 11.
- SIDHU, S. S. (2001) Engineering M13 for phage display. *Biomolecular engineering*, 18, 57-63.
- SMALL, E., MARRINGTON, R., RODGER, A., SCOTT, D. J., SLOAN, K., ROPER, D., DAFFORN, T. R. & ADDINALL, S. G. (2007) FtsZ Polymer-bundling by the Escherichia coli ZapA Orthologue, YgfE, Involves a Conformational Change in Bound GTP. *Journal of Molecular Biology* 369, 210 - 221.
- SMITH, D. S. & EREMIN, S. A. (2008) Fluorescence polarization immunoassays and related methods for simple, high-throughput screening of small molecules. *Analytical and Bioanalytical Chemistry*, 391, 1499-1507.
- SMITH, J. M., SEREBRENNIKOVA, Y. M., HUFFMAN, D. E., LEPARC, G. F. & GARCÍA-RUBIO, L. H. (2008a) A New Method for the Detection of Microorganisms in Blood Cultures: Part I. Theoretical Analysis and Simulation of Blood Culture Processes. *The Canadian journal of chemical engineering* 86, 947-959.
- SMITH, R. G., D'SOUZA, N. & NICKLIN, S. (2008b) A review of biosensors and biologically-inspired systems for explosives detection. *Analyst*, 133, 571-584
- STEINFELD, J. I. & WORMHOUDT, J. (1998) Explosives detection: A challenge for physical chemistry. *Annual review of physical chemistry*, 49, 203-232.
- STEVEN, G. C. S. & GUNARATNA, R. (2004) *Counterterrorism: A reference handbook*, Santa Barbara, ABC-CLIO Inc.
- STEVENS, D. L., BISNO, A. L., CHAMBERS, H. F., EVERETT, E. D., DELLINGER, P., GOLDSTEIN, E. J. C., GORBACH, S. L., HIRSCHMANN, J. V., KAPLAN, E. L., MONTOYA, J. G. & WADE, J. C. (2005) Practice guidelines for the diagnosis and management of skin and soft-tissue infections. *Clinical Infectious Diseases*, 41, 1373-1406.
- SUNG, P. & STRATTON, S. A. (1996) Yeast Rad51 Recombinase Mediates Polar DNA Strand Exchange in the Absence of ATP Hydrolysis. *Journal Biological Chemistry*, 271, 27983-27986.
- TAPIE, P., HAWORTH, P., HERVO, G. & BRETON, J. (1982) Orientation of the pigments in the thylakoid membrane and in the isolated chlorophyll-protein complexes of higher plants. III. A quantitative comparison of the low-temperature linear dichroism spectra of thylakoids and isolated pigment-protein complexes. *Biochimica et Biophysica Acta*, 682, 339-344.
- TARR, P. I., GORDON, C. A. & CHANDLER, W. L. (2005) Shiga-toxin-producing Escherichia coli and haemolytic uraemic syndrome. *The Lancet*, 365, 1073-1086.
- THOMAS, J. H., RONKAINEN-MATSUNO, N. J., FARRELL, S., BRIAN HALSALL, H. & HEINEMAN, W. R. (2003) Microdrop analysis of a bead-based immunoassay. *Microchemical journal*, 74, 267-276.
- ULLMAN, E. F. (1999) Homogeneous immunoassays: historical perspective and future promise. *Journal of chemical education*, 76, 781.
- UNITED NATIONS OFFICE ON DRUGS AND CRIMES (2012) World Drug Report. *United Nations Publication*
- VENKATRAMAN, A. & LENTS, N. H. (2011) Zinc Reduces the Detection of Cocaine, Methamphetamine, and THC by ELISA Urine Testing. *Journal of Analytical Toxicology*, 35, 333-340.
- VILLARI, P., MOTTI, E., FARULLO, C. & TORRE, I. (1998) Comparison of conventional culture and PCR methods for the detection of Legionella pneumophila in water. *Letters in Applied Microbiology* 27, 106-110.

- VON SYDOW, M., GAINES, H., SONNERBORG, A., FORSGREN, M., PEHRSON, P. O. & STRANNEGARD, O. (1988) Antigen detection in primary HIV infection. *British Medical Journal*, 296, 238-240.
- WARSINKE, A. (2009) Point-of-care testing of proteins. *Analytical and Bioanalytical Chemistry*, 393, 1393 - 1405.
- WOODS, G. L. & IWEN, P. C. (1990) Comparison of a Dot Immunobinding Assay, Latex Agglutination, and Cytotoxin Assay for Laboratory Diagnosis of *Clostridium difficile*-Associated Diarrhea. *Journal Of Clinical Microbiology*, 28, 855-857.
- YAMAMOTO, K. R., ALBERTSROLF, B. M., LAWHORNE, L. & TREIBER, G. (1970) Rapid bacteriophage sedimentation in the presence of polyethylene glycol and its application to large-scale virus purification. *Virology*, 40, 734-744.
- YANARI, S. & BOVEY, F. A. (1960) Interpretation of the Ultraviolet Spectral Changes of Proteins. *The Journal of Biological Chemistry* 235, 2818-2826.
- ZITTERKOPF, N. L. (2008) The Advantages of Molecular Diagnostics in the Surveillance of Health Care-Associated Infections. *Lab medicine*, 39, 623-625.